# The development of motuporamine derivatives and an investigation into their biological properties

2016

Kristen Skruber
*University of Central Florida*

# THE DEVELOPMENT OF MOTUPORAMINE DERIVATIVES AND AN INVESTIGATION INTO THEIR BIOLOGICAL PROPERTIES

by

KRISTEN S. SKRUBER
B.S. Chemistry, Beloit College, 2006

A thesis submitted in partial fulfillment of the requirements
for the degree of Master of Science
in the Burnett School of Biomedical Science
in the College of Medicine
at the University of Central Florida
Orlando, Florida

Fall Term
2016

Major Professor: Otto Phanstiel IV

# ABSTRACT

This project investigates the synthesis of a class of compounds derived from a marine-based natural product and probes how iterative changes to its structure affect its derivatives' biological efficacy. The compound class of interest are the motuporamines which were isolated from the sea sponge *Xestospongia exigua* collected off the coast of Motupore island in Papua, New Guinea.[1] The compounds for this project are predicated upon dihydromotuporamine C (Motu33), the compound that has been shown to be both cytotoxic to MDA-MB231 breast carcinoma cells and has antimetastatic efficacy.[1] The motuporamine scaffold contains a large fifteen-membered saturated macrocycle and an appended polyamine component. A series of Motu33 derivatives were synthesized and evaluated for their ability to target the polyamine transport system as well as inhibit cell migration of human pancreatic cancer cells in vitro. By altering the polyamine component of the system we attempted to build smart antimetastatic compounds which target the upregulated polyamine transport system of human pancreatic cancers and block their migration.

## ACKNOWLEDGMENTS

A special thank you to my committee for their feedback and insight, to Dr. Andl for his microscopy help, to all the other members of the Phanstiel lab, to Dr. Naser and Lisa Vaughn for their administrative magic, my Mom for being my academic role model and advice-giver, to Nicole Roberts for both listening to me complain about all of my failed experiments and helping me problem-solve, and most importantly, to Dr. Phanstiel for being a mentor in the truest sense, for giving me guidance and teaching me how to be a better scientist.


.

# TABLE OF CONTENTS

## LIST OF FIGURES

## LIST OF TABLES

## LIST OF SCHEMES

## LIST OF ACRONYMS AND ABBREVIATIONS

| | |
|---|---|
| µL | Microliter |
| µM | Micromolar |
| µm | Micrometer |
| $^{13}C$ | Carbon 13 isotope |
| $^{1}H$ | Hydrogen 1 isotope |
| AcOH | Acetic Acid |
| AG | Aminoguanidine |
| ATCC | American Type Culture Collection |
| Boc | *tert*-Butoxycarbonyl |
| BuLi | Butyllithium |
| $CDCl_3$ | Deuterated chloroform |

| | |
|---|---|
| $CH_3CN$ | Acetonitrile |
| $CHCl_3$ | Chloroform |
| CHO | Chinese hamster ovary wild-type cells |
| CHO-MG | Chinese hamster ovary mutant cells defective in polyamine transport |
| d | Doublet |
| $D_2O$ | Deuterated water |
| DCM | Dichloromethane |
| DFMO | α-Difluoromethylornithine |
| DMSO | Dimethylsulfoxide |
| EtOAc | Ethyl acetate |
| EtOH | Ethanol |
| FBS | Fetal bovine serum |

| | |
|---|---|
| g | Gram |
| h | Hour |
| HCl | Hydrochloric acid |
| $IC_{50}$ | Half maximal inhibitory concentration |
| $KMnO_4$ | Potassium permanganate |
| L | Liter |
| L3.6pl | Metastatic human pancreatic cancer |
| $LiAlH_4$ | Lithium aluminum hydride |
| m | Multiplet |
| *M* | Molarity (moles/L) |
| Motu33 | Dihydromotuporamine C |
| $MotuCH_233$ | $N^1$-(3-aminopropyl)-$N^3$-(cyclopentadecylmethyl)propane-1,3-diamine |

| | |
|---|---|
| MeOH | Methanol |
| mg | Milligram |
| MHz | Megahertz |
| min | Minute |
| MGBG | Methylglyoxal bisguanyl hydrazine |
| mM | Millimolar |
| mmol | Millimole |
| MS | Mass spectrum |
| MsCl | Methanesulfonyl chloride |
| MTD | Maximum tolerated dose |
| $NaBH(OAc)_3$ | Sodium triacetoxy borohydride |
| NCI | National Cancer Institute |
| $NH_4OH$ | Ammonium hydroxide |

| | |
|---|---|
| NMR | Nuclear magnetic resonance |
| NO | Nitric oxide |
| ODC | Ornithine decarboxylase |
| PAO | Polyamine oxidase |
| psi | Pounds per square inch |
| PTI | Polyamine transport inhibitor |
| PTS | Polyamine transport system |
| Put | Putrescine |
| rt | Room temperature |
| Spd | Spermidine |
| Spm | Spermine |
| SSAT | Spermidine/spermine-$N^1$-acetyl transferase |
| t | Triplet |

| | |
|---|---|
| TEA | Triethylamine |
| THF | Tetrahydrofuran |
| TLC | Thin layer chromatography |
| TMS | Tetramethylsilane |
| UV | Ultraviolet |
| δ | Parts per million (ppm) |

# I. INTRODUCTION

Increased metabolism in rapidly dividing cancer cells necessitates a requirement for increased nutrients and metabolic fuels, including polyamines. Polyamines are low molecular weight aliphatic amines that are positively charged at physiological pH (*Figure 1*, Structures **1-3**). In some cases polyamines act similarly to inorganic cations (e.g., magnesium (II) ion) and stabilize the negative charges present in DNA and RNA. Unlike inorganic cations, they can be biosynthesized and their biosynthesis is tightly-controlled and regulated to maintain charge balance and homeostasis. They are crucial for chromatin condensation, the replication of DNA, synthesis of RNA, cell cycle regulation, and in the translation of mRNA into protein.[2] Perhaps the best example of how polyamines are used to facilitate growth is the fact that an aminobutyl fragment of spermidine is annealed to eIF-5A precursor protein to form a critical hypusine residue. Only this hypusinylated form of eIF-5A is functional , thus illustrating a key role for polyamines in mRNA and protein synthesis.[3]

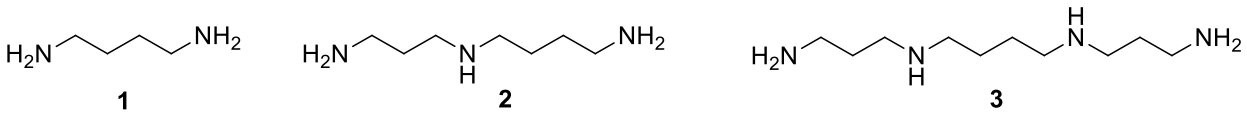


**Figure 1**. Native Polyamines: putrescine **1**, spermidine **2**, and spermine **3**

It has been previously established that an increase in intracellular polyamine content is concomitant with the initiation of cancer and maintained throughout the development of the cancer cell.[4] The concentration of polyamines in cells is under multifaceted biochemical control via regulation of key enzymes in the biosynthetic pathway, the polyamine transport pathway, or by a

combination of both pathways as shown in Figure **2**.[4] The polyamine transport system (PTS) is an important system in the development and progression of metastatic cancers, as it provides a means to scavenge polyamine metabolites from outside the cell. This polyamine addiction by certain cancers can be utilized to selectively target cancer cells over healthy cells.[5]

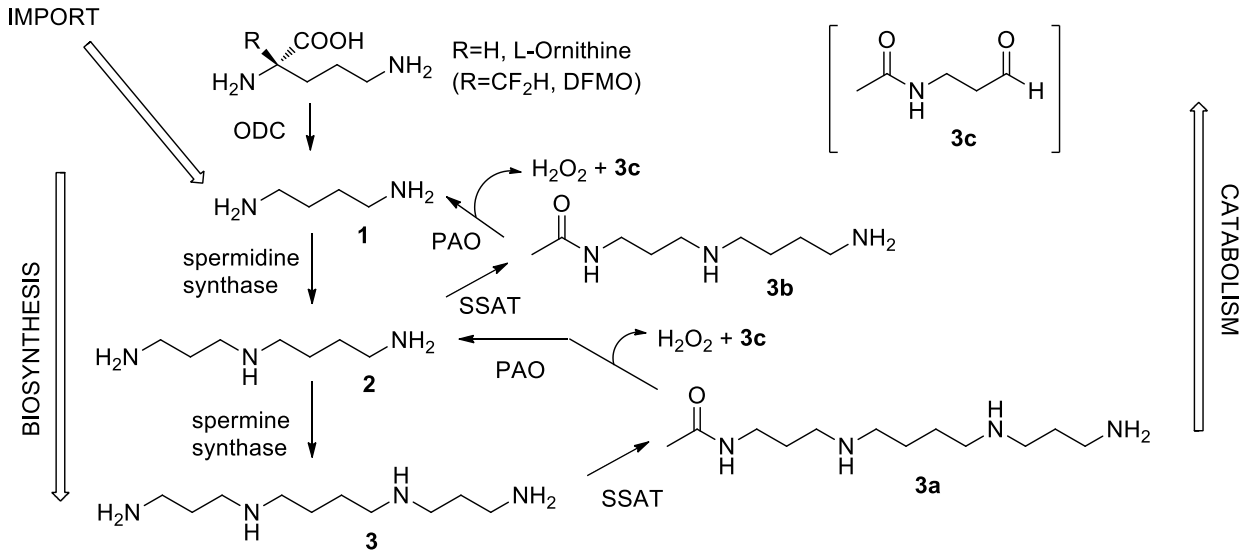


**Figure 2**. Interplay between polyamine metabolism and transport[6]

As the polyamine transport system has wide structural tolerance of its ligands, it can be leveraged to deliver polyamine vectors tethered to anti-metastatic and cytotoxic agents. Assessment of ideal polyamine vectors for the PTS is established through a CHO/CHO-MG screen. Chinese Hamster Ovary cells (CHO-K1 cell line, ATCC) have a highly active PTS while the CHO-MG mutant cell line does not have an active polyamine transport system and relies solely on biosynthesis for polyamine levels through ornithine decarboxylase (ODC) as shown in Figure 2.[6] CHO-MG was derived from CHO cells via random alkylation and was selected for its resistance to a known toxic

PTS ligand (methylglyoxal bisguanyl hydrazine, MGBG).[7] and displays no $^{3}$H-spermidine uptake in radiolabeled polyamine uptake experiments.[8]

The macrocycles for this project are inspired by the motuporamine architecture. The motuporamines contain two key structural elements: a large macrocycle and an appended polyamine component (*Figure 2*, Structures **4**-**7**,). In 1997, the Andersen group isolated and showed that the motuporamines have anti-invasive properties as measured in MDA-231 breast carcinoma cells. The Andersen group synthesized over 40 derivatives of the lead motuporamine, dihydromotuporamine C (*Figure 2*, Structure **7a**), and none exceeded its potency. While the Andersen group probed the nature and size of the macrocyclic ring, they did not change the distance between the ring system and the polyamine message; a strategy which should improve targeting if the polyamine message is facilitating cellular entry. Synthesis of additional analogues of the motuporamines allows the development of additional structure activity relationships and the opportunity to enhance key properties such as inhibition of metastasis and angiogenesis, low cytotoxicity, and increased targeting to cancer cells.[1, 9]

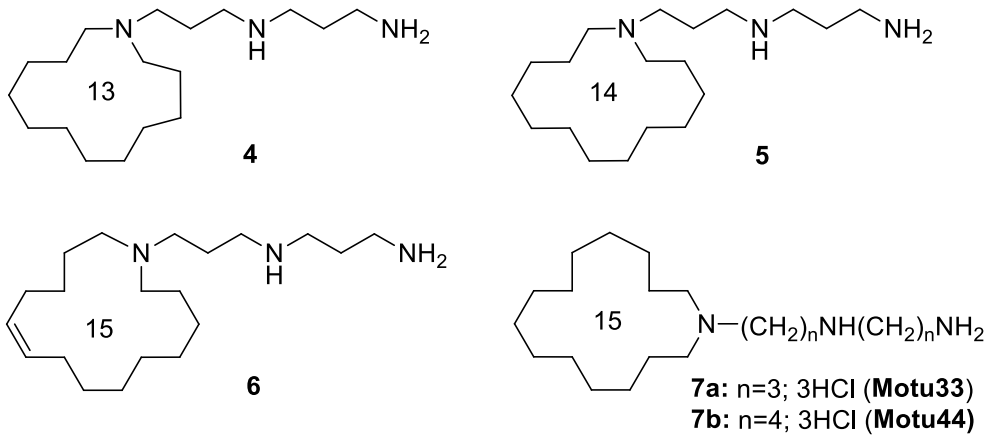


**Figure 3**. Native Motuporamines from *Xestospongia Exigua*. Note the number inside the macrocycle indicates the number of atoms involved in the macrocycle

This project defines key structural requirements of polyamine ligands for targeting the PTS by developing structure activity relationships with a specific set of macrocycle-polyamine conjugates. As the PTS is relatively uncharacterized, most prior progress in the development of drugs attempting to target the PTS has been accomplished via the construction of a homologous series of derivatives and by ranking their ability to gain entry to cells. Members of the proposed series are the result of iterative changes in the degree of saturation in the macrocycle, number of carbons in the macrocycle, length of the tether to the appended polyamine message, and the polyamine message itself. This project builds upon key features already established for aryl-polyamines and extends them to saturated macrocycles. The synthetic schemes focus on changing the length of the tether connecting the polyamine message to the macrocycle as well as by changing the spacer sequence within the the polyamine message itself. By changing the length of the tether, potency has been shown to improve along with cell targeting capabilities because the extended distance

decreases steric crowding near the polyamine ligand and increases the availability of the polyamine message for its putative receptor. Muth et al showed a significant increase in anti-metastatic efficacy with increased distance between the polyamine message and the macrocycle as shown in *Figure 3* (**7a**) to *Figure 4* (**8a** to **10a**).[5] In addition, changing the nature of the polyamine message should increase targeting of the macrocycle as specific polyamine sequences are preferred by the PTS. Outcomes from these studies could lead to improved polyamine transport ligands and inhibitors; both of which have applications as cancer therapies.[6, 10,10b]

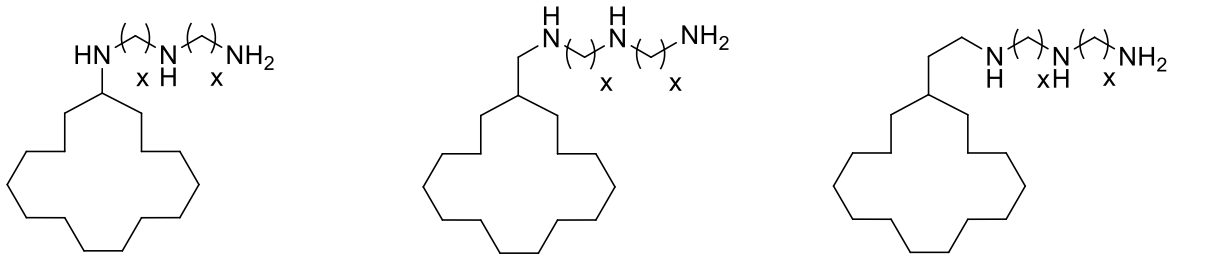


**8a:** x=3; 3HCl (**MotuN33**)
**8b:** x=4; 3HCl (**MotuN44)**

**9a:** x=3; 3HCl (**MotuCH$_2$33**)
**9b:** x=4; 3HCl (**MotuCH$_2$44**)

**10a:** x=3; 3HCl (**MotuCH$_2$CH$_2$33**)

**Figure 4**. Synthesized Motuporamine derivatives **8-10**

Andersen et al established the ideal number of carbons in the macrocycle and degree of saturation for optimal potency and identified dihydromotuporamine C (**Motu33**) as the lead compound.[9] Acetylation of the terminal amino group of Motu33 did not alter the antimetastatic efficacy of the compound, while acetylation of both the secondary amine and the terminal primary amine of Motu33 provided a diacetylated adduct with complete loss of antimetastatic potential.[11] Other studies using $N^1$-(anthracenylmethyl)polyamines as motuporamine derivatives revealed that

generation of a tertiary amine at the $N^1$ position completely eradicated PTS targeting, possibly due to an increase of steric crowding.[10a] Increasing substitution at the $N^1$ amine has also tracked with an increase in $K_i$ values and substitution at both ends of the polyamine increases $K_i$ values, yielding a decrease in affinity for the PTS.[10b]

Previous studies have shown that motuporamines do not use polyamine transport for cell entry.[6] Using prior SAR studies of anthracenylmethyl polyamine compounds and motuporamine derivatives, new motuporamine derivatives were designed in an attempt to create smart polyamine vectors that selectively target polyamine transport active cells. These ethylene amine motifs are based on triethylene tetramine (*Figure 4*, **11c***)* which has been shown to interact with established oncogenic targets such as eIF-5a and telomerase.[12a,b] These motifs are of particular interest when tethered to the motuporamines as they are charge deficient analogues of the native polyamines which further inquiry into the effect of modulating the distance between nitrogen centers and motuporamine efficacy.

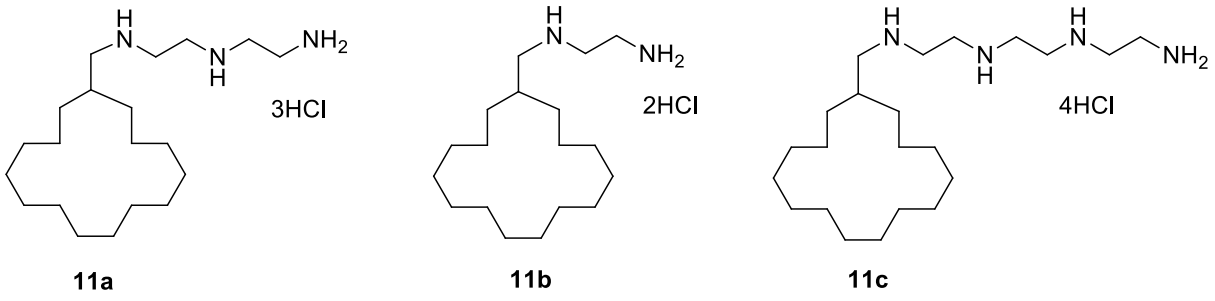


**Figure 5**. Synthesized Ethylene Amine motifs based on Motu$CH_2$33

Prior assessment via a CHO/CHO-MG screen has shown that linear triamine motifs are ideal vectors for the PTS. Using L1210 cells, Phanstiel et al showed that tetra-amines with low $K_i$ values

in the nM range did not enter cells as readily as the less toxic triamines with μM Ki values. Evidently, compounds with too high an affinity for the cell surface receptor (i.e. low Ki values) bind and stick and do not enter as readily. A homospermidine (4,4-triamine) motif (*Figure 3*, Structure **7b**) was selectively delivered via the PTS and displayed 150 fold higher cytotoxicity in polyamine transport active CHO cells versus a transport-deficient CHO-MG cell line.[10b] The distance between nitrogens in the polyamine sequence, therefore, seems to have a large effect on cellular entry and the compound's ability to use the PTS. While the homospermidine message seems to be the optimal polyamine motif for targeting the PTS, this does not necessarily imply that it also provides optimal cytotoxicity or anti-metastatic properties. This was of interest in our investigation into ethylene amine motifs as the decrease from a norspermidine (3,3-triamine) motif to the ethylene amine (2,2-amine) motifs as shown in *Figure 4* was expected to place the nitrogen centers at different distances from the hydrophobic macrocyle substituent and extend our understanding of the motuporamine pharmacophore.

The proposed efficacy of the motuporamines lies in their ability to affect Rho activation. Prior investigators found that Motu33 works as an anti-metastatic agent by over-activating Rho.[13] The Rho pathway is involved in the formation of stress fibers and focal adhesions often found in motile cells. However, McHardy et al found that certain tumor cell lines undergo invasion from primary sites to secondary sites using an elongated cell structure, invadopodia. They proposed that Motu33 efficacy is tied to its ability to block metastasis only when elongation is required for invasion, which is often the case. Further elucidation of this mechanism, including the specifics of how the small molecule alters signal transduction in the Rho pathway, are needed.

Baetz et al found that Motu33 was able to alter sphingolipid profiles in yeast cells using a yeast haplo-insufficiency screen. Genes involved in sphingolipid metabolism were deleted and those mutants were found to be more susceptible to the addition of Motu33.[14] Sphingolipid metabolism is involved in the production of ceramide which has crucial roles in initiation of apoptosis and was also found to be linked directly to migration through a CXCL12/CXCR4 dependent pathway.[15] While the full mechanism as to how motuporamine compounds are able to alter sphingolipid profiles and what the consequences are for the cell are unknown, further elucidating these mechanisms may be key to understanding the pharmacological mechanism behind their antimetastatic and antiangiogenic properties.

Identifying the mechanism of action is important to understanding efficacy of any potential drug candidate as well as managing its off-target effects. This project will complete key structure-activity relationship studies as a continuation of Muth et al[6], Andersen et al[9], optimize the drug design and provide new probes for future elucidation of potential targets of the motuporamines, including the Rho GTPase[14] pathway and sphingolipid metabolism.[15]

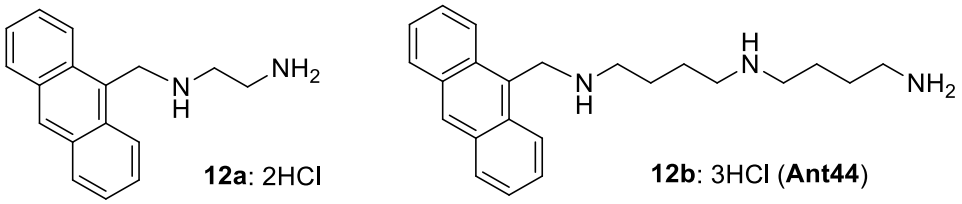


**Figure 6**. Synthesized Anthracenylmethyl amines based on monosubstituted anthracene conjugates

# II. RESULTS AND DISCUSSION

## 2.1 Chemical Synthesis

A number of synthetic approaches were investigated in an attempt to utilize the reactivity of commercially-available ketone, i.e., cyclopentadecanone, to develop extended motuporamine derivatives. This ketone **13** obviated the need for building the fifteen membered ring from scratch through ring closing metathesis as had been accomplished in Furstner et al and which resulted in an undesirable byproduct due to an inability to control stereochemistry during formation of the macrocycle.[16] The Phanstiel group has already previously developed a total synthesis of the parent Motu33 compound via a multistep scheme using ring closing metathesis and protected polyamines.[5]

As shown in Scheme 1, Muth et al demonstrated that it was possible to convert commercially available ketone **13** to its corresponding alkene **14** through a Wittig reagent[5]. The alkene could then undergo hydroboration oxidation to alcohol **15**. From alcohol **15** a number of synthetic routes were attempted to use the alcohol as a platform to create an electrophile or a nucleophile. The synthesis of extended motifs on the motuporamines had been attempted by Muth et al by conversion of alcohol **15** to its corresponding aldehyde resulting in low yields and an impure product.[5] While extended compounds **9a** and **9b** were made from the aldehyde, other chemistries were investigated in an attempt to improve the yields on extended motuporamine structures.

Therefore it was attempted to convert the alcohol to an extended primary amine **18** which could behave as a nucleophile to attack an electrophilic polyamine scaffold, as shown in Schemes **2,3** .

**Scheme 1** [a]

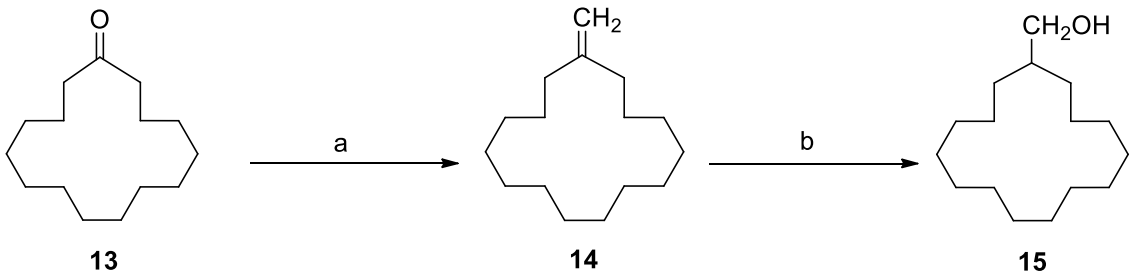


[a] ***Reagents*****:** a) $MePPh_3I$, BuLi; b) $BH_3$/THF

The alcohol **15** was converted into a good leaving group (by conversion to its mesylate **16**) using methane sulfonyl chloride/TEA in DCM in good yields. Mesylate **16** was then converted to nitrile **17** using 18-crown-6 ether and KCN with a yield of 87%. The resultant alkylated nitrile was then reduced to primary amine **18** using lithium aluminum hydride in THF with a 49% yield. Attempts were made to generate the amine on the motuporamine ring with two and three methylene spacers. Synthesis of the two methylene spacer amine **18a** was successful while the three spacer amine **18b** was problematic due to low yields of its corresponding nitrile **17b** (<11%).

**Scheme 2**[a]

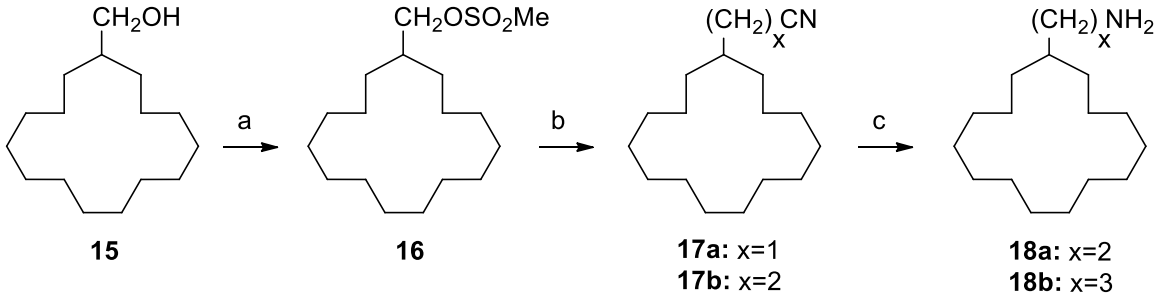


[a]*Reagents*: a) $CH_3SO_2Cl$ b) KCN, c) $LiAlH_4$

The synthesis of **10** was an attempt to further probe the effects of extending the norspermidine message away from the macrocycle core by increasing the number of methylene spacers (Scheme 3). It was shown by Muth et al, that the extended compound **9a** had the best in vivo performance in terms of anti-metastatic efficacy. It was hypothesized this efficacy may have been due to the increased availability of the message for its putative receptor. [5] The synthesis of **10** was therefore an attempt to understand how further extending this message by increasing the number of methylene spacers from two to three would affect anti-metastatic potency.

The polyamine was joined to the macrocycle through a nucleophilic substitution reaction where the polyamine portion behaves as the electrophile and the nucleophilic amine on the macrocycle attacks the mesylate on the polyamine (Scheme 3). Aqueous sodium carbonate ($Na_2CO_3$) was used to facilitate alkylation and 4M HCl was used to deprotect the Bocylated amine. This synthetic scheme began with the conversion of the Boc-protected polyamine **19** to its corresponding mesylate **20** in 80% yield. The N-alkylation of mesylate **20** with amine **18** was performed in the

presence of $Na_2CO_3$ in DCM and resulted in poor yield of 20%. As this step also required the use of amine **18**, a compound that was generated through a long synthetic method and also resulted in low yields, the scheme was less than satisfactory. The low yields in the synthesis of **21** in particular was attributed to the facile formation of a self-cyclized byproduct **22** where (due to the low reactivity of the macrocyclic amine **18)** the terminal carbamate group of **20** was observed to react with and displace the appended mesylate group to form byproduct **22,** thus, lowering the amount of **20** available to react.

**Scheme 3**[a]

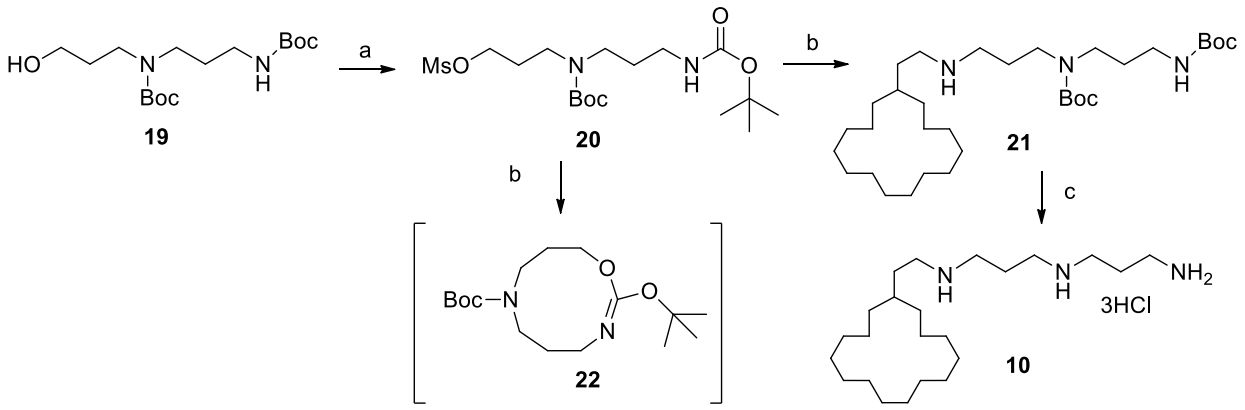


[a]*Reagents*: **a).** TEA, MsCl; b) amine **18a**, $Na_2CO_3$; c) EtOH, 4M HCl

Due to the low yields in the production of amine **18b** and the long synthetic process required for its synthesis starting from ketone **13**, alternative chemistries were investigated on ketone **13** and alcohol **15** in an attempt to create a nucleophilic polyamine motif that could be joined to an electrophilic macrocycle in more efficient manner.

As shown in Scheme 4, the synthesis of alkylbromide **23** began via bromination of alcohol **15** using phosphorus tribromide in hexane to give a 67% yield. It was then attempted to convert bromide **23** to a Grignard reagent **A** (RMgBr) as shown in step d in Scheme 4 by activating magnesium turnings in the presence of dry THF and 1,2-dibromoethane. We envisioned using this Grignard reagent for chain extension using formaldehyde or ethylene oxide to impart new one and two carbon extensions, respectively on the (cyclopentadecyl)-methyl scaffold. The respective alcohols could then be converted to their corresponding mesylates and reacted with Boc-protected

polyamines for the crucial ring-joining step. However, the formation of the Grignard reagent **A** was not observed and the bromide was recovered in full yield.

Chain extension was also attempted using a Suzuki reaction (see Step e in Scheme 4) per the Yang group's 2012 paper on copper mediated cross-coupling of alkyl halides with secondary Grignard reagents to form a carbon-carbon bond[17]. This reaction to form **B** was, thus, attempted with a commercially available Grignard reagent **C**, a cyclic acetal. We envisioned that compound **B** could be subsequently be deprotected to its aldehyde with heat and aqueous acid. This aldehyde could then be coupled via reductive amination to a Boc-protected polyamine as done previously on related systems to afford a chain extended analogue. [5] However, we were unable to form **B** likely again due to the steric hindrance of the macrocycle in **23.**

Due to the lack of formation of the desired macrocyclic Grignard reagent **A** (Scheme 4), we attempted to directly couple ketone **13** and a commercially available Grignard reagent **C**. Step g in Scheme 4 illustrates this attempt to use a pre-formed Grignard reagent on the ketone through nucleophilic addition as an alternative to extend the carbon chain as shown in acetal **D.**.

**Scheme 4**[a]

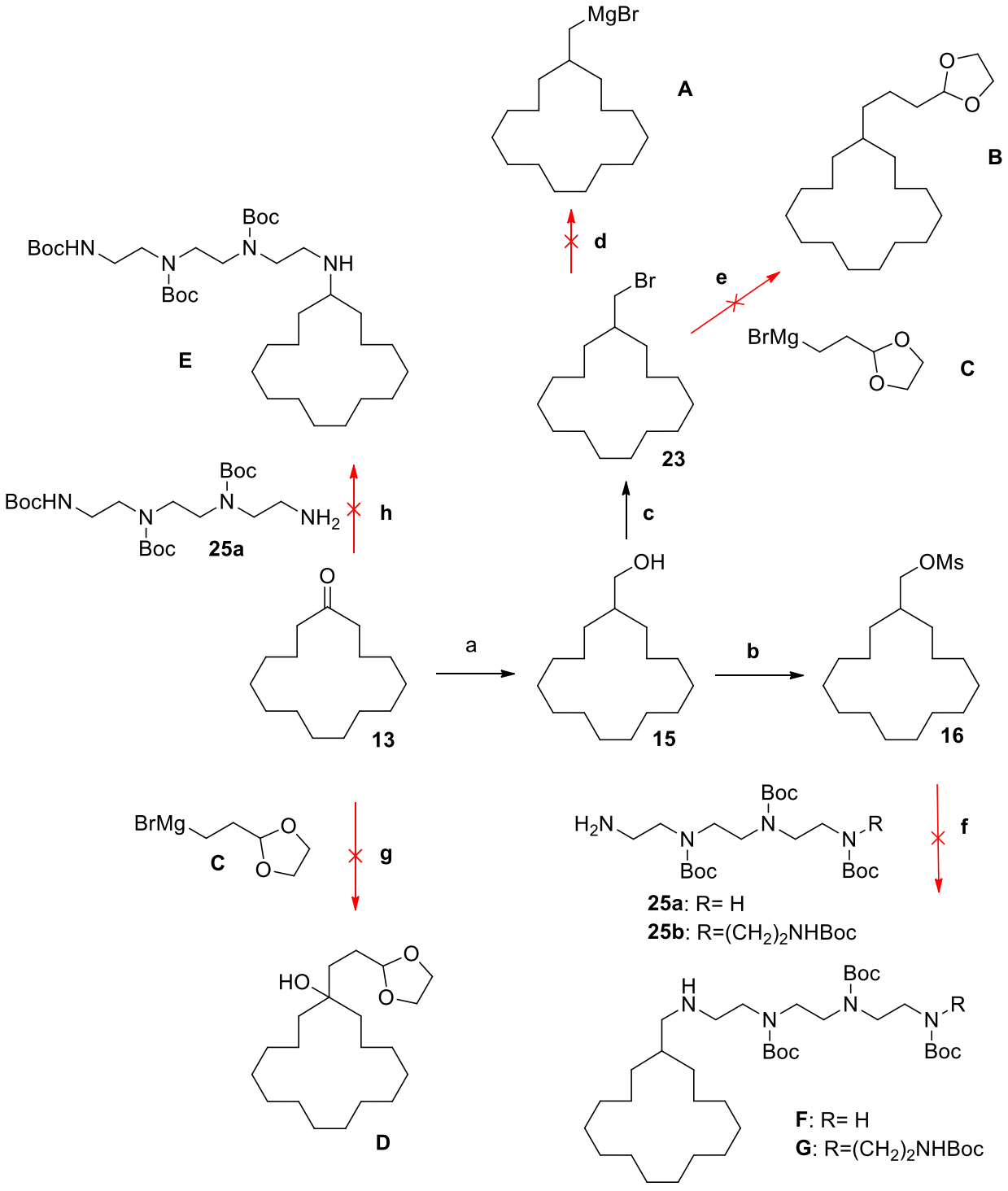


[a]*Reagents*: a) $MePPh_3I$, BuLi; then $BH_3$, THF; b) MsCl; c) $PBr_3$; d) Mg, dry THF; e) CuI, LiOMe, TMEDA; f) $CH_3CN$, $K_2CO_3$; g) THF; h) glacial AcOH, DCE, $NaBH(OAc)_3$

The failed attempts to create the envisioned extended aldehydes through Grignard chemistry, and failure to perform chemistry directly on the ketone to form imine **E**, and the difficulty in synthesis of amine **18a** suggested that alternative chemistries were needed. Due to the observed by product formation seen with the mesylate **20** we elected to reverse the polarity of the two coupling partners and created a nucleophilic polyamine component that could then be appended to an electrophilic macrocycle motif. The development of an electrophilic macrocycle motif was limited by the reactivity of ketone **13.** Many attempts were made to perform chemistry directly on the macrocyclic ketone, to no avail. The only method that worked well was Wittig olefination followed by hydroboration to create alcohol **15**. The conversion of alcohol **15** to its corresponding mesylate **16** afforded our entry to an electrophilic macrocycle modality. Efforts next focused on preparing the nucleophilic polyamine motif for attachment to the alkyl motif in **16**.

In an attempt to maximize yields and minimize the formation of undesirable side products, a regioselective protection of specific nitrogen centers was performed on the free base of triethylene tetramine tetrahydrochloride **24b** and tetraethylenepentamine pentahydrochloride **24c**. The general strategy was to cap all the free secondary amine centers on the polyamine chain as carbamates containing *t*-butoxycarbonyl (Boc) groups. Failure to cap these potential nucleophilic centers would result in undesired non-linear, branched byproducts.

Selective protection was performed by formation of an imine on the primary amine of the free base form of the polyamine using salicylaldehyde.[18] Salicylaldehyde will selectively protect primary amines but leave the secondary amines untouched and therefore the secondary amines are subject

to protective Bocylation using di-*tert*-butyl dicarbonate. After the Boc protection of the secondary amine and remaining primary amine centers was complete, cleavage of the imine was performed with methoxyamine under acid-free conditions to maintain the fidelity of Boc protection.[19] Deprotection of the salicylimine afforded a polyamine chain with one available primary amine as a reactive center for selective alkylation with the macrocycle mesylate **16**.

**Scheme 5**[a]

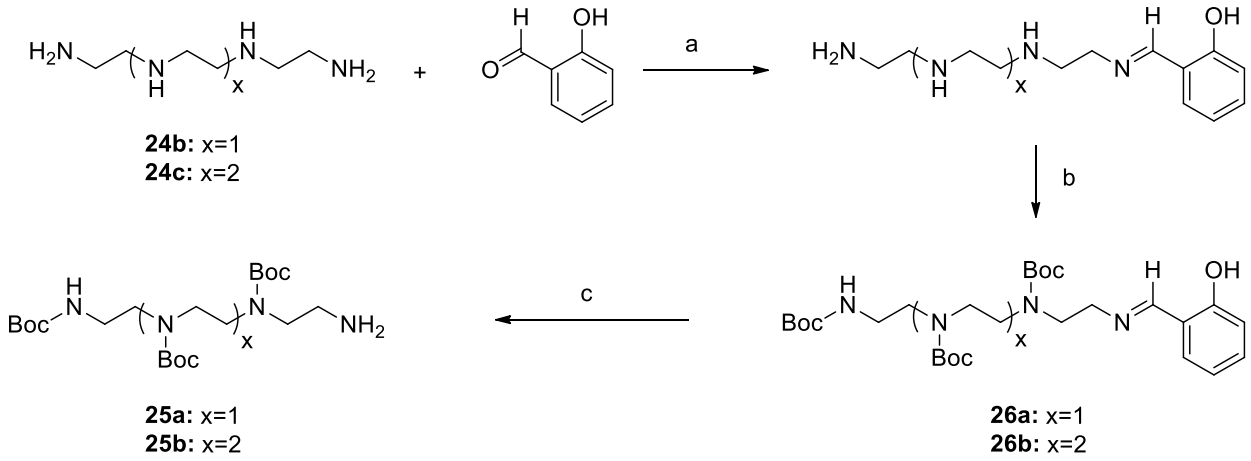


[a]*Reagents*: a) NaOH; b) di-*tert*-butyl dicarbonate; c) $MeONH_2$

Following work done by Abdel-Magid et al, a reductive amination was attempted between tetramine **25a** and ketone **13** with $NaBH(OAc)_3$ to give amine **E** (Scheme 4). The reaction was monitored for disappearance of the ketone and showed no conversion in DCM or in THF after 48 h in each solvent at both rt and at 40°C.[20]

We speculated that the failure of the reductive amination using **25a** and **13** was due to steric occlusion of the reactive ketone center by the bulky macrocycle. Therefore, attempts were made with the extended electrophile of mesylate **16** and the Boc-protected polyamines generated in Scheme 5, (i.e., **25a** and **25b**).

Step f in Scheme 4 illustrates the attempts to use regioselectively protected polyamines **25a** and **25b** to generate the Boc protected motuporamine structures **F** and **G.** The alkylation reaction with

pentaamine **25b** and mesylate **16** was performed in $CH_3CN$ initially at rt and monitored by TLC (1% $NH_4OH$/3%MeOH/DCM, $R_f$ **25b:** 0.4) for disappearance of starting material. After 48 h and no disappearance of starting material, the temperature was raised to 40°C. After the reaction was run for an additional 12 days NMR showed a 60% conversion of starting materials. **25b** and mesylate were both still present when the reaction was stopped by removal of $CH_3CN$ and then re-solvation in DCM for a crude red oil mixture (0.563g). A column was run to separate the mixture (100% DCM, mesylate: $R_f$ 0.6, suspected product: $R_f$ 0.4, pentamine **25b**: $R_f$ 0.1) and mesylate **16** was recovered (33mg, 0.102mmol). The suspected product appeared to be the motuporamine ring with a cyclized polyamine based-urea byproduct. The failure of this reaction indicated the low reactivity of the primary amine on **25b**, possibly due to the large bulky Boc substituents a short distance away from each other. In the case of **25b** there are four Boc groups two carbons away from each other. Thus, the steric constraints associated with each of the reactants disfavored the coupling chemistry.

This coupling was also attempted with the regioselectively-protected tetraamine **25a** also in $CH_3CN$ starting at 40°C and after 48 h raising it to 80 °C. It was shown with the previous attempt that the purported self-cyclization of the polyamine portion was facilitated at rt and that raising the temperature reduced the formation of the undesirable urea byproduct. Unfortunately, starting the reaction with **25a** at 40°C did not abate the formation of the byproduct nor did it facilitate the formation of the desired linear motuporamine motif, nor did the temperature increase to 80 °C yield the desired result. The reaction was also monitored by TLC (1% $NH_4OH$/3%MeOH/DCM, $R_f$ **25a:** 0.4) and by $^1H$ NMR but also showed a self-cyclized byproduct and was aborted after 7 days.

Mono N-Boc diamine **28** was available commercially (Sigma Aldrich) and was the only Boc protected ethylene amine motif to be used successfully in forming the desired motuporamine structure. The Boc protected polyamine **28** was heated at 50 $^{o}$C overnight and then for 5 days at reflux (80 $^{o}$C). The reaction rate was shown to increase after 48 h when the volume of the solvent ($CH_3CN$) was reduced. The product **27c** was able to be separated by column chromatography (7% MeOH/DCM $R_f$ of **27c**: 0.4) from a cyclized urea byproduct that was present in large quantities for a total yield of **27c** of 53% (Scheme 6). Subsequent removal of the Boc group with acid provided the desired adduct **11c** in high yield but at a disappointing 10% overall yield from **16**.

**Scheme 6**[a]

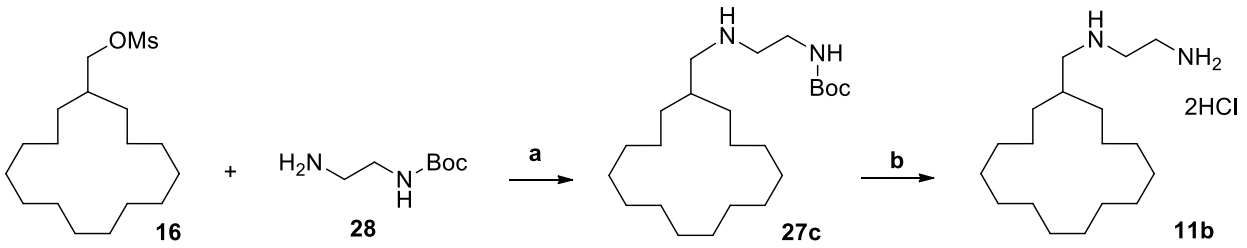


[a]*Reagents*: a) $CH_3CN$, $K_2CO_3$ b) 4M HCl, EtOH

As polyamines **25a** and **25b** appeared to have hindered reactivity due to their Boc groups and displaced their own *t*-butyl groups to form cyclic ureas in favor of reacting with the mesylate, a 'naked polyamine' approach was attempted with the free base of **24a,b,c** as shown in Scheme **7**. This approach was not initially attempted due to the probability of the secondary internal amines reacting with the mesylate and creating tertiary branched motuporamine structures instead of the desired secondary amine containing linear motuporamine motifs. Nevertheless, this 'naked polyamine' approach avoided the possibility of the polyamine portion reacting with its own Boc group prior to alkylation. Indeed, the reaction was much more facile without the bulky Boc substituents crowding the primary amine reaction center. This approach was successful with **24a** and **24b** while **24c** was less productive. In the production of **11a**, triamine **24a** was reacted with bromide **23** while in the production of **11c**, tetraamine **24b** was reacted with mesyl **16**. With both **24a** and **24b** the respective alkylations were performed in $CH_3CN$ and showed complete disappearance of each starting material after 72 h. Workups were performed with 0.1M NaOH and DCM to remove the salts and in the case of **24b**, the displaced methanesulfonate. These provided the expected mixture of secondary and tertiary alkylated products. These were separated by

installing Boc groups at every secondary and primary amine center via bocylation. Since the tertiary amine would not be N-bocylated, the byproduct retained its amine functional group whereas the desired product was converted to a polycarbamate motif. This change in functional group allowed for easy separation by column chromatography of the undesired tertiary amine byproduct (which had one less Boc group and was chemically distinct) and the desired motuporamine motif. Using this approach, a 25% yield was achieved for both products.

The use of the pentamine **24c** with this method achieved a different result. The free base of pentamine **24c** was prepared and mesylate **16** was added in $CH_3CN$ and refluxed for 72 h and monitored by NMR (similar to **24a** sequence in Scheme 7). The mixture was then per-bocylated and separated by column chromatography (1% $NH_4OH$/4.5%MeOH/DCM, $R_f$ of suspected product 0.4 and an additional unknown spot at $R_f$ 0.47). Multiple attempts to separate the product failed and ultimately the final product was both unresolvable from its upper spot and appeared to be the cyclized byproduct by NMR. The crude weight also suggested it was a significantly less productive reaction due to the low conversion of starting material at high temperatures and over a long period of time. Therefore, there were clear limitations to using this approach.

**Scheme 7**[a]

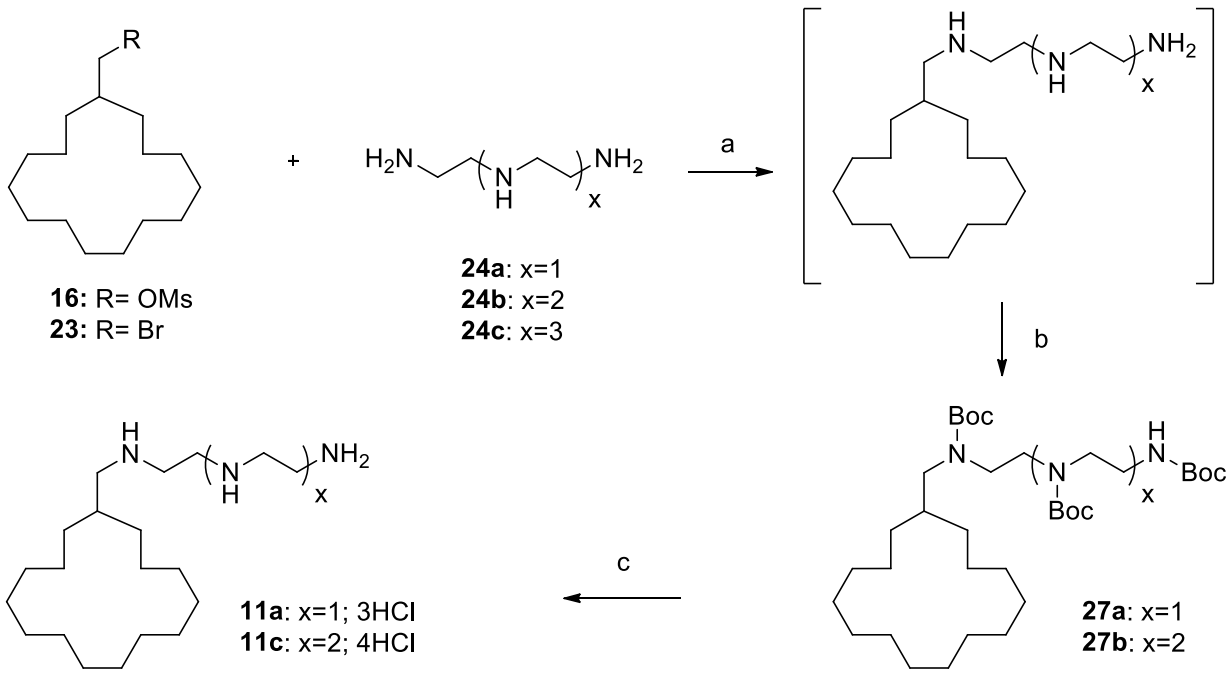


[a]*Reagents*: a) $CH_3CN$, $K_2CO_3$; b) di-*tert*-butyl dicarbonate; c) EtOH, 4M HCl

**Scheme 8**[a]

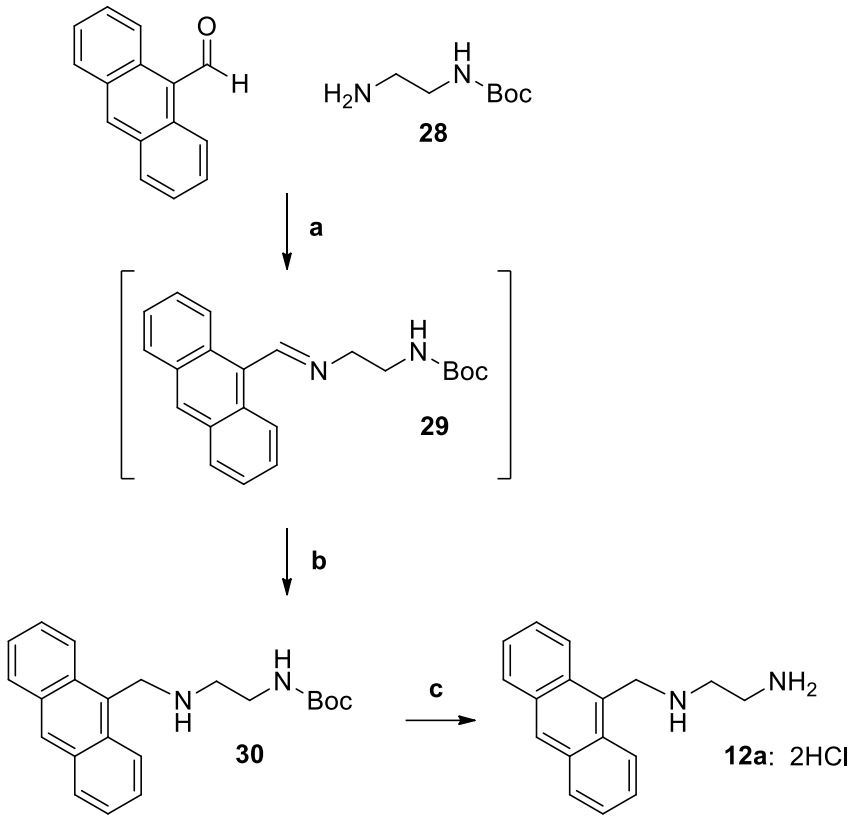


[a]*Reagents*: a) 25%MeOH/DCM; b) $NaBH_4$; c) EtOH, 4M HCl

The synthetic scheme for $N^1$-Anthracen-9-ylmethyl-ethane-1,2-diamine **12a** is shown in Scheme 8 and was based on prior work established in Gardner et al[21] to synthesize Ant44 (**12b**) . In the synthesis of **12a**, the ethylene amine motif was joined via reductive amination to the commercially available 9-anthraldehyde (Sigma Aldrich) which resulted in 75% yield over 3 steps via the intermediate imine **29**.

## 2.2 Biological Evaluation

After synthesis, all compounds were screened for cytotoxicity in CHO, CHO-MG and L3.6pl cells. The wild type (wt) CHO cells have high polyamine transport activity and are very sensitive to compounds, which exploit the PTS for cell entry. In contrast, the CHO-MG cell line was obtained by random DNA-alkylation of CHO cells and selected for their ability to for survival in the presence of a cytotoxic PTS targeting compound, methylglyoxal bisguanyl hydrazine (MGBG).[7] L3.6pl cells are a hyper-metastatic human pancreatic cancer cell line obtained from Dr Isaiah Fidler at MD Anderson Cancer Center in Houston, Texas. To synthesize this cell line, COLO-357 cells were injected into the pancreas of nude mice and allowed to metastasize to the liver. The cells were then harvested from the liver and re-injected into the pancreas. This process was repeated six times to generate the L3.6pl cell line, which provides a model of very aggressive human cells primed for metastasis in vivo.[22]

## 2.3 Polyamine Transport Selectivity Studies

The CHO and CHO-MG cell screen uses cytotoxicity measurements to assess transport preference.[23] Since the CHO-MG cell line is defective in polyamine transport, compounds which selectively enter via the PTS should be less toxic to these cells and give a high CHO-MG $IC_{50}$ value. In contrast, PTS dependent compounds should be lethal to wt CHO cells which have high PTS activity and low $IC_{50}$ value. A ratio of the CHO-MG/CHO $IC_{50}$ values is then used to assess PTS targeting. A compound, which does not enter cells via the PTS, should give similar toxicity in both cell lines and an $IC_{50}$ ratio near 1. In contrast, a compound, which targets the PTS, should give a high CHO-MG/CHO $IC_{50}$ ratio.

Compounds **10**, **11a,b,c**, **12a**, and **15** were tested in both the CHO and CHO-MG cell line at a range of concentrations from 0.1 µM to 100 µM for 48 h in the presence of aminoguanidine (1 mM), an inhibitor of an amine oxidase present in calf serum that will oxidize amine-containing compounds.[5]

As shown in Table 1, all of the motuporamine derivatives did not target the PTS in CHO cells and gave ratios near 1. In contrast, **Ant44** (**12b**) and its derivative Anthracene Diamine **12a** gave a CHO-MG/CHO $IC_{50}$ ratios of 148[24] and 5.8, respectively. As mentioned before, previous studies have shown that dihydromotuporamine C does not use the PTS for cellular entry[6] and one of the goals of this project was to design derivatives that are able to target the PTS. The results of this study suggest that the appended aliphatic macrocycle may not be suitable for PTS targeting. Indeed, modulation of both the polyamine message itself and the distance between the polyamine message and the ring did not improve PTS targeting. The polyamine message of **11b**, when appended to the anthracene core in compound **12a,** was able to accomplish modest PTS targeting while compound **15**, the compound that most closely resembles the naked macrocycle, did not.

**Table 1.** Biological Evaluation of Motuporamine derivatives on cytotoxicity in CHO and CHO-MG cells to assess PTS targeting at 48h[a]

| Compound | CHO-MG $IC_{50}$ (μM) | CHO $IC_{50}$ (μM) | $IC_{50}$ ratio CHO-MG/ CHO |
|---|---|---|---|
| Motu Diamine **11b** | 2.37 (±) 0.12 | 2.66 (±) 0.11 | 0.9 |
| Motu Triamine **11a** | 2.55 (±) 0.07 | 2.48 (±) 0.10 | 1 |
| Motu Tetramine **11c** | 2.62 (±) 0.13 | 2.37 (±) 0.09 | 1.1 |
| Ant Diamine **12a** | **11.33 (±) 0.34** | **1.96 (±) 0.11** | **5.8** |
| Motu$CH_2OH$ **15** | > 100 μM | >100 μM | ND |
| Motu$CH_2CH_2$33 **10** | 2.80 (±) 0.11 | 2.51(±) 0.06 | 1.1 |

[a] All compounds were dosed as aqueous solutions and were compared to a media control with no drug, except compound **15.** Compound **15** was not soluble in water and was dosed in such a manner that the final DMSO concentration was 1% DMSO and was thus compared to a 1% DMSO in PBS control with no drug. For all replicates, n =3. ND= not determined.

### 2.4 L3.6pl cytotoxicity studies

Compounds **10**, **11a-c**, **12a**, and **15** were tested in the human pancreatic cancer cell line L3.6pl which as mentioned earlier, provides a model for aggressive human metastatic cancer. The K-Ras mutation present in the cell line has been shown to correlate with high polyamine uptake due to its ability to affect caveolin-mediated endocytosis,[25] which would lead to an increase in uptake of polyamine-like compounds, if they were polyamine-transport selective. For this study, L3.6pl cells were treated with a range of compound concentrations (0.1 μM to 100 μM) for 48 h in the presence of aminoguanidine (250 μM), a polyamine oxidase inhibitor. Prior studies have shown that an oxidase inhibitor was needed to maintain the polyamine compound integrity and potency. Cell viability was evaluated through the MTS assay and the $IC_5$ /$IC_{50}$ values were calculated from the

plots. Each value represents the concentration of the drug needed to produce the designated level of toxicity (n=3). The $IC_5$ value is the concentration of the compound, which gives 95% viability and represents the dose where minimum toxicity from the compound is expected. The $IC_{50}$ value is the concentration of the compound needed to reduce viability by 50%. The results are shown in Table 2, and accompanying cytotoxicity curves are shown in Figures 7-9.

**Table 2**. Cytotoxicity evaluation of Motuporamine Derivatives (**10**,**11a-c**, **15**) and anthryl derivative (**12a**) in L3.6pl cells for 48h[a]

| **Compound** | | **L3.6pl $IC_{50}$ (**μM) | **L3.6pl $IC_5$ (**μM) |
|---|---|---|---|
| Motu$CH_2CH_2$33 | **10** | 3.34 ± 0.09 | 1.64 ± 0.09 |
| Motu Triamine | **11a** | 1.25 ± 0.05 | 0.6 ± 0.05 |
| Motu Diamine | **11b** | 1.44 ± 0.09 | 0.6 ± 0.09 |
| Motu Tetraamine | **11c** | 1.64 ± 0.05 | 0.92 ± 0.05 |
| Ant Diamine | **12a** | 24.1 ± 1.2 | 4.15 ± 0.2 |
| Motu$CH_2$OH | **15** | 42.0 ± 3.4 | 8.4 ± 0.6 |

[a] All compounds were dosed as aqueous solutions and were compared to a media control with no drug, except compound **15.** Compound **15** was not soluble in water and was dosed in such a manner that the final DMSO concentration was 1% DMSO and was thus compared to a 1% DMSO in PBS control with no drug. For all replicates, n =3.

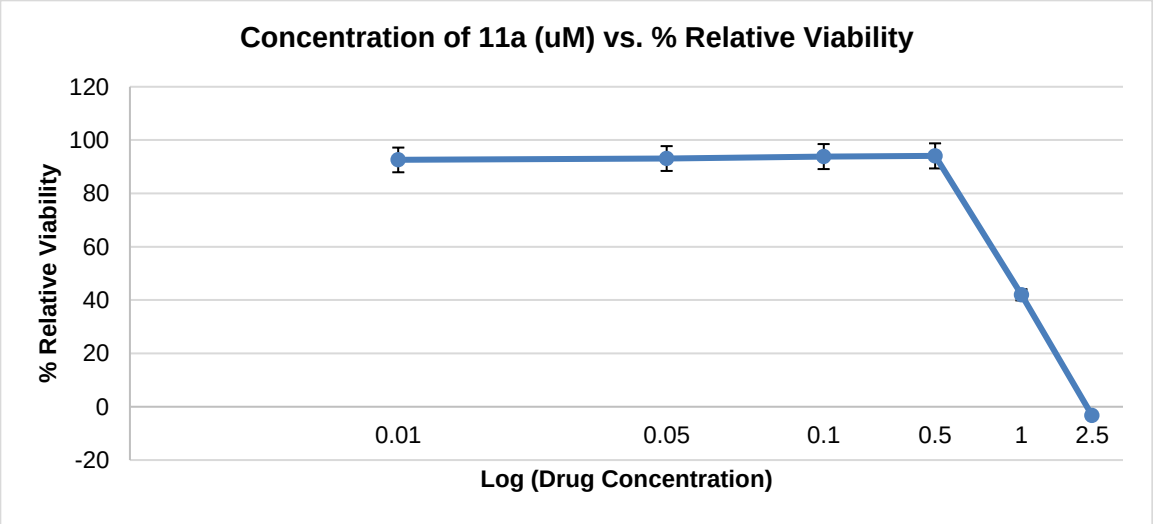


**Figure 7**. Cytotoxicity Profile of **11a** in L3.6pl cells at 48 h

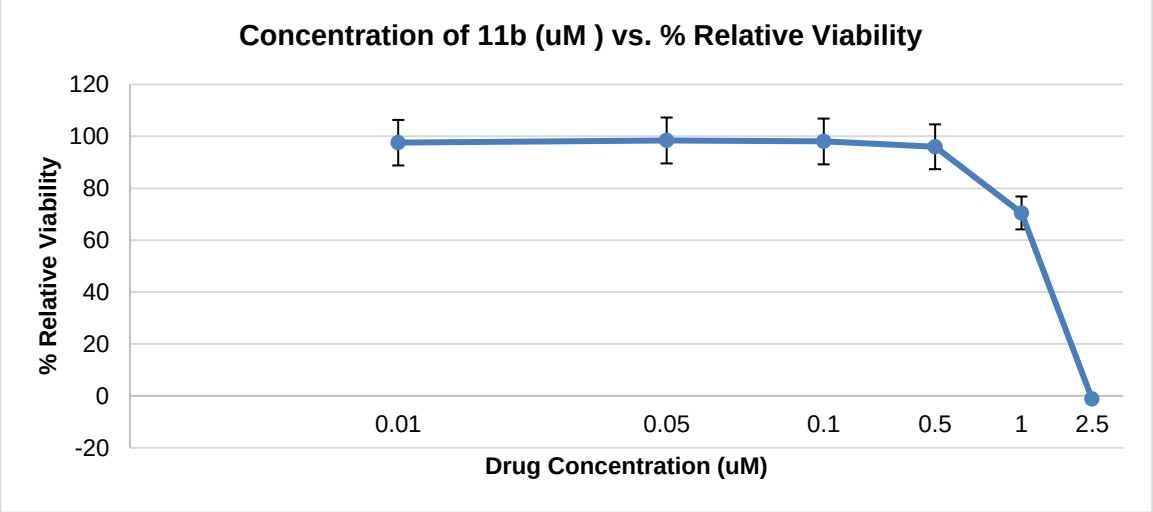


**Figure 8**. Cytotoxicity Profile of **11b** in L3.6pl cells at 48 h

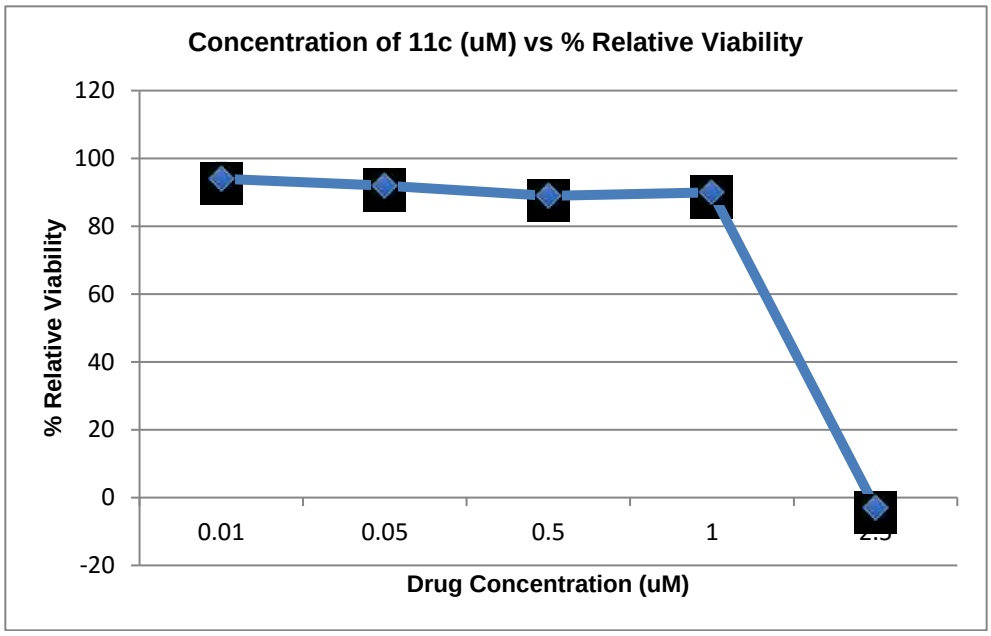


**Figure 9**. Cytotoxicity profile of **11c** in L3.6pl cells at 48h

The motuporamine derivatives (**10, 11a-c**) displayed sharp cytotoxicity curves with their respective $IC_5$ value (where ≤5% toxicity was observed, i.e., maximum tolerated dose (MTD)) was very close to their half maximal inhibitory concentration ($IC_{50}$). These data follow trends from prior members of the series. Interestingly, the toxicity of the motuporamine derivatives was not dramatically altered through modulation of the message or the distance of the message away from the macrocycle. However, the absence of the polyamine component (such as in **15**) or the addition of an unsaturated anthracene core in place of the aliphatic macrocycle (e.g., **12a**) were sufficient to improve toxicity profiles, and in the case of **12a,** PTS targeting (Table 1). These results suggest that the specific combination of polyamine and the macrocycle core seems to be responsible for the cytotoxicity of these compounds. We noted that no cell lysis was observed at the $IC_{50}$

concentrations of these compounds, and cell lysis was discarded as a potential mechanism of action for these amphiphilic molecules.

*Scratch assay.* A scratch assay was performed to assess the anti-migratory properties of compounds **10, 11a,b,c, 12a,** and **15** in L3.6pl cells. The parent compound **7a** and extended compound **9a** were tested as controls, and non-native polyamines **28** and **24a,b** were tested to comment on the anti-migratory ability of the non-native motifs. Compounds were dosed at the MTD (0.5 μM) of the parent compound **7a** to comment on potency by comparison and at 1 μM which was close to the MTD of all newly synthesized compounds (**10** and **11a-c**).

Untreated cells were plated out in 96 well plates using 90 μL of a L3.6pl cell suspension (55,500 cells/mL). Every compound except **15** was dissolved in water to make its respective stock solution. Compounds were delivered at a volume of 10 μL of the appropriate stock solution to 90 μL of media and cells such that the final volume was 100 μL. Due to solubility constraints, compound **15** was dissolved in 100% DMSO and was diluted down to a total delivered concentration of 10% DMSO in PBS prior to addition in the well. Each final stock solution of **15** was in 1% DMSO in PBS and 10 μL of this stock was added into 90 μL of cells and media (total volume = 100 μL). Two untreated controls were run in parallel to account for the difference in vehicle; one containing a water control where 10 μL of water was added to the well containing cells and media and the other control was performed by adding 1% DMSO in PBS (10 μL) to the well containing cells and media. The total volumes used for all scratch experiments was 100 μL. The untreated cells migrated 72± 8.8% of the wound area after 24 h for the motuporamine and anthracene derivatives experiments (compounds **10, 11a-c, 12a, 15**) and 81± 8.9% for the experiments screening the non-

native polyamine derivatives (compounds **24a,b** and **28**). Cell migration was assessed by measuring the area devoid of cells (white space) over a 24 h period and migration measurements calculated as the following:

% Cell Migration at 24h = ((Area with no cells at 0h)-(Area with no cells at 24h))/Area with no cells at 0h x 100%.

% Cell Migration normalized to control = % Migration with drug at 24h/ % Migration of control at 24h * 100

% Cell inhibition at 24h =(1-(% Migration with drug at 24h/% Migration of control at 24h))*100

All experiments were run in triplicate at minimum and representative microscopy images are shown in their respective figures and the numeric results are shown in Tables 3 and 4.

**Table 3.** Inhibition of L3.6pl Cell Migration by Motuporamine derivatives (**7a, 9a, 10, 11a-c, 15**) and Anthracene Derivative (**12a**)[a,b]

| Compound | % Cell Migration at 24 h[a] | % Migration normalized to the control[a] | % Migration inhibition compared to control[a] |
|---|---|---|---|
| 1% DMSO in PBS Control | 44.3 ± 2.5 | - | - |
| 10% aqueous control | 72.3 ± 8.8 [b] | - | - |
| Motu33 (0.5 µM) **7a** | **57.4** ± 5.0 [b] | **79.4** ± 6.9 [b] | **20.61** ± 6.9 [b] |
| Motu33 (1 µM) **7a** | **43.6** ± 4.4 | **60.2** ± 6.6 | **39.76** ± 6.6 |
| Motu$CH_2$33 (0.5 µM) **9a** | 57.7 ± 1.6 | 79.8 ± 6 | 20.24 ± 6 |
| Motu$CH_2$33 (1 µM) **9a** | 50.7 ± 6.8 | 70.1 ± 7.8 | 29.92 ± 7.8 |
| Motu$CH_2CH_2$33 (0.5 µM) **10** | 83.5 ± 3.2 | 115.2 ± 6 | -15.52 ± 6 |
| Motu$CH_2CH_2$33 (1 µM) **10** | 71.2 ± 4.2 | 98.5 ± 6.5 | 1.55 ± 6.5 |
| Motu Triamine (0.5 µM) **11a** | 64.9 ± 7.5 | 89.8 ± 8.2 | 10.22 ± 8.2 |
| Motu Triamine (1 µM) **11a** | 52.9 ± 3.7 | 73.2 ± 6.3 | 26.76 ± 6.3 |
| Motu Diamine (0.5 µM) **11b** | 67.8 ± 5.6 | 93.8 ± 7.2 | 6.22 ± 7.2 |
| Motu Diamine (1 µM) **11b** | 53.3 ± 13.0 | 73.7 ± 10 | 26.27 ± 10 |
| Motu Tetramine (0.5 µM) **11c** | 67.9 ± 8.2 | 93.9 ± 8.5 | 6.09 ± 8.5 |
| Motu Tetramine (1 µM) **11c** | 60.2 ± 5.5 | 83.2 ± 7.2 | 16.78 ± 7.2 |
| Anthracene Diamine (0.5µM) **12a** | 67.8 ± 4.0 | 93.8 ± 6.4 | 6.24 ± 6.4 |
| Motu$CH_2$OH (1 µM) **15** | 60.7 ± 1.6 | 137.2[a] ± 2.1 | -37.19 ± 2.1 |

[a] All compounds were dosed as aqueous solutions and were compared to the 10% water control, except compound **15.** Compound **15** was not soluble in water and was dosed in such a manner that the final DMSO concentration was 1% DMSO and was thus compared to the 1% DMSO in PBS control. For all values n=3 with the exception of those marked otherwise; [b] n=4.

As mentioned earlier, the Andersen group did not probe the effect of changing the distance between the ring system and the polyamine message. The synthesis of **9a** by Muth et al[5] and **10** allows an understanding of the effect of increased distance on facilitating cellular entry. Interestingly, anti-migration efficacy appears to decrease with the increase of spacers away from the macrocycle (from **7a** to **9a**) and complete loss of efficacy is seen with the two methylene spacer extension **10**.

Targeting to the PTS was not achieved by any modification to the parent compound **7a**. Anthracene Diamine **12a** and Motu$CH_2OH$ **15** were tested well below their MTD in order to comment on their efficacy in comparison to the parent compound. Neither control showed any anti-migration behavior (see Table 3). Interestingly, both the macrocyclic alcohol **12a** and the extended system Motu$CH_2CH_2$33 **10** appear to promote migration at low doses.

As both compound **10** and the **11a-c** series exhibit sharp cytotoxicity curves, the window between the maximum tolerated dose and half maximal inhibitory concentration was very small and a dose-limiting toxicity was observed. This dose-limiting toxicity may have been the reason for the reduced anti-migratory efficacy observed. All compounds were also tested at 1 μM, a concentration that doubles the potency of the parent compound **7a**. In a similar outcome the efficacy for the ethylene amine motifs improved at the higher 1 μM concentration, but did not surpass the anti-migration efficacy seen with the parent compound **7a**.

**Table 4**. Inhibition of L3.6pl Cell Migration by non-native polyamines **24a,b**, and **28**

| Compound | % Cell Migration at 24 h | **%** Migration Inhibition |
|---|---|---|
| 10% water control | 81.9 ± 8.9 | - |
| Triamine HCl (1 µM) **24a** | 100% | 0 |
| Tetramine HCl (1 µM) **24b** | 100% | 0 |
| Diamine HCl (1 µM) **28** | 100% | 0 |

The non-native ethylene amine motifs were also assessed for their anti-migratory properties via scratch assay. However, incubation with each amine for 24 h at 1 µM showed an increase in migration compared to control and complete wound closure at 24 h. This experiment clarifies the importance of both the macrocycle (e.g., **15**) and the polyamine (e.g., **24a**) for efficacy of the moturporamines as each of these compounds independently is less effective than the compound that has both the macrocycle and the amine motif (e.g., **11a**).

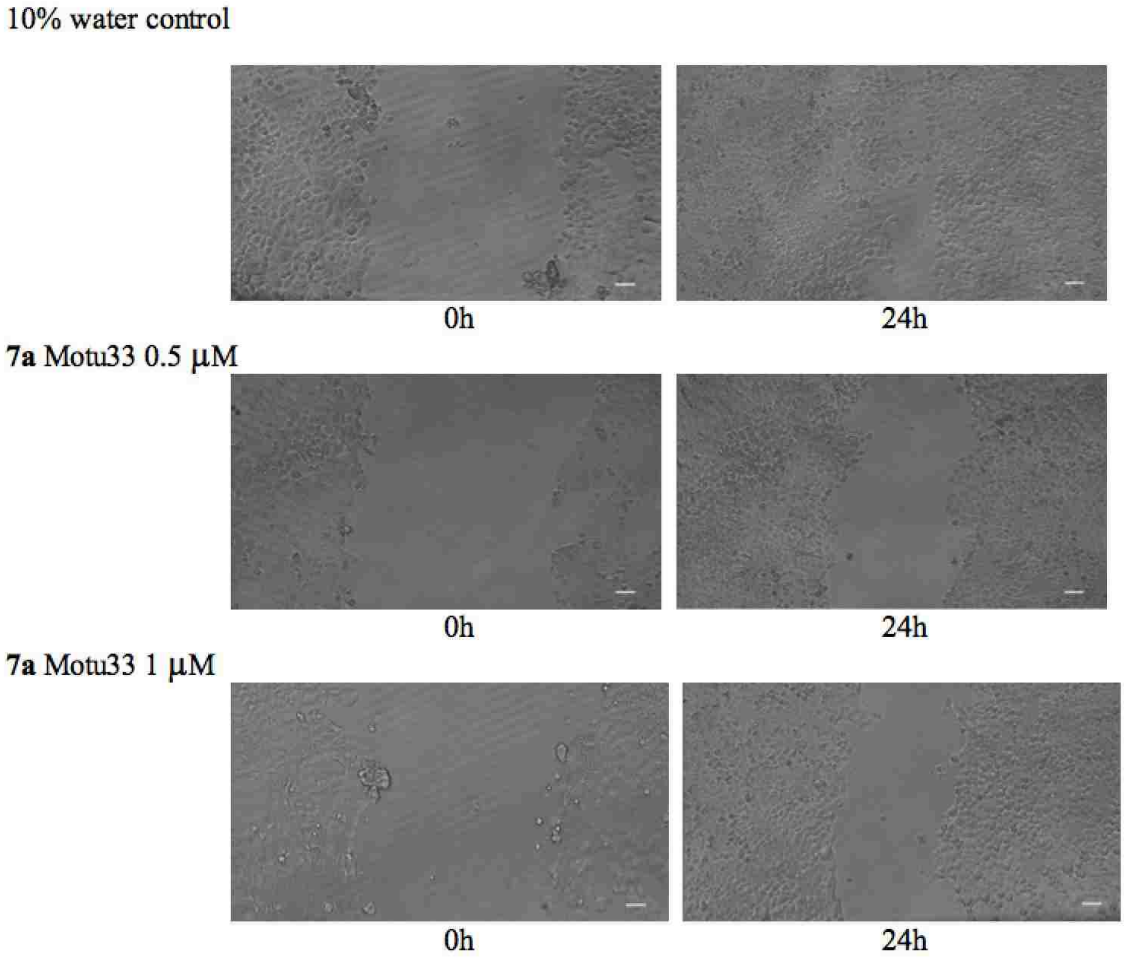


**Figure 10.** L3.6pl Cell Migration studies with **7a** using a scratch assay. L3.6pl cells were incubated with 250 µM AG for 24 h prior to the addition of compound **7a** at 0.5 or 1µM. The white scale bar indicates 20 µm.

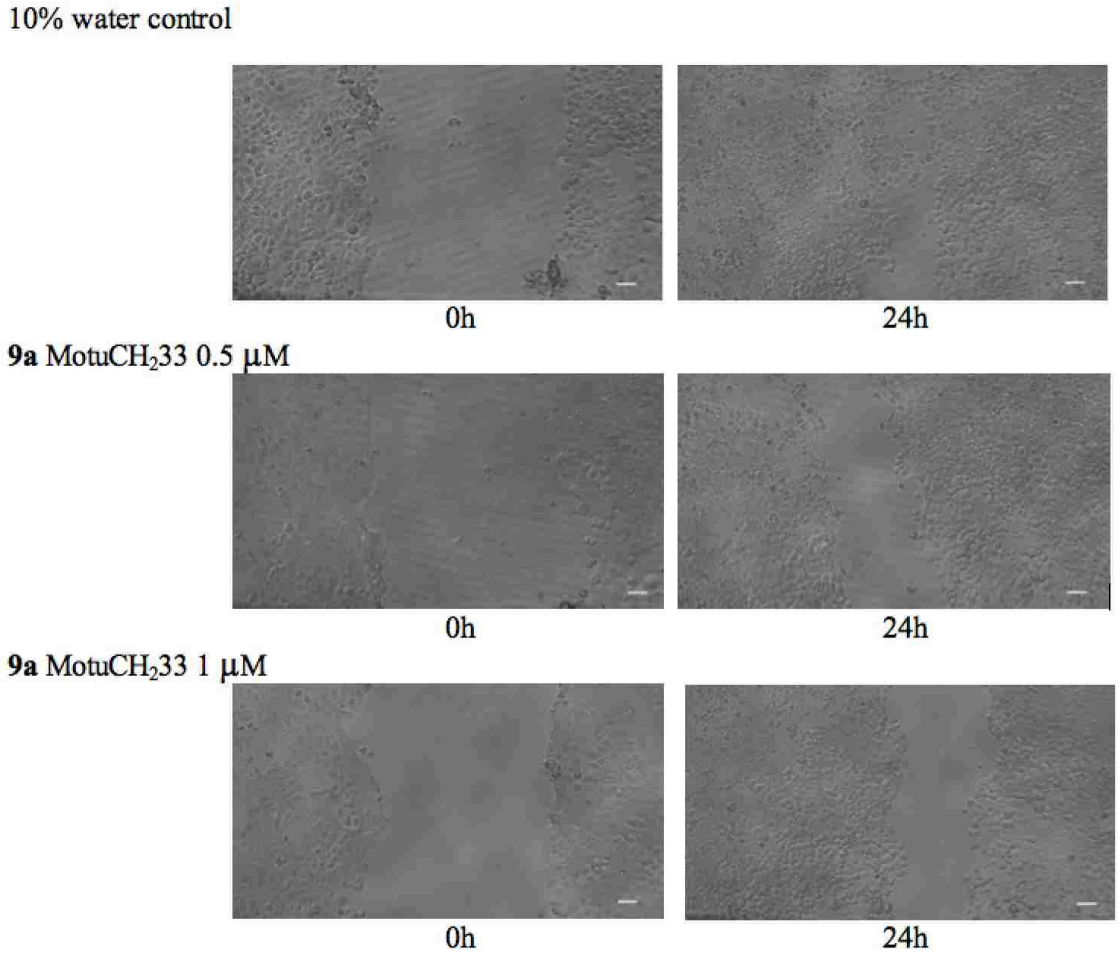


**Figure 11.** L3.6pl Cell Migration studies with **9a** using a scratch assay. L3.6pl cells were incubated with 250 µM AG for 24 h prior to addition of compound (0.5 or 1µM). The white scale bar indicates 20 µm.

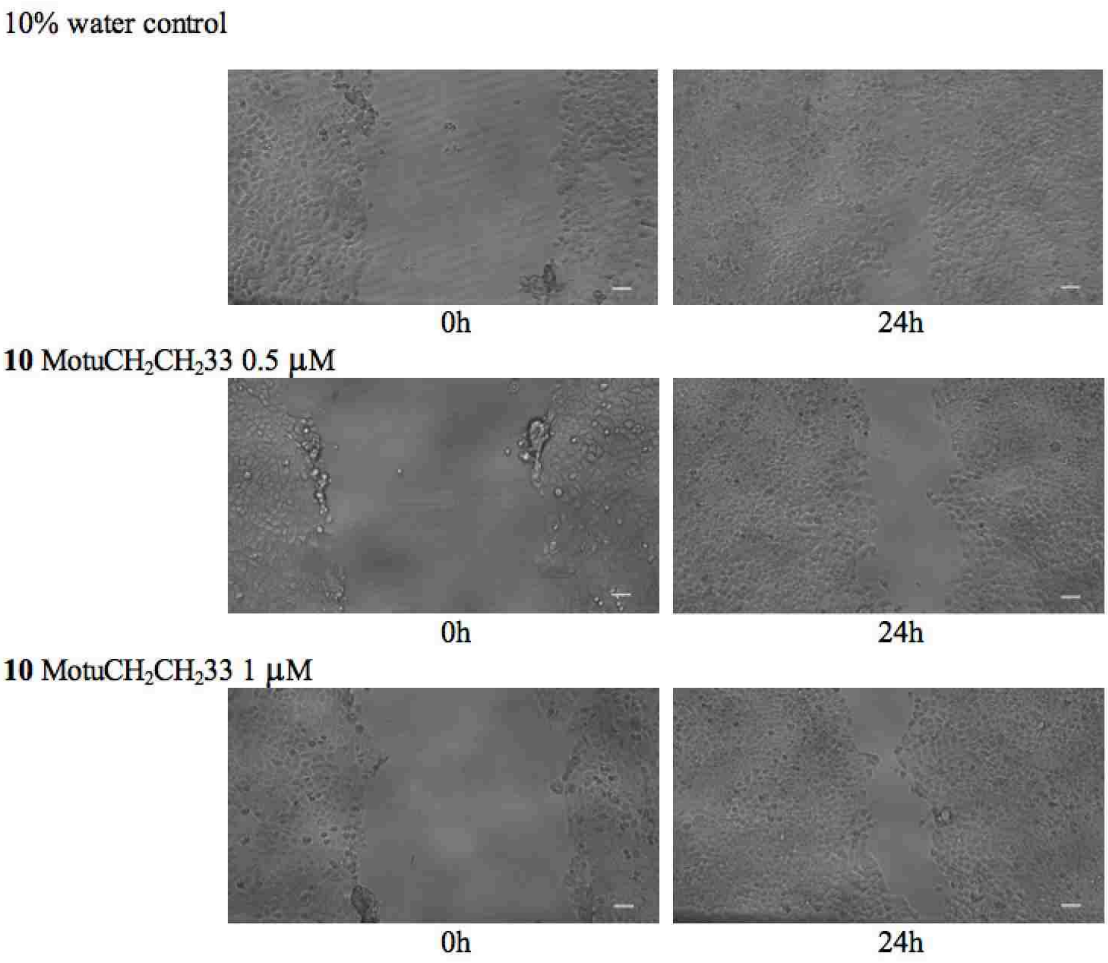


**Figure 12.** L3.6pl Cell Migration with **10** using a scratch assay. L3.6pl cells were incubated with 250 µM AG for 24 h prior to addition of the compound (0.5 or 1µM). The white scale bar indicates 20 µm.

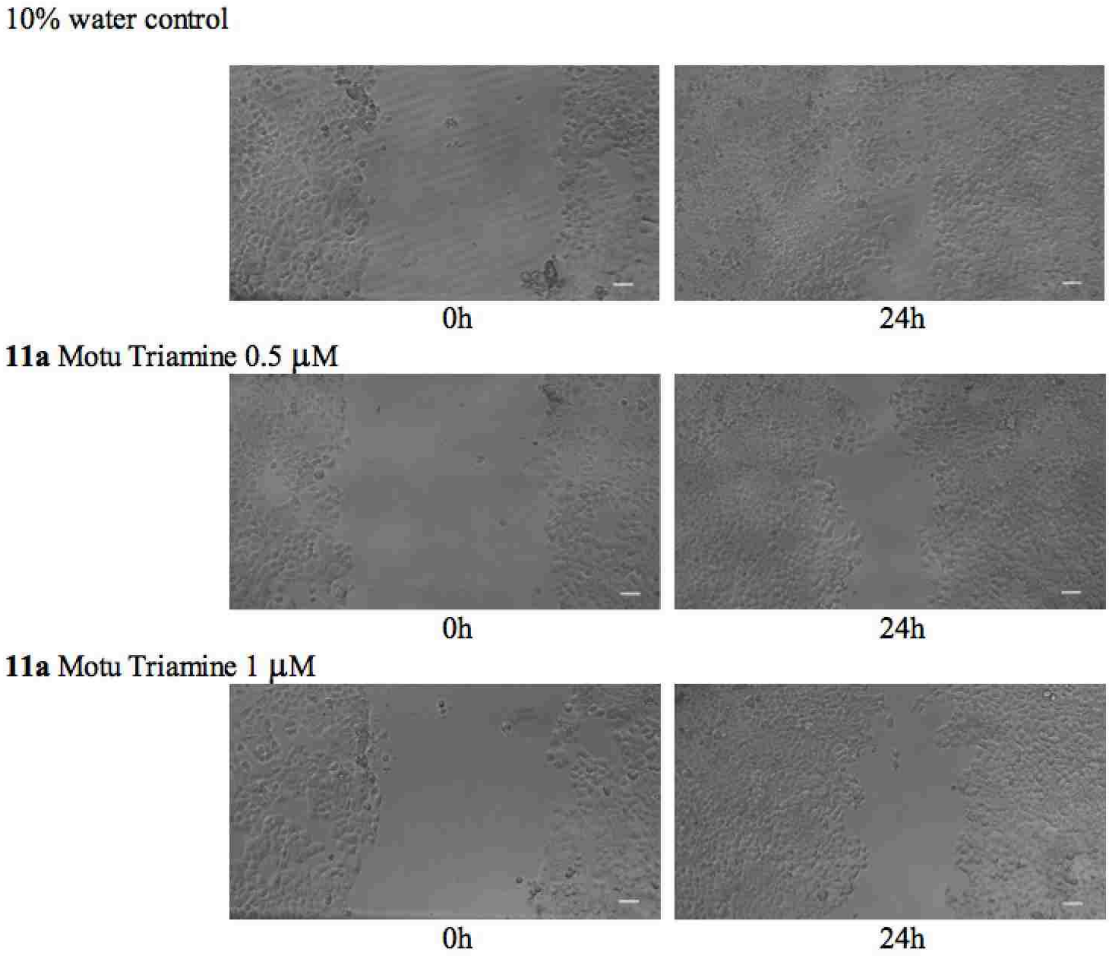


**Figure 13.** L3.6pl Cell Migration with **11a** via scratch assay. L3.6pl cells were incubated with 250 µM AG for 24 hours prior to addition of compound (0.5 or 1µM). The scale bar indicates 20 µm.

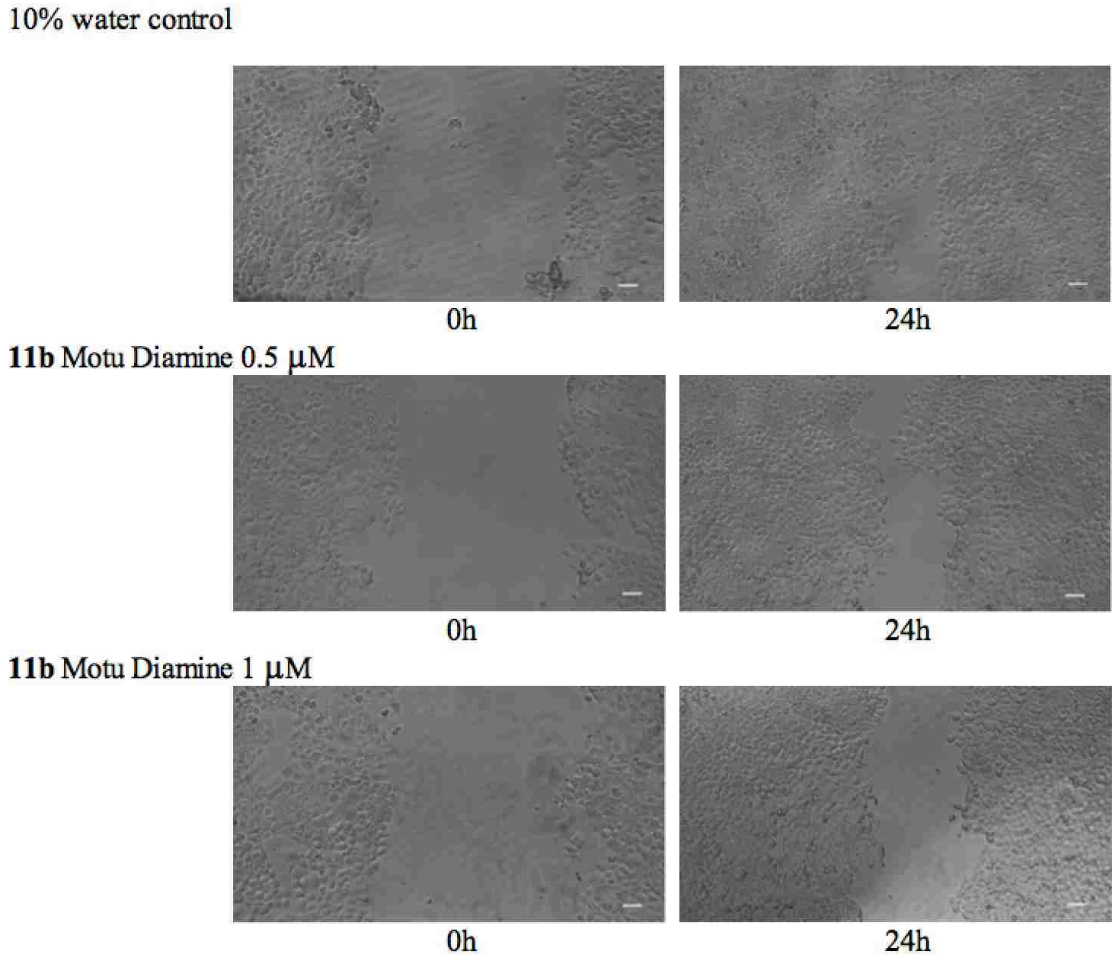


**Figure 14.** L3.6pl Cell Migration with **11b** via scratch assay. L3.6pl cells were incubated with 250 µM AG for 24 hours prior to addition of compound (0.5 or 1µM). The scale bar indicates 20 µm.

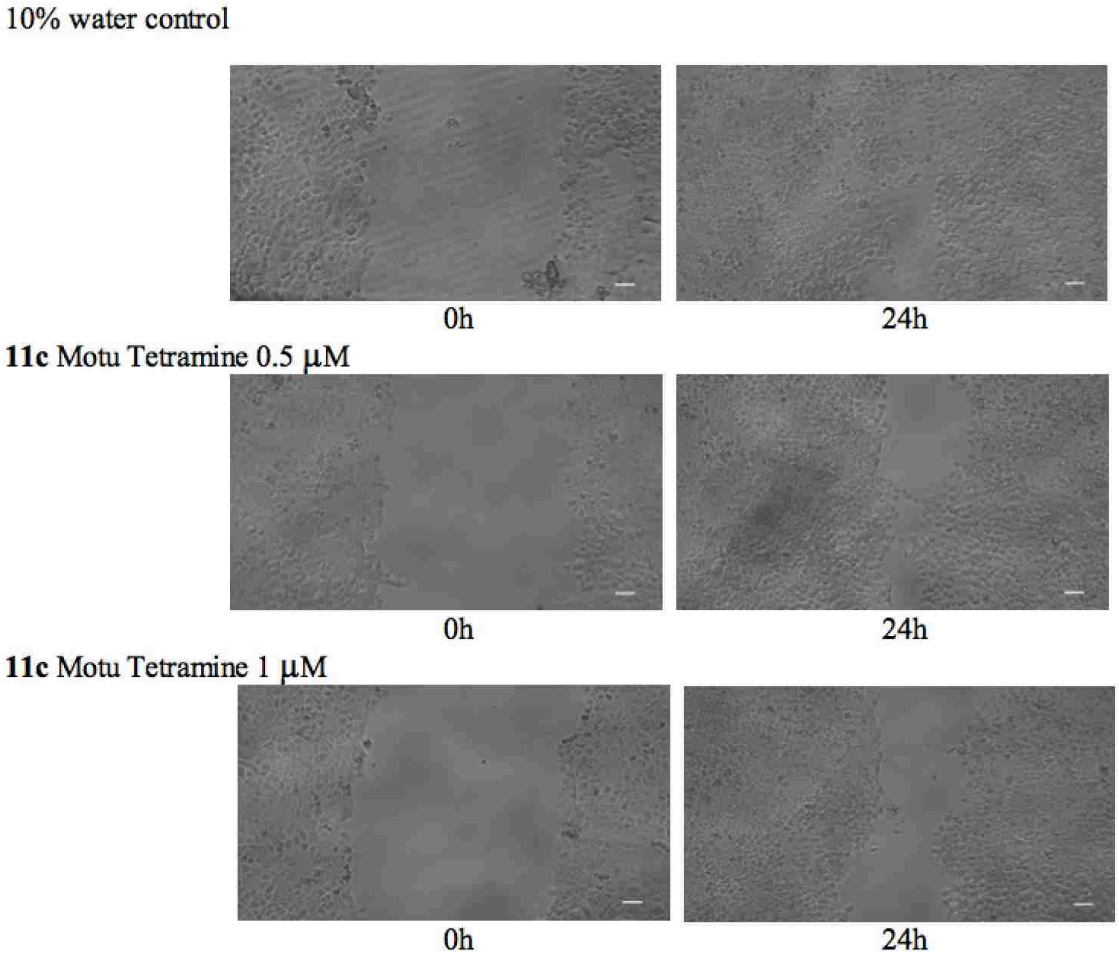


**Figure 15.** L3.6pl Cell Migration with **11c** via scratch assay. L3.6pl cells were incubated with 250 µM AG for 24 hours prior to addition of compound (0.5 or 1µM). The scale bar indicates 20 µm.

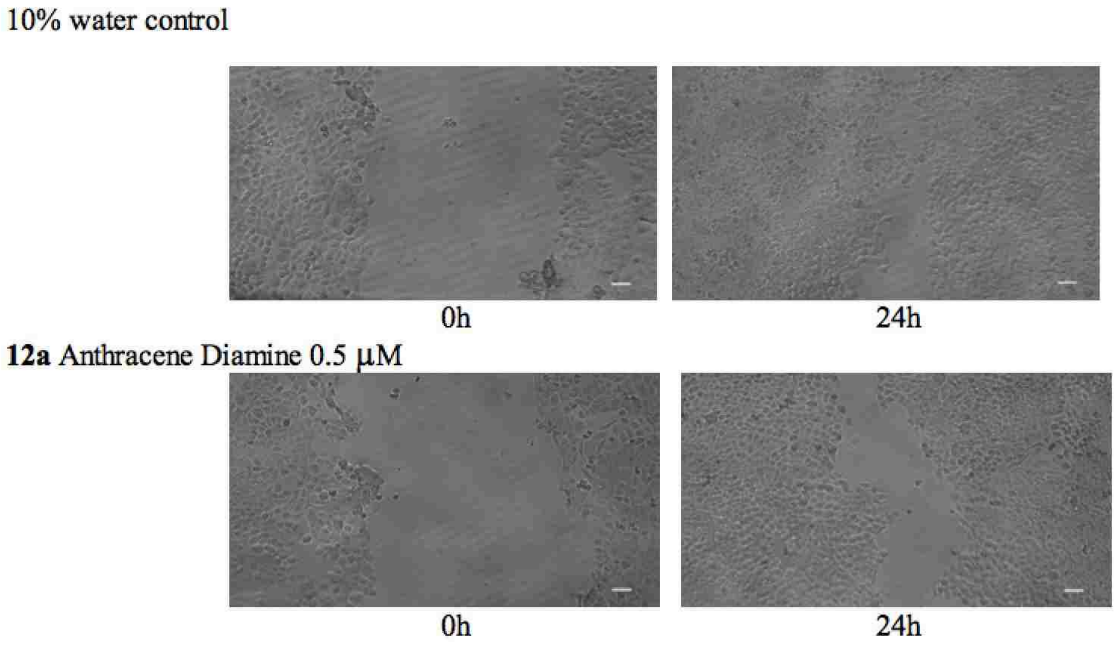


**Figure 16.** L3.6pl Cell Migration with **12a** via scratch assay. L3.6pl cells were incubated with 250 µM AG for 24 hours prior to addition of compound (0.5µM). The scale bar indicates 20 µm.

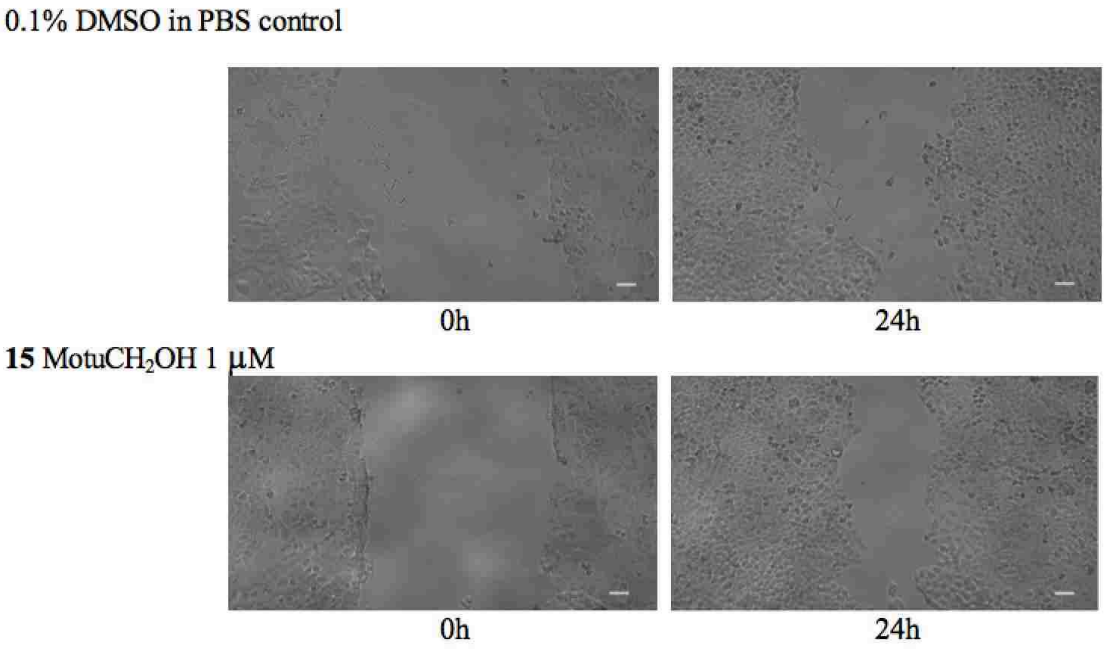


**Figure 17.** L3.6pl Cell Migration with **15** via scratch assay. L3.6pl cells were incubated with 250 µM AG for 24 hours prior to addition of compound (1µM). The scale bar indicates 20 µm.

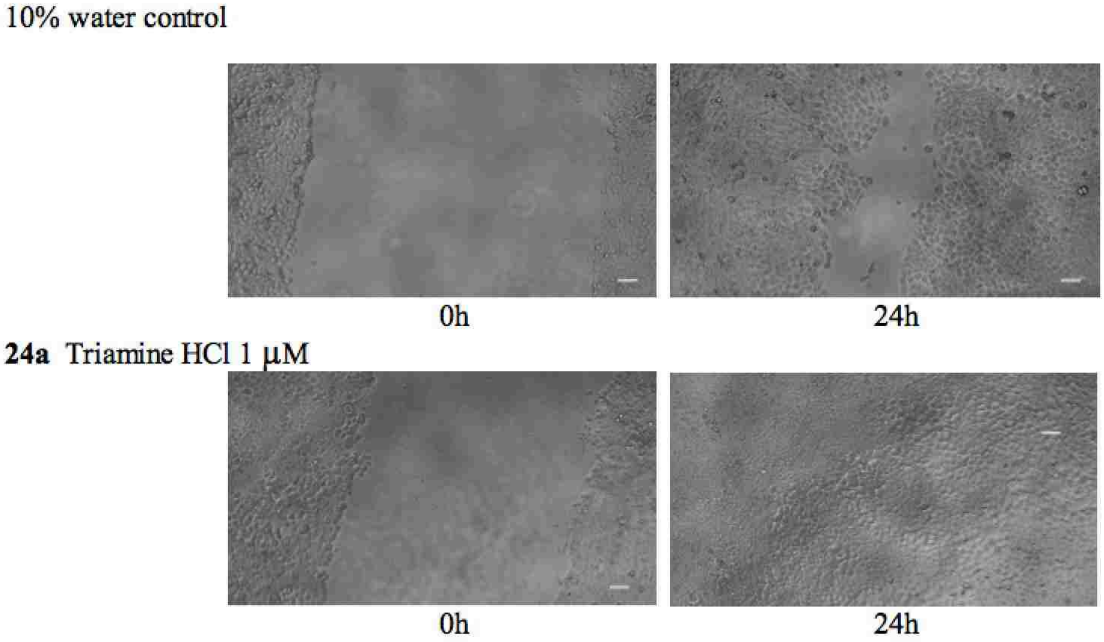


**Figure 18.** L3.6pl Cell Migration with **24a** via scratch assay. L3.6pl cells were incubated with 250 µM AG for 24 hours prior to addition of compound (1 µM). The scale bar indicates 20 µm.

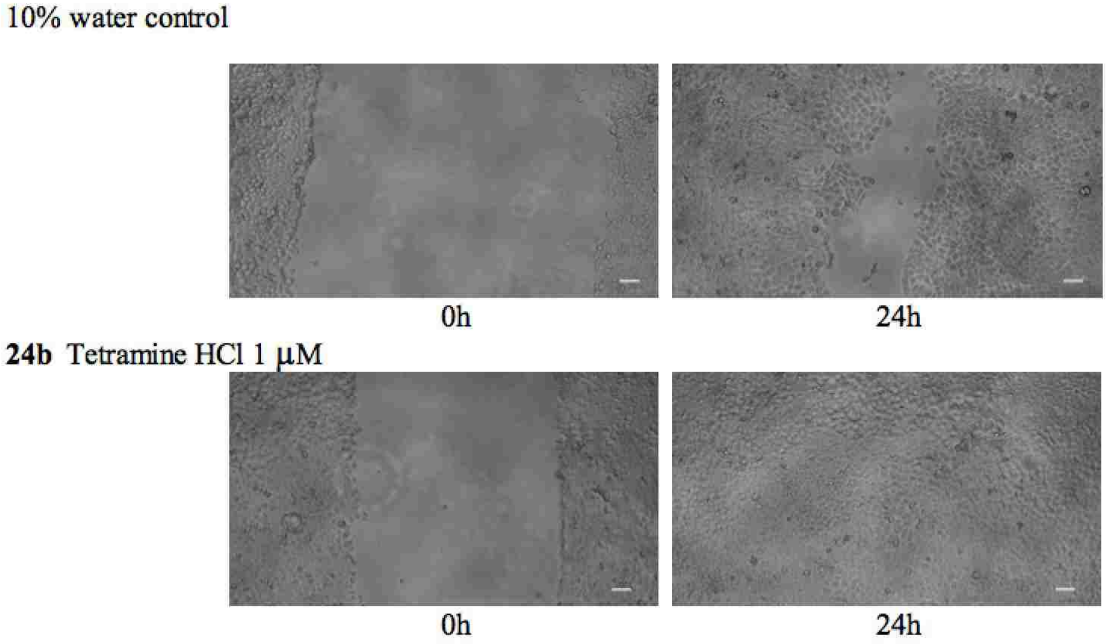


**Figure 19.** L3.6pl Cell Migration with **24b** via scratch assay. L3.6pl cells were incubated with 250 µM AG for 24 h prior to addition of compound (1µM). The scale bar indicates 20 µm.

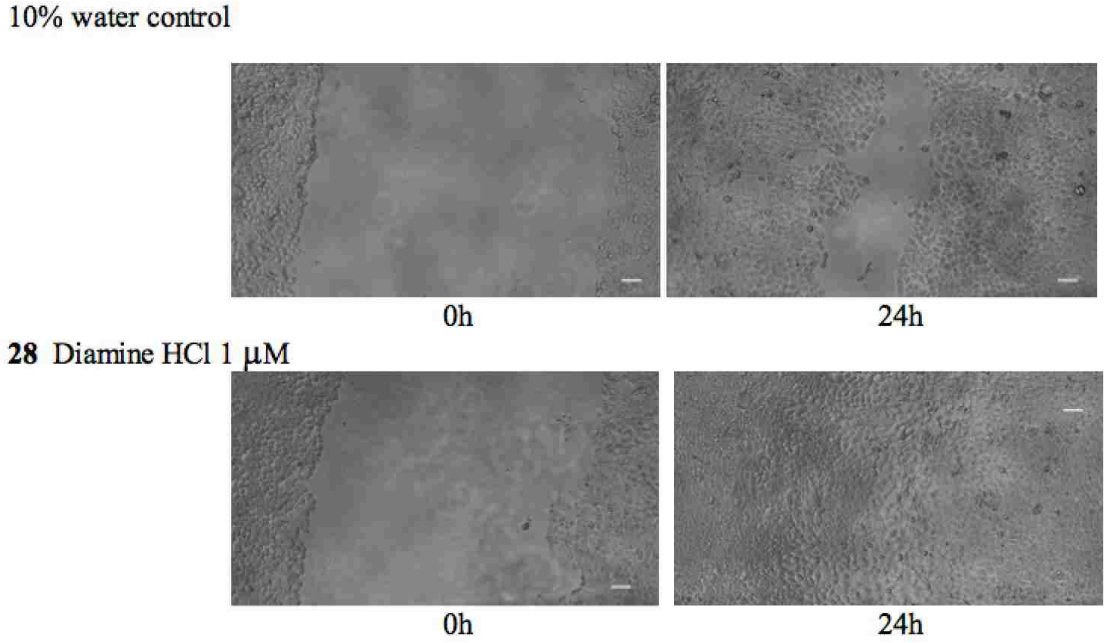


**Figure 20.** L3.6pl Cell Migration with **28** via scratch assay. L3.6pl cells were incubated with 250 µM AG for 24 hours prior to addition of compound (1 µM). The white scale bar indicates 20 µm.

# III. SUMMARY

This project continued the investigation of the synthesis and biological evaluation of extended motuporamine derivatives based on the parent compound, Motu33 (**7a**). Synthetic strategies were developed for the extended derivatives **8a,b** and **9a,b** and involved joining the polyamine component to the macrocycle via reductive amination. A correlation was seen between the distance separating the polyamine $N^1$ nitrogen and the macrocycle. Steric crowding dramatically influenced both synthetic access to the target structures and their observed biological potencies. While the synthesis of **8a,b** resulted in yields of >70%, those yields decreased to <45% for the synthesis of **9a,b**.[5] A different approach was developed for the synthesis of the extended compound **10**, but resulted in a significant reduction in yield.

This project also builds on the performance of compounds **9a,b,** but with the ethylene amine motifs **24a-c**. The synthesis of these motifs was initially attempted with a regioselective protection strategy to mitigate the low yields expected from tertiary amine formation. This occurs when the unprotected secondary amines become alkylated during the coupling step to form undesired tertiary amines. Ironically, due to unanticipated steric issues, the naked non-regioselective approach resulted in the sole productive strategy for accessing the triamine and tetramine motifs, **11c** and **11a**.

Initial chemistries focused on the modification of the bulky macrocycle. The steric hindrance of the bulky 15-membered ring system, seems to be a significant determining factor in synthesizing motuporamine derivatives. Few chemistries were found to react with this large macrocyclic ketone **13**. In a similar vein, the low reactivity of polyamine chains containing nearby bulky Boc

substituents also severely limited the feasibility of the regioselective strategies employed here. In this regard the steric demands of the polyamine component was also important in facilitating reactivity. It was of particular interest that while coupling reactions completely failed, the use of naked motifs **24a-c** was productive. The ethylene amine motifs are shorter than norspermidine (**9a**) and homospermidine (**9b**) and the decrease in distance between nitrogen centers coupled with the closeness in proximity of Boc groups to the reactive site appears to make the nitrogen to carbon coupling reaction especially challenging.

For example, while mesylate **16** and Boc protected tetra-amine **25a** failed to generate the desired product **F**, the mesylate **16** and the naked tetraamine **24b** produced the desired linear motif in fair yields. The non-regioselective approach also worked with bromide **23** and the free base of tetra-amine **24a**. This suggests that once the reactive centers on the macrocycle and the polyamine component are accessible to each other (without bulky Boc substituents or buried in the ring system like ketone **13**) the reaction can occur. Interestingly, diamine **11b** was able to be produced with the starting mono Boc-protected amine **28**, but gave very low yields while the bocylated polyamines **25a,b** were unable to be used to synthesize the desired linear motifs. This suggests that while the Boc group itself may be hindering the reaction by physically blocking access to the reaction site. The steric hindrance is not solely responsible for the low yields because the length of the chain and the $N^1$-nitrogen's ability to react with Boc groups further down the chain is also an issue.

The naked polyamine strategy unexpectedly failed with the pentamine motif and further studies are necessary to develop synthetic strategies for synthesis of these longer polyamine chains. The

non-regioselective naked strategy, while productive, also facilitates a loss in yield due to the formation of tertiary branched byproducts. Interestingly this loss of yield is also seen in the regioselective protection step for the polyamine components (**25a,b**) themselves. While salicylaldehyde selectively protects primary amines, it is not absolute and to a smaller extent, reacts with secondary amines resulting in the eventual formation of undesired polyamines with unprotected secondary amines. While these are easily separated by chromatography, a loss in yield by either method seems to be unavoidable and investigations into synthetic processes that lead to higher yields for these systems is warranted for future two carbon polyamine systems.

The $IC_{50}$ and PTS targeting determinations for the synthesized compounds showed that the two carbon polyamine systems **11a-c** were unable to target the PTS and have similar cytotoxicity profiles as other members of the series. The effect of the reduced distance between nitrogen centers had no significant effect on improving potency when appended to the large macrocycle. Studies with the naked macrocycle **15** or the ethylene motif appended to an anthracene core (**12a**) showed that the motifs responsible for cytotoxicity appear to be both the polyamine and the macrocycle component. Studies with **12a** in particular, showed that PTS targeting with the motuporamines may not be possible due to the complete lack of targeting seen with derivatives containing the macrocycle core. For example, **12a** which contain the same polyamine motif as **11b** had some PTS selectivity, whereas **11b** did not. This suggests that replacing the saturated motuporamine macrocycle with the anthracene core would improve PTS targeting.

The macrocyclic alcohol **15** and the unsubstituted non-native ethylene amine motifs (as their respective HCl salts), were all found to be non-toxic and displayed no anti-migration properties.

Compounds **11a-c**, while unable to improve upon the efficacy of **7a**, still had modest performance as anti-migration compounds. These results suggest that both the polyamine and macrocycle components are required for efficacy. Compound **10** demonstrates that chain extension between these two components has its limits, where extended compounds like **10** showed loss of activity.

In summary, this study revealed that moving the linear triamine message of **7a** away from the ring (as performed here with **9a** and **10**), indeed probed the limits of anti-migration efficacy for this compound class. While **9a** retained the anti-migration properties of **7a**, all efficacy was lost when two methylene spacers were present between the polyamine message and the macrocycle, as in **10**. This study shows that efficacy can be significantly altered by minor structural changes in the motuporamine architecture and suggests that an optimal placement of the appended nitrogen centers is necessary to fully interact with the putative biological target.

# IV. EXPERIMENTAL

## 4.1 Materials.

Silica gel (32-63 μm) and chemical reagents were purchased from commercial sources and used without further purification. All solvents were distilled prior to use or purchased as analytical grade. All reactions were carried out under atmospheric pressure unless an $N_2$ atmosphere was specified. $^{1}H$ and $^{13}C$ spectra were recorded at 500 or 125 MHz, respectively. TLC solvent systems were listed as volume percentages. All tested compounds provided satisfactory elemental analyses.

## 4.2 Biological Studies.

CHO and CHO-MG as well as L3.6pl cells were grown in RPMI 1640 medium with the addition of 10% fetal bovine serum and 1% penicillin/streptomycin and grown at 37°C under a humidified 5% $CO_2$ atmosphere. CHO and CHO-MG cells were seeded at 10,000 cells/mL while L3.6pl cells were grown at 5,000 cells/mL for cytotoxicity studies and 55,500 cells/mL for anti-migration experiments. Cells were treated with aminoguanidine (AG, a known inhibitor of polyamine oxidase present in bovine serum) through addition to the growth medium at a concentration of 1mM for CHO/CHO-MG cells and 250 μM for L3.6pl cells, 24 h prior to drug addition. The presence of AG was important as the compounds tested contained polyamines within their structure and active amine oxidase could cause degradation during the course of the assay.

**$IC_{50}$ determinations.** Cell viability was assessed in sterile 96-well plates (Costar 3599, Corning). Drug solutions (10 μL/well) in their listed concentrations were added after overnight incubation (90 μL/well cell suspension in media with AG). After incubation with the drug for 48 h, cell viability was assessed through a metabolic assay by measuring formazan formation from 3-

(4,5-dimethylthiazol-2-yl)-5-(3-carboxymethoxyphenyl)-2-(4-sulphenyl)-2H-tetrazolium (MTS) via absorbance (490 nm) with a SynergyMx Biotek microplate reader.

**Anti-Migratory Assay.** Anti-migratory properties were assessed in sterile 96-well plates (Costar 3599, Corning) Drug solutions (10 µL/well) in their listed concentrations were added after overnight incubation (90 µL/well cell suspension in media with AG). 24 h after seeding, a channel was scratched laterally across the plate using a 100 µL pipette tip. The cells were then washed with PBS (1X, 100 µL) and media was replaced (90 µL/well cell suspension in media with AG) and the respective drugs solutions were added (10 µL/well) in quadruplicate. After 24 h, cells were imaged (Nikon TE 200) with a 10X objective. To image the same location at two time points, images were taken next to a line bisecting each well perpendicular to the channel scratched. To standardize each image, all images were cropped in image J to 700x1280 pixels. Cell migration was assessed by measuring the area devoid of cells over a 24 h period and calculated as the following:

% Cell Migration at 24h = ((Area with no cells at 0h)-(Area with no cells at 24h))/Area with no cells at 0h x 100%.

% Cell Migration normalized to control = % Migration with drug at 24h/ % Migration of control at 24h * 100

% Cell inhibition at 24h =(1-(% Migration with drug at 24h/% Migration of control at 24h))*100

### 4.3 Synthetic Procedures and Characterization

**N-(3-Amino-propyl)-N'-(2-cyclopentadecylethyl)-propane-1,3-diamine 10.** Compound **21** was dissolved in 200 proof EtOH (1 mL) and slowly added dropwise to 4M HCl (1.56 mL) at 0$^{o}$C.

After the addition was complete, the solution was brought to rt and stirred for 24 h. It was then concentrated under reduced pressure to yield the product **10**. (20 mg, 0.042 mmol, 74% yield). **10:** $^{1}$H NMR ($D_2O$): δ 3.10(m, 10H, $J^{3}_{H-H}$ = 6.1Hz), 2.09(m, 4H), 1.58(m, 2H), 1.45(m, 1H), 1.29 (s, 28H); $^{13}$C NMR ($CDCl_3$): δ 45.89, 43.89, 36.80, 33.65, 33.49, 31.28, 30.92, 30.27, 28.69, 28.07, 27.44, 27.41, 26.46, 25.77, 25.60, 23.98, 23.48. HRMS calc for $C_{23}H_{49}N_3$ (M+H) 367.392, found 367.3926. Compound **10** was 93% pure by HPLC analysis [UV detection at 210 nm showed a major peak eluted (~5 min) on a $C_{18}$ column using 60% acetonitrile/an aqueous heptane sulfonate buffer at pH 3.8 with a flowrate of 1 mL/min].

**N-(2-Amino-ethyl)-N'-cyclopentadecylmethyl-ethane-1,2-diamine 11a.** Compound **27a** (96 mg, 0.153 mmol) was then dissolved in EtOH (3 mL) and 4M HCl in EtOH (3mL) while stirring overnight at rt. The solvent was then removed under reduced pressure to give a white solid **11a** (60 mg, 0.138 mmol, 90% yield). **11a.** $^{1}$H NMR ($D_2O$): δ 3.45 (m, 8H), 3.02 (br s, 2H), 1.83 (br s, 1H), 1.32 (br s, 28H); $^{13}$C NMR ($D_2O$): δ 55.57, 47.12, 46.04, 37.92, 36.74, 31.84, 29.29, 28.94, 28.88, 28.55, 26.09. HRMS for $C_{20}H_{43}N_3$ (M+H) Theory: 325.3439 Found: 325.3457. Anal Calcd $C_{20}H_{46}Cl_3N_3$ 0.56 $H_20$: Theory: C 53.98, H 10.67, N 9.44 Found: C 54.38, H 10.68 N 9.05

**N1-Cyclopentadecylmethyl-ethane-1,2-diamine 11b**. Compound **27c** (61mg, 0.16 mmol) was dissolved in EtOH (1 mL) and 4M HCl/EtOH (1mL) was added dropwise and stirred at rt overnight. The solvent was then removed under reduced pressure for a white solid **11b** (50 mg, 0.157 mmol, 98% yield). **11b**: $^{1}$H NMR ($D_2O$): δ 3.39 (br s, 4H), 3.01 (br s, 2H), 1.82 (br s, 1H), 1.33 (br s, 28H); $^{13}$C NMR ($D_2O$): δ 55.48, 47.30, 37.97, 36.73, 31.84, 29.29, 28.90, 28.56, 26.09.

Anal Calcd for $C_{18}H_{40}Cl_2N_2$ 0.05 $H_20$: theory C 60.83, H 11.34, N 7.88; found C 61.12, H 11.44, N 7.72.

**N-[2-(2-Amino-ethylamino)-ethyl]-N'-cyclopentadecylmethyl-ethane-1,2-diamine 11c.** Removal of the Boc groups of **27b** was performed in 4M HCl/EtOH by first dissolving the product in 200 proof EtOH (5 mL) which required sonication. 4M HCl in EtOH (5 mL) was then added dropwise while stirring. Reaction proceeded overnight, the solvent was then removed under reduced pressure for a weight of the final product, a white solid, **11c** (252 mg, 0.49 mmol, 98% yield). **11c**: $^1$H NMR ($D_2O$): δ 3.51 (m, 12H), 3.04 (br s, 2H), 1.86 (br s, 1H), 1.33 (s, 28H); $^{13}$C NMR ($D_2O$): δ 55.43, 47.07, 46.44, 46.15, 38.03, 36.64, 31.79, 30.50, 29.42, 29.05, 28.80, 26.08. HRMS $C_{22}H_{48}N_4$ (M+H) Theory: 368.3878, Found: 368.3879; Anal Calcd $C_{22}H_{52}Cl_4N_4$ Theory: C 51.36, H 10.19, N 10.89 Found: C 51.35, H 10.46, N 10.62.

**N1-Anthracen-9-ylmethyl-ethane-1,2-diamine 12a**. To a stirred solution of monoBoc diamine **28** (268 mg, 1.67 mmol) in 25% methanol/DCM (10 mL) was added a solution of 9-anthraldehyde (289 mg, 1.40 mmol) in 5 mL of 25% methanol/DCM under $N_2$. The solution was allowed to stir at rt overnight until imine formation was complete (monitored by $^1$H NMR). The solvent was removed in vacuo and the crude imine **29** was re-dissolved in 50% Methanol/DCM and cooled to 0$^o$C. $NaBH_4$ (167 mg, 4.28 mmol) was added and the mixture was stirred at rt overnight. The solvents were removed under vacuum, and the residue was redissolved in DCM and washed with saturated $Na_2CO_3$. The organic layer was separated, dried over anhydrous $Na_2SO_4$, filtered and concentrated to give a solid (521 mg crude) which was purified by 5% MeOH/$CHCl_3$ to yield 412 mg (1.18 mmol) of the desired adduct **30** (80% yield). Debocylation with 2 mL of ethanol and 2

mL of 4M HCl gave the product (340 mg, 1.05 mmol, 89% yield) for an overall yield of 75%. **12a:** $^{1}$H NMR ($D_2O$): δ 8.40 (s, 1H), 8.05 (m, 2H), 7.63 (m, 2H), 7.53 (m, 2H), 4.95 (s, 2H), 3.55 (m, 2H), 3.35 (m, 2H); $^{13}$C NMR (25% $d_6$-DMSO in $D_2O$): δ 133.4, 132.8, 131.9, 130.3, 128.3, 125.4, 124.3, 47.3, 46.0, 38.26

**Methylenecyclopentadecane 14**.To a stirred solution of methyltriphenyl phosphonium iodide (27.17g, 66.9 mmol) in freshly distilled anhydrous THF (300 mL) was added n-Butyl Lithium (n-BuLi, 66.9 mmol, 1.6M in hexanes) dropwise under $N_2$ via syringe at 0$^{o}$C. The solution immediately turned a dark brown-reddish color and the contents of the solution dissolved. Prior to addition of n-BuLi, attempts were made to dissolve the $MePh_3PI$ in THF but dissolution only occurred upon n-BuLi addition. After the Wittig reagent had formed (20 minutes), ketone **13** (5 g, 22.3 mmol) was added in a minimal amount of THF followed by an additional 5.0 g of ketone (for a total of 44.6 mmol). The reaction was allowed to warm to room temperature and stir overnight. The reaction was monitored for the presence of ketone **13** by TLC (5% ethyl acetate/hexane with $KMnO_4$ staining and by $^{1}$H NMR). Additional butyl lithium (10 mL) was added under the same conditions after 48 h after NMR showed only 45% conversion. An additional 10 mL of BuLi was added at the 72 h time point. After 96 h the reaction was worked up by quenching excess BuLi at 0$^{o}$C with deionized water. The contents were then filtered with minimal amounts of white solid present and the THF was removed under reduced pressure revealing a biphasic red-yellow mixture. The mixture was redissolved in DCM, the layers were separated, the aqueous layer was washed with DCM (3x) and then the DCM was removed to yield a biphasic crude with a red solid and a

yellow oil (30.9 g). The red solid was assumed to be the triphenyl phosphonium oxide. The residue was then washed 3x with hexanes and then the solvent was removed to reveal a yellow non-viscous oil (10.7 g). The crude mixture was then separated by column chromatography (10% DCM, hexanes) to yield alkene **14** as a colorless oil. (4.9 g, 22.4 mmol, 50% yield).

**Cyclopentadecylmethanol 15**.[5] Alkene **14** (4.97 g, 22.4 mmol) was added dropwise at 0°C to a $BH_3$-THF solution (67 mmol, 5.7 g, 14.9 mL). The reaction was stirred for 1 h at 0°C and then allowed to warm to room temp and stir for 2 h. The reaction progress was monitored for disappearance of the alkene and then the excess $BH_3$ was quenched with deionized water (31 mL) after pre-cooling the mixture to 0°C. 3M NaOH (31 mL) followed by 30% $H_2O_2$ (31 mL) was added over the course of 1 h at 0°C for the oxidation step in the workup and the reaction was stirred overnight. $K_2CO_3$ (300 mg: 2.17 mmol) was added and then the THF was removed under reduced pressure. DCM was then added, the layers were separated, and the aqueous layer was extracted three times with DCM, the organic layers were pooled, dried over anhydrous $Na_2SO_4$, filtered and concentrated to give a viscous light yellow oil (5.2g). TLC (20% Hexanes/DCM, visualization with phosphomolybdic acid, $R_f$ 0.3). Column (100% DCM) was run to separate the crude for a clear oil (3.9 g, 16.2 mmol, 73% yield). $^1$H NMR analysis matched the literature spectrum for this compound.[5]

**Methanesulfonic acid cyclopentadecylmethyl ester 16**. Alcohol **15** (998 mg, 4.15mmol) was added to TEA (643 µL, 4.58mmol) in DCM. Methanesulfonyl chloride was then dispensed by syringe (355 µL, 4.58mmol) at 0 °C and stirred overnight at rt. The reaction was monitored by

TLC (100% $CH_2Cl_2$, $R_f$ mesylate **16** :0.63; $R_f$ alcohol **15**: 0.37) and then quenched with 1M NaOH (2 mL). The organic phase was washed three times with 1M NaOH (5 mL), then separated, dried over anhydrous $Na_2SO_4$, filtered and concentrated to give the mesylate **16** as a yellow oil (1.12 g, 3.52 mmol, 85% yield). $^1$H NMR ($CDCl_3$): δ 4.15 (d, 2H, $J^3_{H-H}$6.1Hz), 3.0 (s, 3H), 1.34 (br s, 29H).

**Cyclopentadecyl-acetonitrile 17.** KCN (3.09 g, 47.6 mmol), 18-crown-6 ether (145 mg, 0.48 mmol), and dry $CH_3CN$ (48 mL) were added to mesylate **16** (1.69 g, 5.29 mmol) and the reaction was refluxed overnight. The reaction was monitored by TLC (70%Hexanes/$CH_2Cl_2$, $R_f$=0.28) and then volatiles were removed, the residue was redissolved in DCM and washed with water. The layers were separated, the organic layer was dried over anhydrous $Na_2SO_4$, filtered and concentrated to give a yellow crude oil (1.29g, 5.17mmol) which was then purified by column chromatography (70% Hexanes/$CH_2Cl_2$) and concentrated under reduced pressure and subjected to high vacuum yielding a colorless oil (0.92g, 3.69 mmol, 82% yield, 91% conversion). Mesylate **16** was recovered as a white crystalline solid (0.15 g, 0.47 mmol, 9% recovery) in (50% Hexanes/$CH_2Cl_2$, $R_f$ 0.3). $^1$H NMR: δ 2.30 (d, 2H, $J^3_{H-H}$6.6Hz), 1.80 (m, 1H), 1.34 (br s, 28H). $^{13}$C NMR: δ 119.2, 33.7, 31.8, 27.1, 26.8, 26.7, 26.6, 26.5, 24.3, 22.9. HRMS for $C_{17}H_{31}N$ (M+H):250.2535, found 250.2527. Anal. $C_{17}H_{31}N$: Theory: C 81.86, H 12.53, N 5.62 Found: 82.04, 12.63, N 5.51.

**2-Cyclopentadecyl-ethylamine 18.** Nitrile **17** (412 mg, 1.64 mmol) was dissolved in dry THF (5 mL, 55.5 mmol) and added dropwise to a stirred solution of $LiAlH_4$ (207 mg, 5.46 mmol) in THF (5 mL) at 0$^o$C. The reaction was then warmed to rt and refluxed overnight. The reaction was

monitored for the disappearance of the nitrile with TLC (1% $NH_4OH$/15%MeOH/$CH_2Cl_2$, $R_f$ Amine=0.28, $R_f$ Nitrile=0.55). After disappearance of the starting material was confirmed by TLC, the reaction mixture was concentrated and redissolved in DCM. The organic phase was washed with a solution of water (0.9 mL) and 5M NaOH (0.15 mL), and the organic layer was separated, dried over anhydrous $Na_2SO_4$, filtered and concentrated under reduced pressure to yield a colorless oil. Column chromatography (85% $CH_2Cl_2$, 15% Methanol, 1 drop $NH_4OH$) provided amine **18** (203 mg, 0.80 mmol, 49% yield). **18**: $^1$H NMR: δ 2.72 (m, 2H), 1.41 (m, 4H), 1.34 (m, 28H); $^{13}$C NMR: δ 40.00, 38.86, 34.17, 32.42, 27.58, 26.93, 26.59; HRMS for $C_{17}H_{35}N$ (M+H):253.2789, found 253.277; Anal. $C_{17}H_{35}N$ 0.2 $H_20$ Theory: C 79.43, H 13.88, N 5.45 Found: C 79.24, H 13.94, N 5.37.

**Methanesulfonic acid 3-[tert-butoxycarbonyl-(3-tert-butoxycarboynlamino-propyl)-amino]-propyl ester 20**. DiBoc 33 triamine alcohol **19**[10b] (3-tert-Butoxycarbonylaminopropyl)-(3-hydroxypropyl) carbamic acid tert-butyl ester, 100mg, 0.3mmol) was added to TEA (127 µL, 0.9 mmol) and $CH_2Cl_2$ (3 mL). Methane sulfonyl chloride (34.9 µL, 0.45 mmol) was added dropwise at 0 $^o$C via syringe under a nitrogen atmosphere. Once the addition was complete, the syringe was rinsed with $CH_2Cl_2$ (0.6 mL). Reaction progress monitored by TLC (5% MeOH/$CH_2Cl_2$, $R_f$ alcohol 0.25; $R_f$ mesylate 0.37). After 24 h, 4M NaOH (5 mL) was added with stirring. The organic layer was separated, dried over anhydrous $Na_2SO_4$, filtered and concentrated under reduced pressure to yield mesylate **20** (99 mg, 0.24 mmol, 80% yield).

**19:** $^1$H NMR ($CD_3OD$): δ 3.55 (t, 2H), 3.28 (t, 2H), 3.24 (t, 2H), 3.04 (q, 2H), 1.62-1.81 (m, 4H), 1.44 (s, 9H), 1.42 (s, 9H).[10b]

**20:** $^{1}$H NMR ($CDCl_3$): δ 4.25 (t, 2H, $J^{3}_{H-H}$= 6.2Hz), 3.28 (br s, 4H), 3.11 (br s, 2H), 3.02 (s, 3H), 1.99 (m, 2H), 1.67 (m, 2H), 1.56 (s, 3H), 1.47 (s, 9H), 1.44 (m, 9H)

**(3-tert-Butoxycarbonylamino-propyl)-[3-(2-cyclopentadecylethylamino)-propyl]-carbamic acid tert-butyl ester 21**

2-Cyclopentadecyl-ethylamine **18** (0.07g, 0.28 mmol) was dissolved in $CH_2Cl_2$ and added to $Na_2CO_3$ (75 mL, 1.79 mmol) while stirring at rt. Di Boc Mesylate **20** (121mg, 0.2957mmol) was dissolved in $CH_2Cl_2$ (1 mL) and added to the solution dropwise. The reaction was stirred for 48 h and was monitored by TLC (10% MeOH/$CH_2Cl_2$; $R_f$ 0.34).

After the reaction was complete, $CH_2Cl_2$ (2 mL) was added and the solution was washed three times with aq. $Na_2CO_3$ (10% by w/v, 3 mL). The organic layer was separated, dried over anhydrous $Na_2SO_4$, filtered, and concentrated under reduced pressure to yield a crude yellow oil (248 mg). Column chromatography (10% MeOH/$CH_2Cl_2$, followed by 10% MeOH/1% $NH_4OH$, $CH_2Cl_2$) provided the crude as a clear oil (60 mg, 0.106 mmol, 38% yield) with a self-cyclized starting material **22** which was separated by running a second column (4.5% MeOH/$CH_2Cl_2$) to yield the byproduct **22** (27.3 mg, 0.0572 mmol, 21% yield) and the desired product **21** (32 mg, 0.056 mmol, 20% yield) as a yellow oil.

**21**: $^{1}$H NMR ($CDCl_3$): δ 3.31(br s, 2H), 3.16 (br s, 2H), 3.03 (br s, 2H), 2.84 (br s, 4H), 2.06 (m, 2H), 1.65 (m, 4H), 1.40 (s, 18H), 1.36 (br s, 29H); $^{13}$C NMR: δ 46.89, 44.97, 37.80, 34.55, 32.38, 31.26, 29.69, 29.06, 28.33, 27.46, 26.76, 26.60, 26.50, 24.98, 24.25, 22.67. HRMS for $C_{33}H_{65}Cl_3N_3O_4$ (M+H) 567.4973, found 567.4975.

**22**: $^{1}$H NMR ($CDCl_3$): δ 4.25 (m, 2H), 3.30 (br s, 4H), 3.11 (s, 2H), 2.0 (m, 2H), 1.66 (m, 2H), 1.46 (s, 18H).

**Bromomethyl-cyclopentadecane 23.** The alcohol **15** (250 mg, 1.04 mmol) was placed under an inert atmosphere. Phosphorus tribromide (0.52 mmol, 49 µL) was added by syringe. The reaction immediately turned yellow and started bubbling and was stirred at rt for 1.5 h. Hexane (3 mL) was added and the reaction was refluxed at 69$^{o}$C for another 1.5 h. The reaction turned a brownish yellow color. The vessel was rinsed and the brown crude (0.48g) was isolated. Column chromatography (100% n-hexane) was performed (with a 30:1 ratio of silica gel: crude) due to the large $R_f$ difference ($R_f$ **15**: 0, $R_f$ **23**: 0.8). Visualization of the TLC plate using phosphomolybdic acid and heat provided a convenient monitoring tool. The product **23** was isolated and concentrated under reduced pressure to yield a clear oil (0.21g, 0.695 mmol, 67% yield). **23**: $^{1}$H NMR ($CDCl_3$): δ 3.38(d, 2H, $J^{3}_{H\text{-}H}$ = 6.1Hz), 1.72 (m, 1H), 1.38 (br s, 28H); $^{13}$C NMR ($CDCl_3$): δ 40.39, 38.65, 31.17, 27.25, 26.87, 26.64, 26.53, 24.59.

**Synthesis N-(2-Amino-ethyl)-N'-[2-(cyclopentadecylmethyl-amino)-ethyl]-ethane-1,2-diamine 25a.** The free base of 2,2-tetraamine **24b** was generated using N,N'-Bis-(2-amino-ethyl)-ethane-1,2-diamine (3.00 g, 10.27 mmol, Sigma-Aldrich) with 4 equivalents of aq. NaOH (1M, 41 mmol, 41 mL). The water was removed and then dried by adding and removing benzene under reduced pressure to remove the excess water. Anhydrous $Na_2SO_4$ (8 equivalents, 82.3 mmol, 11.69 g) was added to a dried vessel with 25% MeOH/$CH_2Cl_2$ (50 mL). One equivalent of salicyclaldehyde (10.27 mmol, 1.10 mL) in MeOH (10 mL) was then added dropwise over 2 h at 0$^{o}$C while stirring. Upon addition of the reagent, the reaction immediately turned yellow. Imine

formation was monitored by $^{1}$H NMR. After imine formation, the additional reactive centers were protected with di-*tert*-butyl dicarbonate (3 equiv., 30.87 mmol, 6.74 g) and stirred overnight. The reaction progress was checked by $^{1}$H NMR for full bocylation and additional di-*tert*-butyl dicarbonate was then added (0.3 equiv., 0.67g) while heating at 40$^{o}$C overnight to drive the reaction to completion. The reaction was again checked for N-bocylation and confirmed to be complete. Then $MeONH_2 \cdot HCl$ (10.27mmol, 0.8578g) was added in 1.5 mL of TEA. Note: $MeONH_2$ HCl was initially not soluble in the TEA, which was used to generate the free base. Upon addition of 25%MeOH/ $CH_2Cl_2$ (5 mL) the methoxyamine easily dissolved and the TEA/MeOH/$CH_2Cl_2$ solution was then added dropwise to the stirring solution. Imine cleavage was monitored by NMR. Note: an oxime byproduct is formed via methoxyamine exchange with the imine. The MeOH was then removed under reduced pressure, the residue was re-dissolved in $CH_2Cl_2$ and then washed with saturated $Na_2CO_3$ (22g/100mL solution, 10 mL). The aqueous layer was extracted three times with $CH_2Cl_2$ and then the organic layer was concentrated under reduced pressure to yield a yellow oil (3.65g). The product was separated from the crude by column chromatography (1% $NH_4OH$/10%MeOH/$CH_2Cl_2$, Product $R_f$ **25a**: 0.65). The product **25a** eluted as a light yellow solid (1.48g, 3.31mmol, 32% yield). **25a**: $C_{21}H_{42}N_4O_6$ $^{1}$H NMR ($CDCl_3$): δ 3.31 (br s, 10H), 2.84 (br s, 2H), 1.79 (br s, 2H), 1.46 (br s, 27H); $^{13}$C NMR ($CDCl_3$): δ 155.52, 76.59, 46.24, 45.45, 40.24, 39.08, 28.06; HRMS for $C_{21}H_{42}N_4O_6$ (M+H) Theory 446.3121, Found 446.3104; Anal $C_{21}H_{42}N_4O_6$ 0.2 $H_2O$ Theory: C 56.03, H 9.49, N 12.45 Found: C 55.87, H 9.39, N 12.23.

**N-[2-(2-Amino-ethylamino)-ethyl]-N'-(2-cyclopentadecylamino-ethyl)-ethane-1,2-diamine**

**25b**. The free base of tetraethylenepentamine pentahydrochloride **24c** (N-(2-Amino-ethyl)-N'-[2-(2-amino-ethylamino)-ethyl]-ethane-1,2-diamine, Sigma Aldrich) (3g, 8.07 mmol) was generated with 5 equivalents of NaOH (40.4 mmol, 1.61g, 40.35 mL). The water was then removed by addition of benzene as an azeotrope and then removal of benzene under reduced pressure. Anhydrous sodium sulfate was added (64.6 mmol, 9.18 g) and 25% MeOH/DCM added as solvent (30 mL). After the generation of the free base, one equivalent of salicylaldehyde was added (8.07 mmol, 1.160g/mL, 850 μL) to protect the terminal amine and the solution immediately turned bright yellow. After protection was complete by NMR, the remaining amines were protected with di-*tert*-butyl dicarbonate (4 equivalents, 7.05g, 32.29 mmol) and the reaction was heated at 40$^{o}$C overnight.. After complete bocylation was verified by NMR, the imine was cleaved with 1 equivalent of methoxyamine (8.07 mmol, 0.674g, in 1.13 mL of TEA and 5 mL of MeOH/$CH_2Cl_2$) and the disappearance of the imine peak at 8.34 ppm by $^{1}$H NMR. After conversion to the free amine was complete, the solvent (MeOH) was removed and residue was redissolved in DCM and then washed with saturated aq. $Na_2CO_3$ (30 mL) to generate the free base. The organic layer was separated, dried over anhydrous sodium sulfate, filtered and concentrated to give a red brown solid (6.24g). The crude solid was separated by column chromatography (1% $NH_4OH$/10% MeOH/$CH_2Cl_2$, product $R_f$ **25b**: 0.5) to generate a light red solid (1.23g, 2.09 mmol, 26% yield). **25b**: $^{1}$H NMR ($CDCl_3$): δ 3.32 (br s, 14H), 2.86 (br s, 2H), 1.89 (br s, 2H), 1.46 (s, 36H).; $^{13}$C NMR ($CDCl_3$): δ 156.12, 80.1, 50.12, 47.32, 45.72, 40.82, 39.40, 28.4; Anal $C_{28}H_{55}N_5O_8$ Theory: C 57.02, H 9.40, N 11.87 Found: C 56.75, H 9.31, N 11.61; HRMS for $C_{28}H_{55}N_5O_8$ (M+H) Theory 589.4079, Found 589.4051.

**(2-tert-Butoxycarbonylamino-ethyl)-[2-(tert-butoxycarbonyl-cyclopentadecylmethyl-amino)-ethyl]-carbamic acid tert-butyl ester 27a.** Triamine **24a** (N1-(2-Amino-ethyl)-ethane-1,2-diamine, Sigma, 255mg, 2.47 mmol) was added to bromide **23** (250 mg, 0.82 mmol) dropwise in $CH_3CN$ (3 mL) along with $K_2CO_3$ (1.17 g, 8.47mmol) at 120 $^oC$. After 48 h, $^1H$ NMR showed complete disappearance of starting material and the reaction was concentrated and ressuspended in DCM and washed with 0.1M NaOH. The organic layer was separated, dried over anhydrous $Na_2SO_4$, filtered and concentrated to give a light yellow oil (272 mg). Di-*tert*-butyl dicarbonate was added (540 mg, 2.47 mmol) in 25% MeOH/DCM (10 mL) at 40 $^oC$ and the reaction stirred overnight. Bocylation was assessed by NMR and when complete the reaction was concentrated and redissolved in DCM and washed with aq. $Na_2CO_3$. The organic layer was separated, dried over anhydrous sodium sulfate, filtered and concentrated under reduced pressure to give a yellow oil (706 mg). The crude was then purified by column chromatography (2% MeOH/DCM $R_f$ **27a**: 0.4) to give **27a** as a viscous yellow oil (154 mg, 25% yield). **27a:** $^1H$ NMR ($CDCl_3$): δ 3.30 (m, 8H), 3.06 (m, 2H), 3.04 (m, 1H), 1.68 (s, 1H), 1.45 (s, 27H), 1.31 (br s, 28H). $^{13}C$ NMR ($CDCl_3$): δ. 155.85, 79.89, 52.46, 46.72, 45.50, 39.78, 36.20, 30.17, 28.42, 26.76, 24.43; HRMS for $C_{35}H_{67}N_3O_6$ (M+H): theory 625.5043; found 625.5030; Anal Calcd for $C_{35}H_{67}N_3O_6$ : theory C 67.16, H 10.79, N 6.71; found C 67.42, H 10.92, N 6.63.

**[2-(tert-Butoxycarbonyl-{2-[tert-butoxycarbonyl-(2-tert-butoxycarbonylamino-ethyl)-amino]-ethyl}-amino)-ethyl]-cyclopentadecylmethyl-carbamic acid tert-butyl ester 27b.** Triethylene tetra-amine tetra HCl (N,N'-Bis-(2-amino-ethyl)-ethane-1,2-diamine, Sigma) (1.0 g, 3.42 mmol) was dissolved in 1M NaOH (13.8 mL) to give the free tetraamine base **24b**. The aqueous layer was then removed and chased with benzene for complete water removal to give dry

**24b** plus NaCl. Mesylate **16** (628 mg, 2 mmol) was dissolved in $CH_3CN$ with $K_2CO_3$ (391mg: 2.83 mmol), the reaction showed complete conversion after 72 h at 50 $^oC$ by $^1H$ NMR. The reaction was concentrated to provide a residue, which was dissolved in DCM and washed with 0.1M NaOH (30 mL). A difficult emulsion ensued. The organic layer was separated, dried over anhydrous $Na_2SO_4$, filtered and concentrated to give organic layer #1. The remaining emulsion/aqueous layer was concentrated and re-dissolved in DCM at a lower temperature and any remaining precipitates were filtered off. The precipitates were washed with DCM and the organic filtrate was pooled with organic layer #1 and concentrated to give a yellow viscous oil (806 mg). The crude oil was re-dissolved in 25% MeOH/DCM and reacted with di-*tert*-butyl dicarbonate (8.75 mmol, 1.91g). The reaction was monitored for bocylation by NMR and then worked up in saturated aq. $Na_2CO_3$ and DCM. The organic layer was separated, dried over anhydrous $Na_2SO_4$, filtered and concentrated to give a yellow oil (1.57 g). Column chromatography (25% EtOAc/hexanes, $R_f$ **27b**: 0.39) gave **27b** as a viscous oil (383 mg, 0.5 mmol, 25% yield).

**27b**: $^1H$ NMR ($CDCl_3$): δ 3.32 (m, 12H), 3.08 (br s, 1H), 3.03 (br s, 2H), 1.46 (s, 36H), 1.33 (br s, 29H); $^{13}C$ NMR ($CDCl_3$): δ 155.4, 80.16, 79.41, 51.68, 45.41, 36.13, 35.78, 36.13, 35.78, 30.18, 28.45, 26.77, 26.38, 24.44; HRMS $C_{42}H_{80}N_4O_8$ (M+H) Theory: 768.5987, Found: 768.5976; Anal Calcd $C_{42}H_{80}N_4O_8$ Theory: C 65.59, H 10.48, N 7.28 Found: C 65.89, H 10.64, N 7.26.

**[2-(Cyclopentadecylmethyl-amino)-ethyl]-carbamic acid tert-butyl ester 27c.** The commercially-available mono N-Boc diamine **28** ((2-Amino-ethyl)-carbamic acid tert-butyl ester, Sigma, 286 mg, 1.78 mmol) was added to mesylate **16** (508 mg, 1.59 mmol) in $CH_3CN$ (20 mL) with $K_2CO_3$ (0.72 g) at 50 $^oC$. After 5 days the reaction showed 50% conversion, most of the

$CH_3CN$ was stripped off (leaving 5 mL) and heated overnight for complete conversion. The solvent was removed under reduced pressure, re-dissolved in DCM and washed with water. The crude (620 mg) was then purified by column chromatography (7% MeOH/DCM Rf **27c**: 0.4) to give **27c** as a clear oil (75 mg, 0.196 mmol, 12% yield) as well as a large amount of what appeared to be a cyclized urea byproduct **27d** (250 mg) **27c**: $^{1}$H NMR ($CD_4O$): δ 3.23 (broad s, 2H), 2.78 (br s, 2H), 2.60 (br s, 2H), 1.63 (s, 1H), 1.45 (s, 9H), 1.37 (br s, 28H);$^{13}$C NMR ($CD_4O$): δ 150.80, 68.01, 50.44, 31.87, 28.88, 28.22, 28.03, 27.91, 27.75; HRMS for $C_{23}H_{46}N_2O_2$ (M+H) Theory: 382.3558 Found: 382.3559; Anal Calcd for $C_{23}H_{46}N_2O_2$ 0.3 $H_20$: theory C 71.19, H 12.10, N 7.22; found C 71.02, H 12.05, N 7.20.

**Attempted Synthesis of Grignard A**. Briefly, in an attempt to produce the Grignard reagent from bromomethyl-cyclopentadecane **23**, dried magnesium turnings (64mg, 2.63mmol) were placed in a dried 3 neck flask under $N_2$ with 1mL of dried THF. A 0.1:1 ratio of 1,2-dibromoethane (22.7µL, 0.26 mmol) was added to the turnings dropwise in an effort to activate the surface. The bromide **23** was then added in a minimal amount of THF by syringe (201mg, 0.659mmol) and allowed to stir overnight under reflux. Ethylene oxide was then added in THF by syringe (595 µL, 1.48mmol in a 2.5M solution in THF,) and the reaction stirred overnight. The reaction was checked by TLC for presence of bromide (100% hexanes, visualization in phosphomolybdic acid and heat) and showed no conversion of bromide to the alcohol. The reaction was then quenched with saturated $NH_4Cl$. The water layer was extracted with DCM to recover the unreacted bromide.

**Attempted synthesis of Acetal B**. Briefly, copper (I) iodide (314 mg, 0.165mmol,) and lithium methoxide (63 mg, 1.65mmol) were added together under $N_2$ and then the Grignard reagent **C** (i.e.,

bromo-[2-(1,3-dioxan-2-yl)ethyl]magnesium)(0.5M in THF, Sigma, 631 mg, 3.3 mmol, 6.6mL), alkyl bromide (500 mg, 1.65 mmol) in 1mL of dry THF, and TMEDA (38 mg, 50 µL, 0.33 mmol) were added sequentially at 0$^{o}$C while stirring. The reaction was stirred for 24 h, $^{1}$H NMR showed no sign of reaction and again there was 100% recovery of bromide **23**.

**Attempted synthesis of Acetal D**. Briefly, the commercially available Grignard reagent **C** (i.e., bromo-[2-(1,3-dioxan-2-yl)ethyl]magnesium, 0.5M in THF, Sigma) was placed in a dry three neck flask under $N_2$ (9.84 mL, 4.92 mmol) while stirring at rt. Ketone (1.0 g, 4.45 mmol) in THF (0.75 mL) was added to dioxolane **C** while stirring. The reaction was refluxed overnight and monitored by TLC (5% MeOH, DCM, $R_f$ 0.6) for the quenched Grignard acetal product and monitored for the loss of ketone **(**5% EtOAc/Hexanes, $R_f$ **13**: 0.3). TLC showed no signs of conversion, another 3-4 equivalents of Grignard reagent were added under reflux over 7 days with continuous addition of $N_2$ . No loss of ketone was seen by TLC or by $^{1}$H NMR. The no conversion observed in this reaction further illustrates the poor reactivity of the bulky ketone.

**Attempted Synthesis of Amine E.** Briefly, tri-Boc-protected tetraamine **25a** (500mg, 1.12mmol) in 5 mL of $CH_2Cl_2$ was added to ketone **13** (230mg, 1.02 mmol) in $CH_2Cl_2$ (5 mL) while stirring at rt. $NaBH(OAc)_3$ (1.1g, 5.18 mmol) and glacial acetic acid (58.3µL) were added to the mixture at rt. The reaction showed no disappearance of starting material after 24 h at rt or after 48 h at 40$^{o}$C. Note: the ketone was monitored by TLC using 5% EtOAc/Hexanes stained with $KMnO_4$. The solvent was removed and changed to THF. Reaction was stirred for 48 h at 40$^{o}$C and monitored for loss of ketone (5% EtAc/Hexanes, visualization with $KMnO_4$, $R_f$ **13**: 0.3) and appearance of the secondary amine **E** (5% MeOH,/$CH_2Cl_2$, $R_f$ 0.3). None was observed.

## APPENDIX : NMR SPECTRA

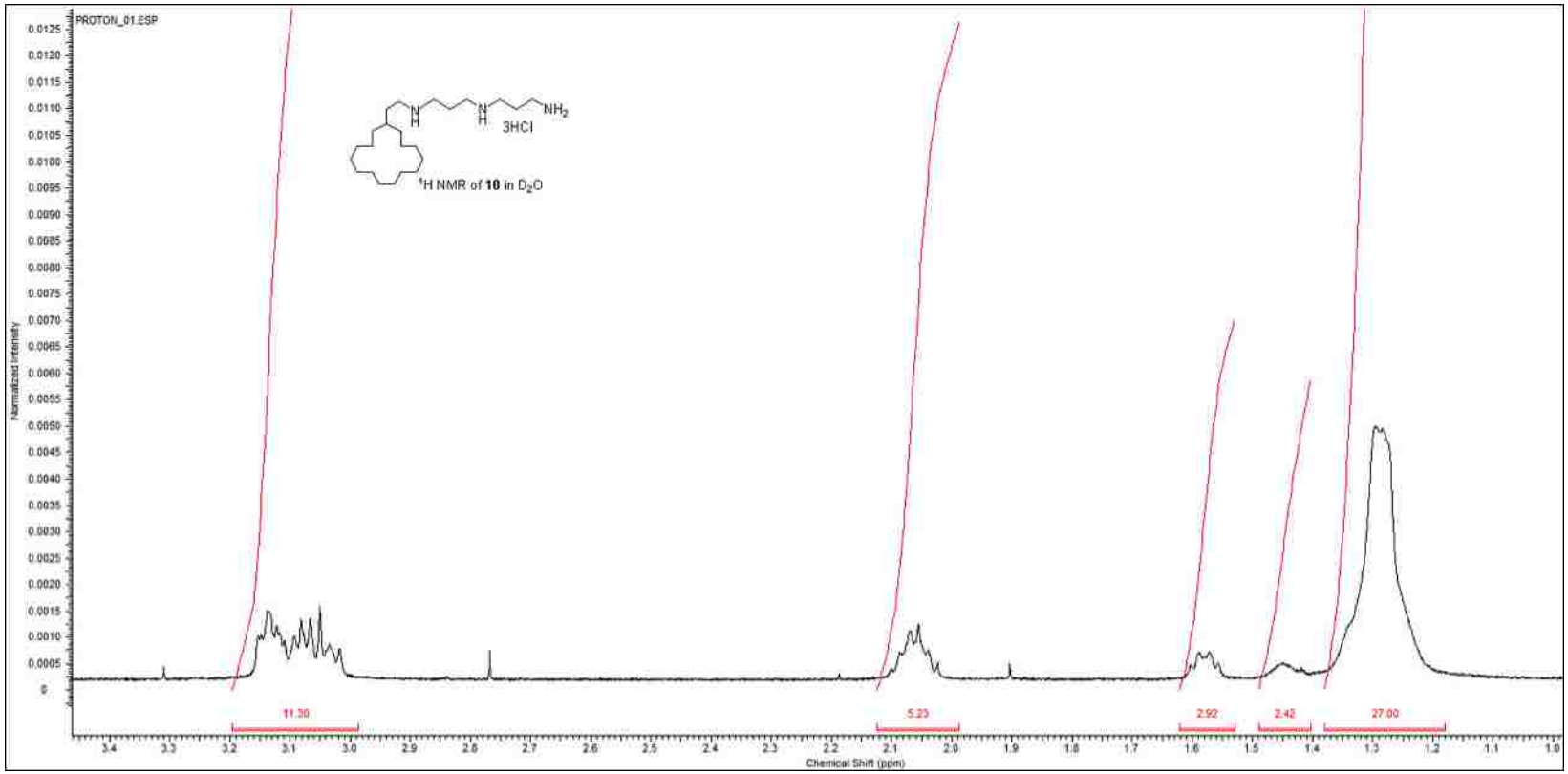
PROTON_01.ESP
NH2
3HCl
1H NMR of 10 in D2O
Normalized Intensity
Chemical Shift (ppm)
11.30
5.23
2.92
2.42
27.00

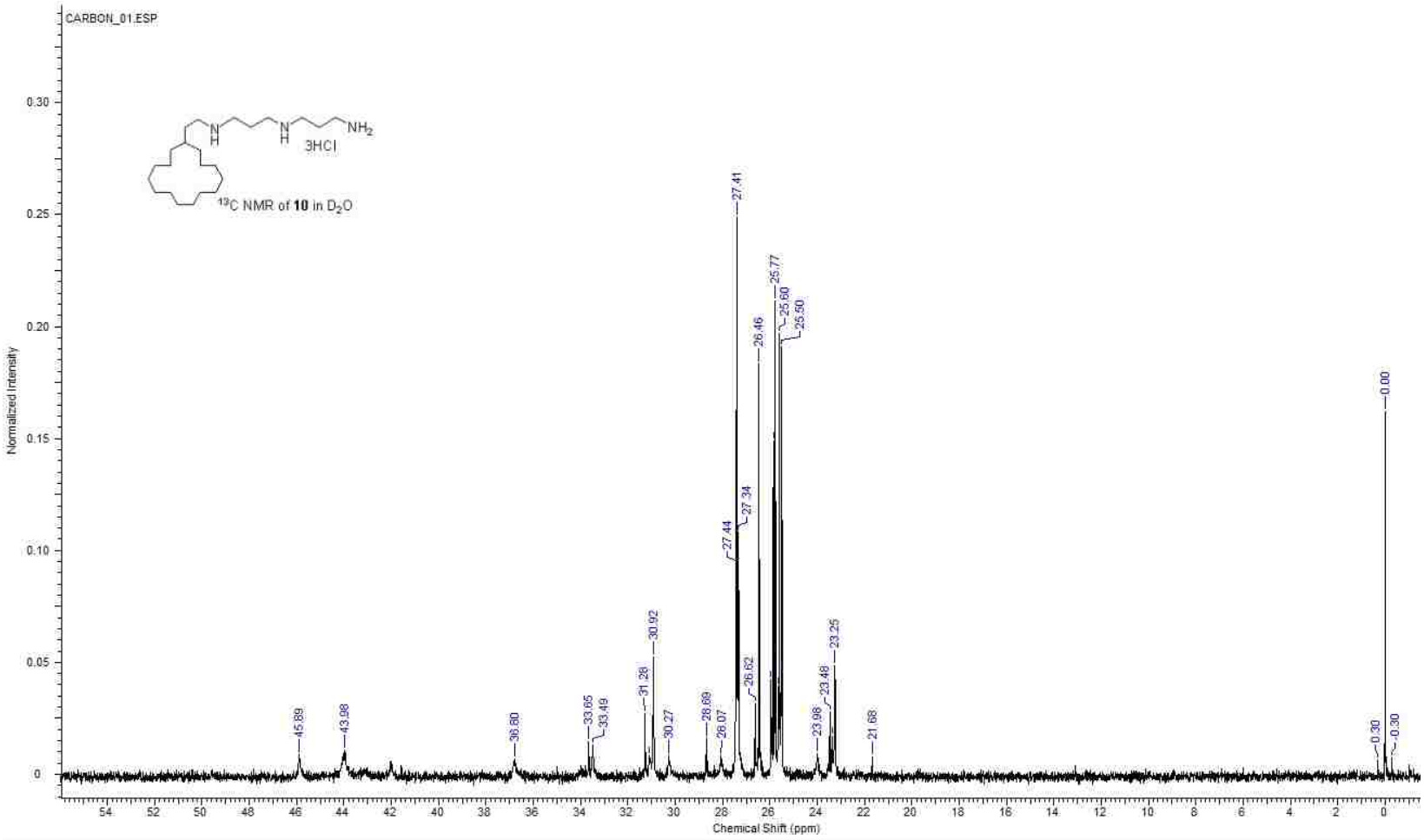
CARBON_01.ESP
3HCl
$^{13}$C NMR of **10** in $D_2O$
Normalized Intensity
Chemical Shift (ppm)
45.89
43.98
36.80
33.65
33.49
31.28
30.92
30.27
28.89
26.07
27.44
27.41
27.34
26.62
26.46
25.77
25.60
25.50
23.98
23.48
23.25
21.68
0.30
0.00
-0.30

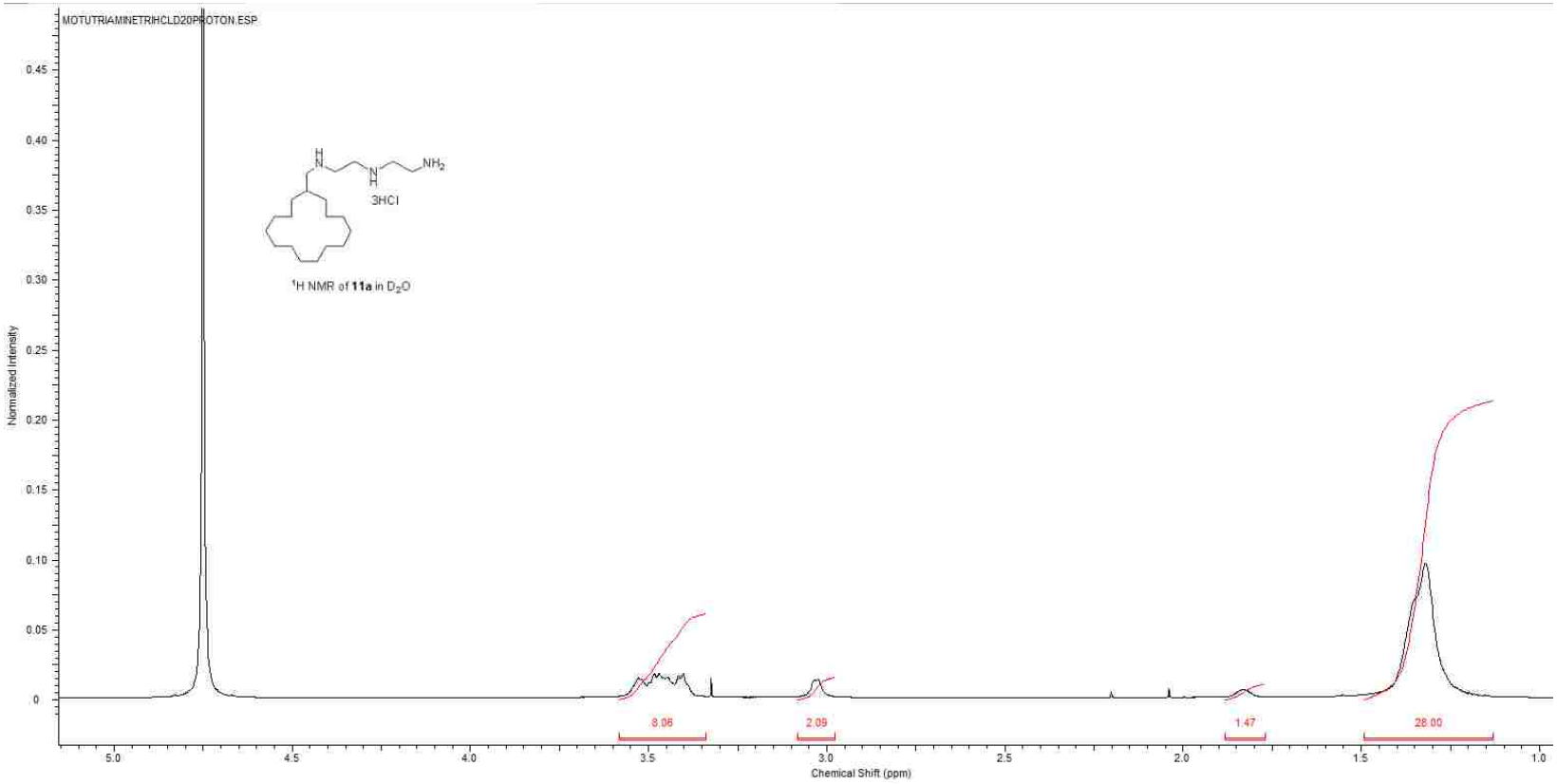
MOTUTRIAMINETRIHCLD20PROTON.ESP
3HCl
$^1$H NMR of **11a** in $D_2O$
Normalized Intensity
Chemical Shift (ppm)
8.06
2.09
1.47
28.00

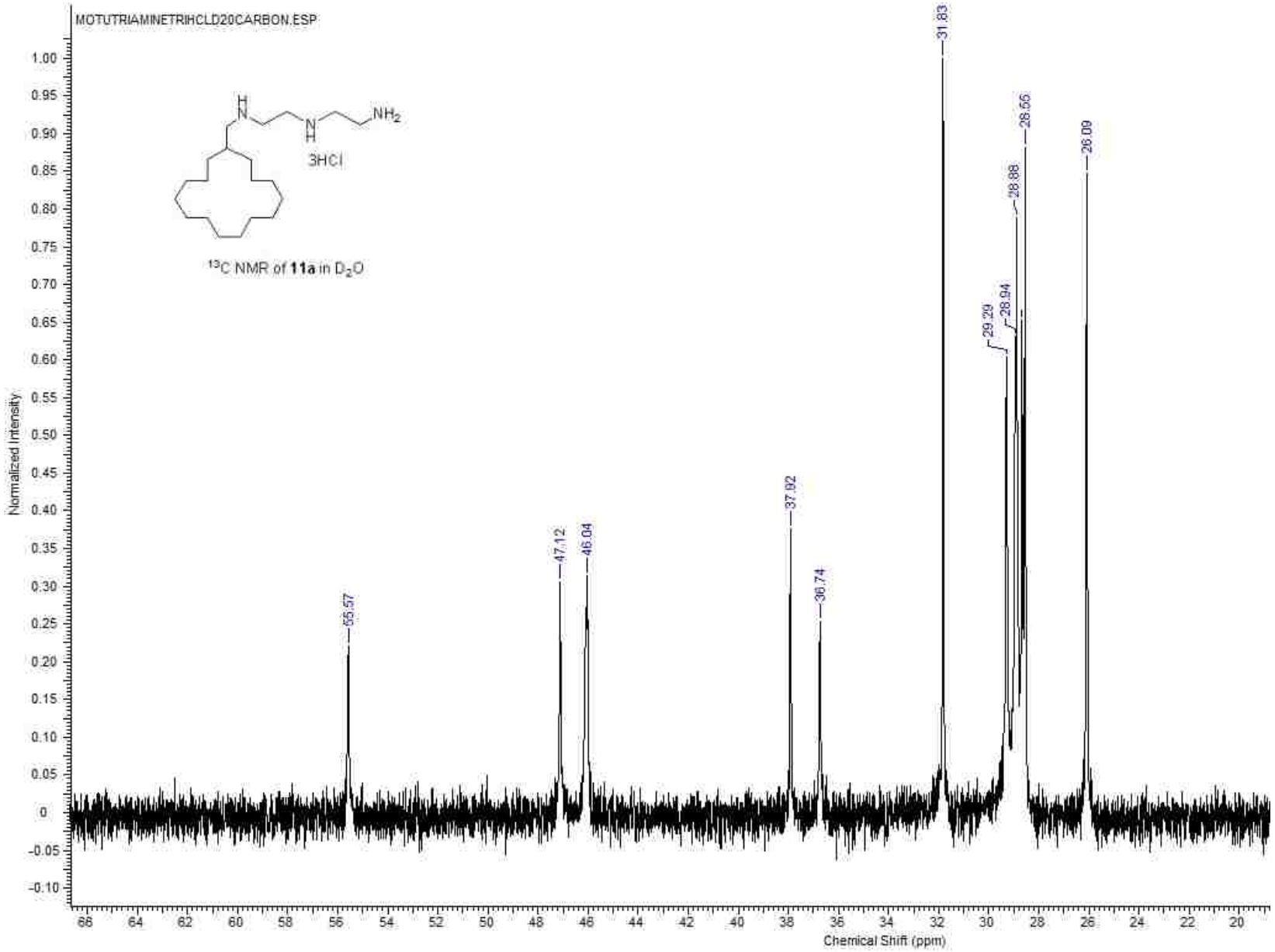
MOTUTRIAMINETRIHCLD20CARBON.ESP
3HCl
$^{13}$C NMR of **11a** in $D_2O$
Normalized Intensity
Chemical Shift (ppm)
55.57
47.12
46.04
37.92
36.74
31.83
29.29
28.94
28.88
28.55
26.09

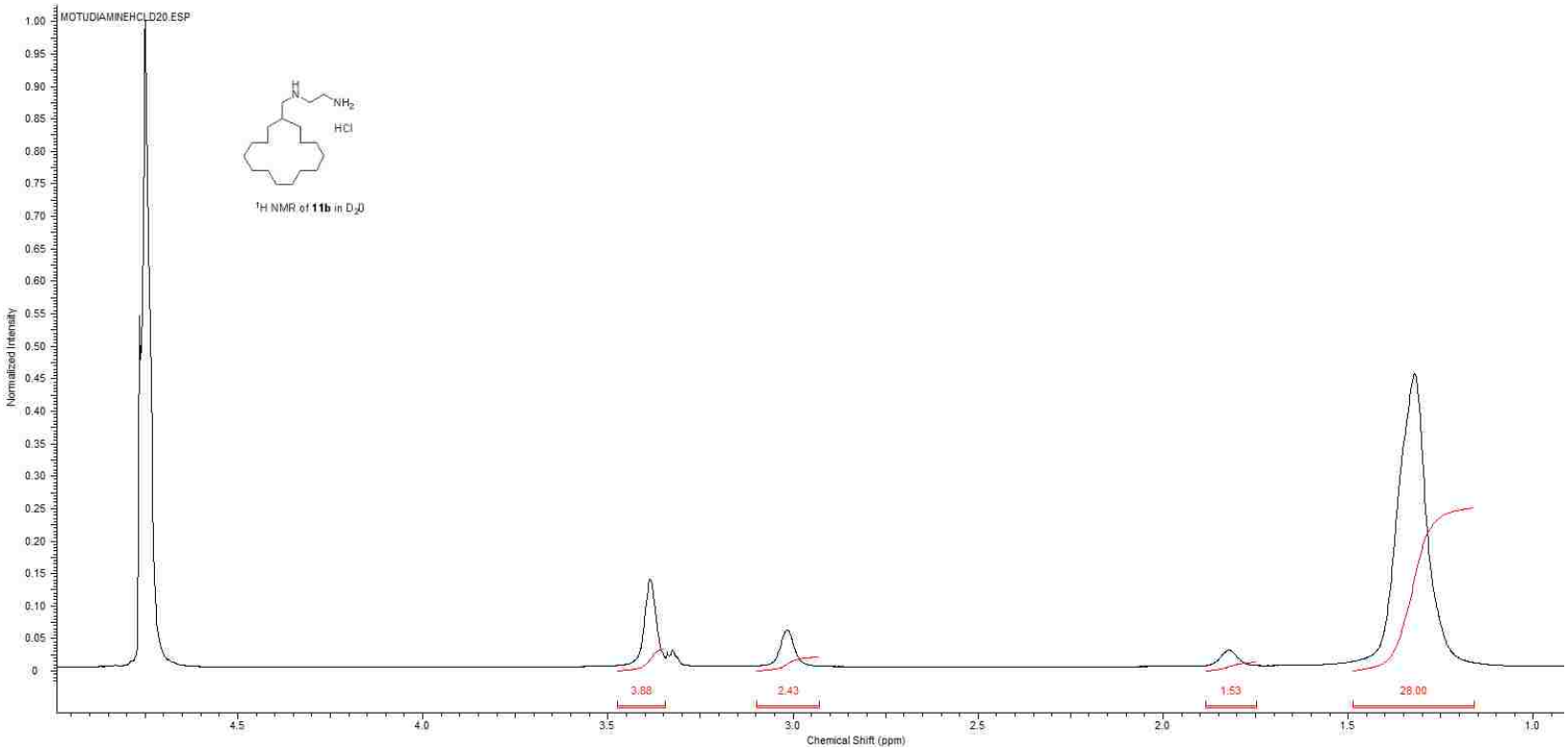
MOTUDIAMINEHCLD20.ESP
NH2
HCl
1H NMR of 11b in D2O
Normalized Intensity
Chemical Shift (ppm)
3.88
2.43
1.53
28.00

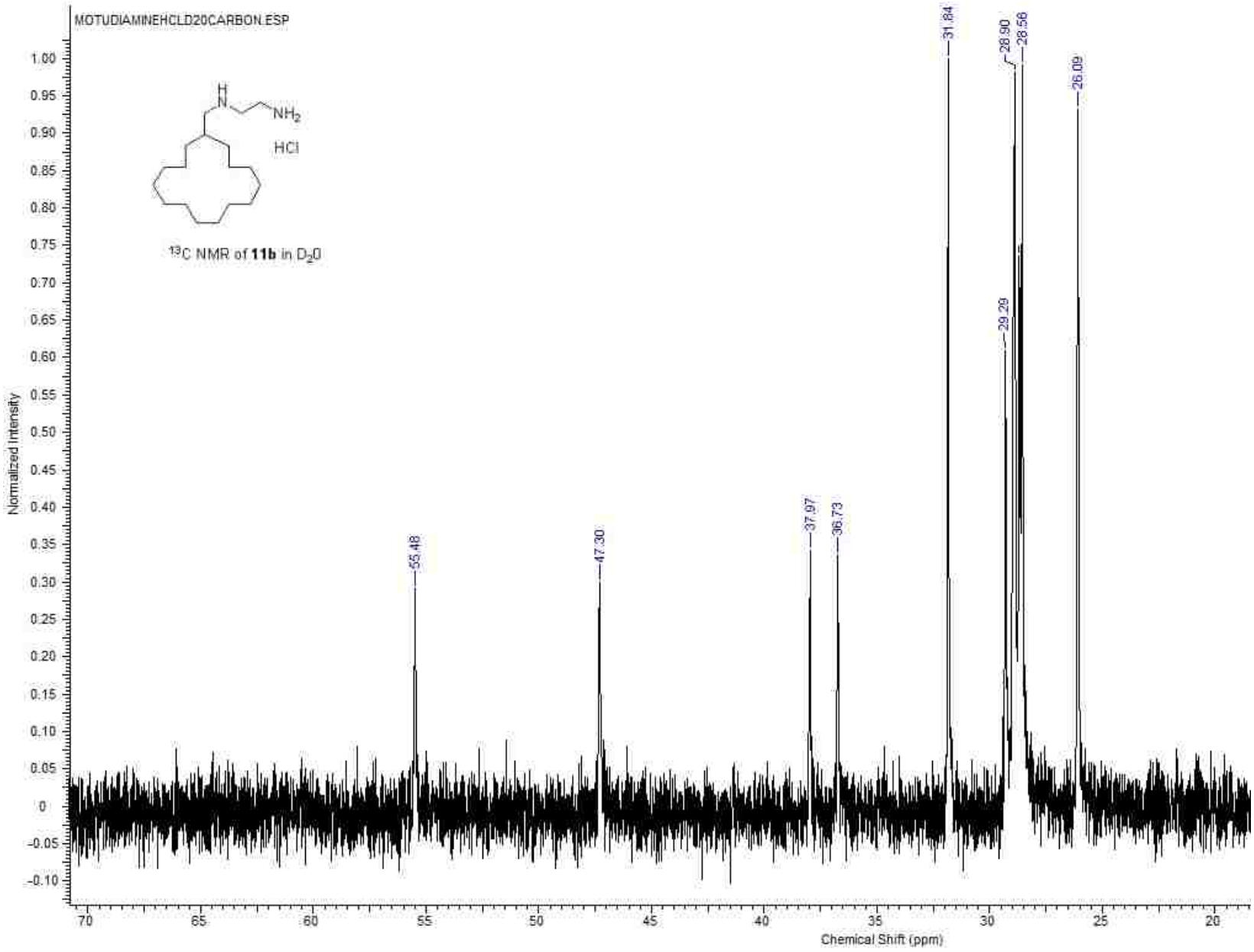
MOTUDIAMINEHCLD20CARBON.ESP
HCl
$^{13}$C NMR of **11b** in $D_2O$
Normalized Intensity
Chemical Shift (ppm)
55.48
47.30
37.97
36.73
31.84
29.29
28.90
28.56
26.09

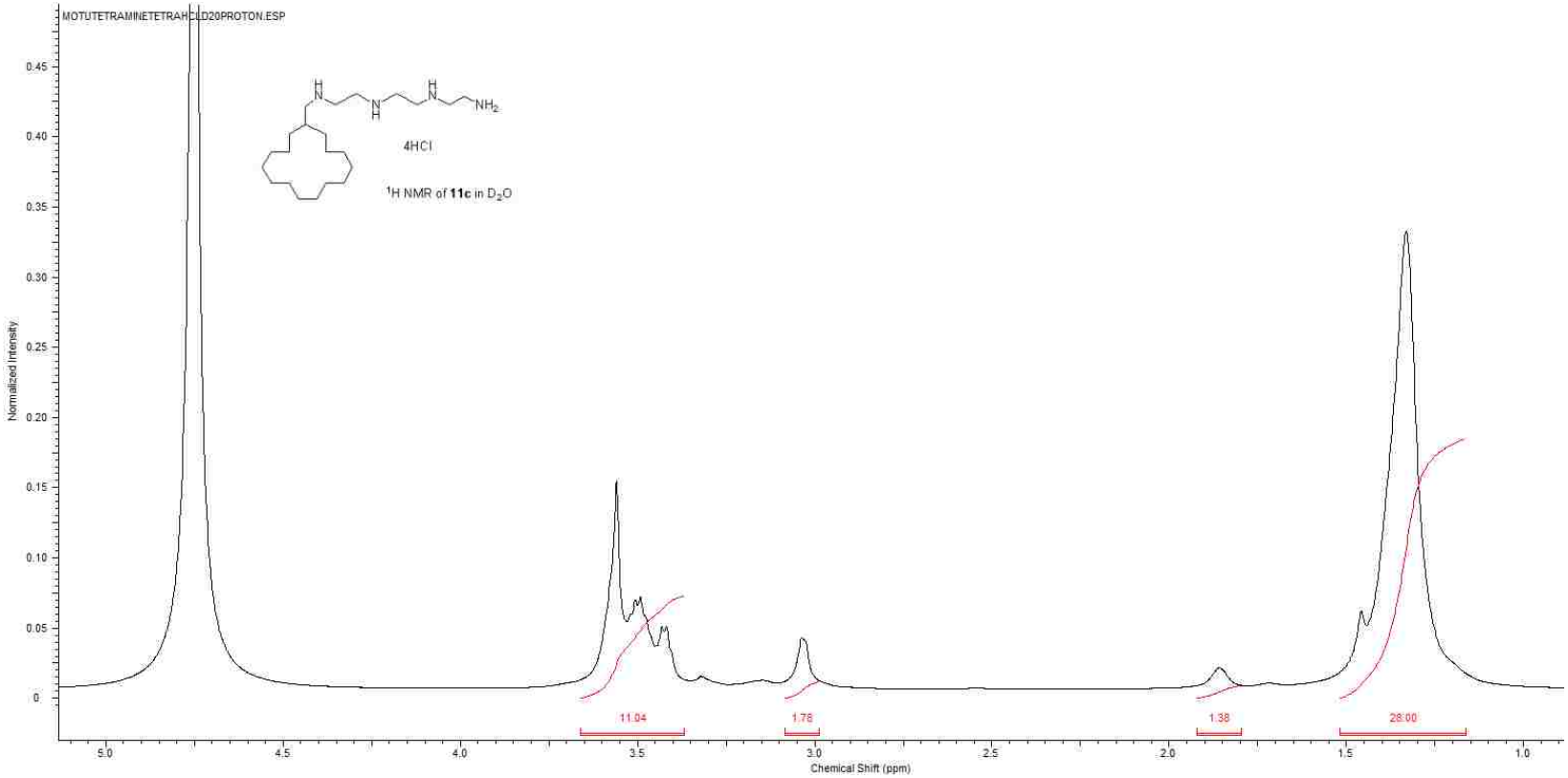
MOTUTETRAMINETETRAHCLD20PROTON.ESP
4HCl
$^1$H NMR of **11c** in $D_2O$
Normalized Intensity
Chemical Shift (ppm)
11.04
1.78
1.38
28.00

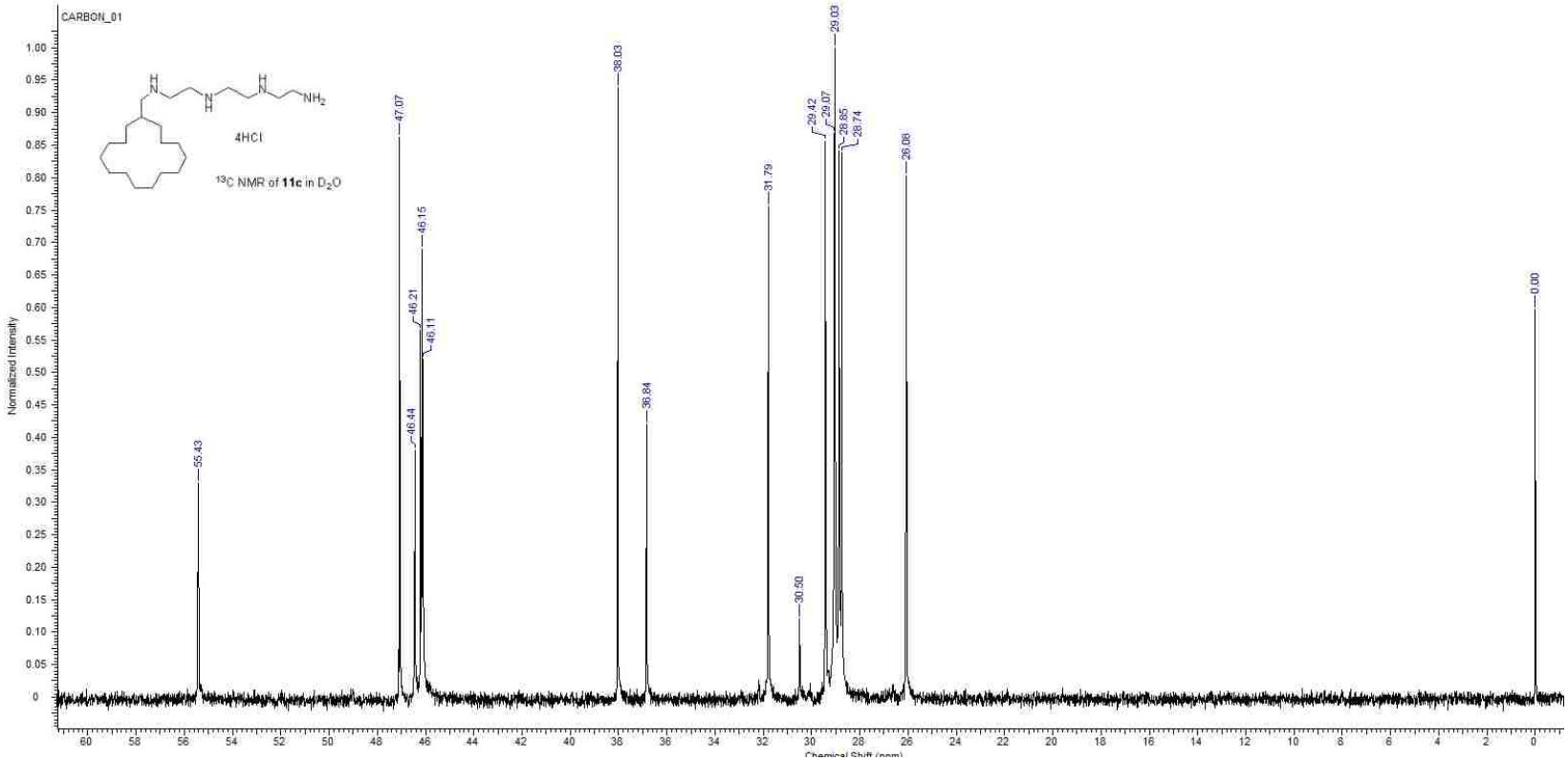
CARBON_01
4HCl
$^{13}$C NMR of **11c** in $D_2O$
Normalized Intensity
Chemical Shift (ppm)
55.43
47.07
46.44
46.21
46.15
46.11
38.03
36.84
31.79
30.50
29.42
29.07
29.03
28.85
28.74
26.08
0.00

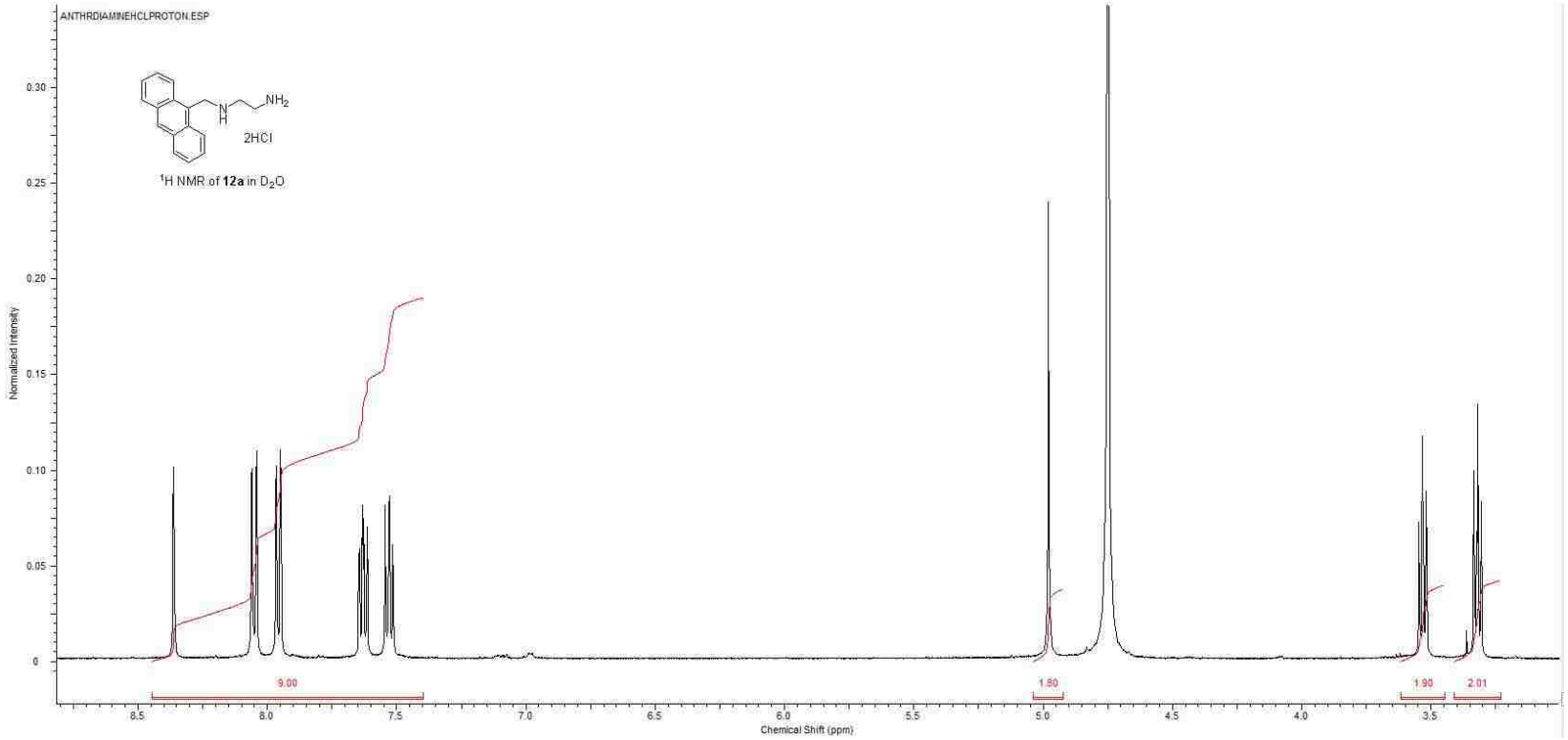
ANTHRDIAMINEHCLPROTON.ESP
NH2
N
H
2HCl
1H NMR of 12a in D2O
Normalized Intensity
0.30
0.25
0.20
0.15
0.10
0.05
0
9.00
1.80
1.90
2.01
8.5
8.0
7.5
7.0
6.5
6.0
5.5
5.0
4.5
4.0
3.5
Chemical Shift (ppm)

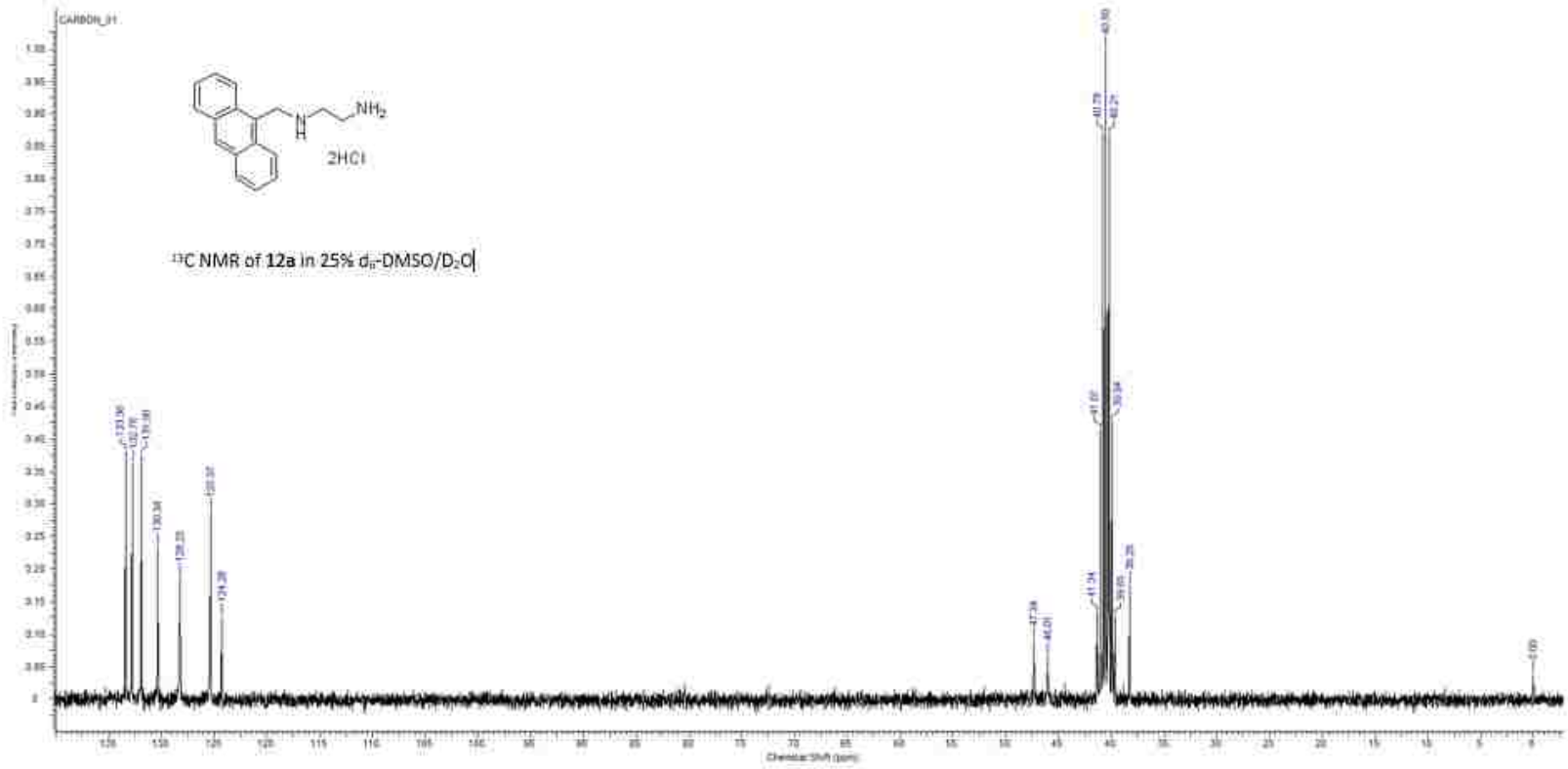
NH2
2HCl
13C NMR of 12a in 25% d6-DMSO/D2O

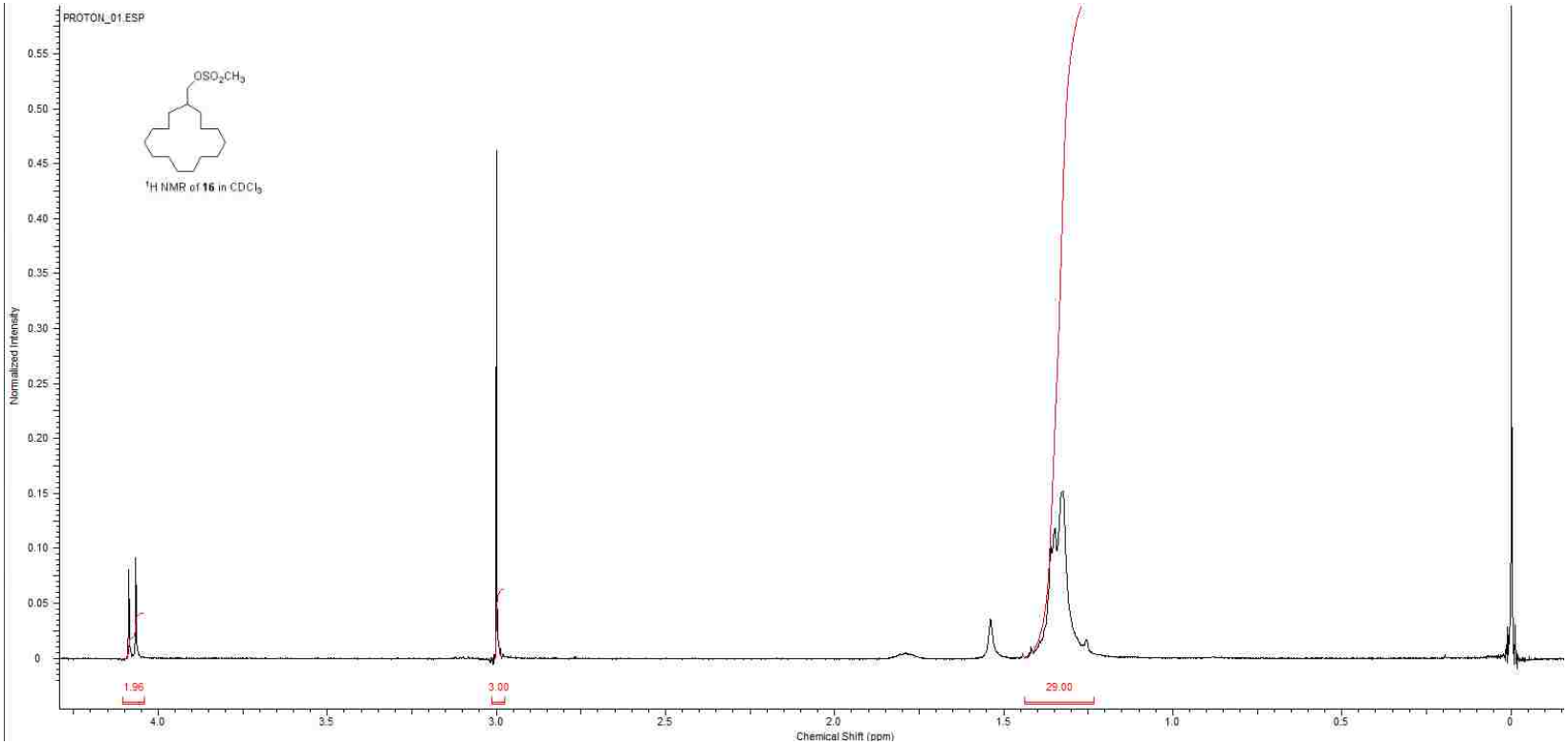
PROTON_01.ESP
OSO2CH3
1H NMR of 16 in CDCl3
Normalized Intensity
0.55
0.50
0.45
0.40
0.35
0.30
0.25
0.20
0.15
0.10
0.05
0
1.96
3.00
29.00
4.0
3.5
3.0
2.5
2.0
1.5
1.0
0.5
0
Chemical Shift (ppm)

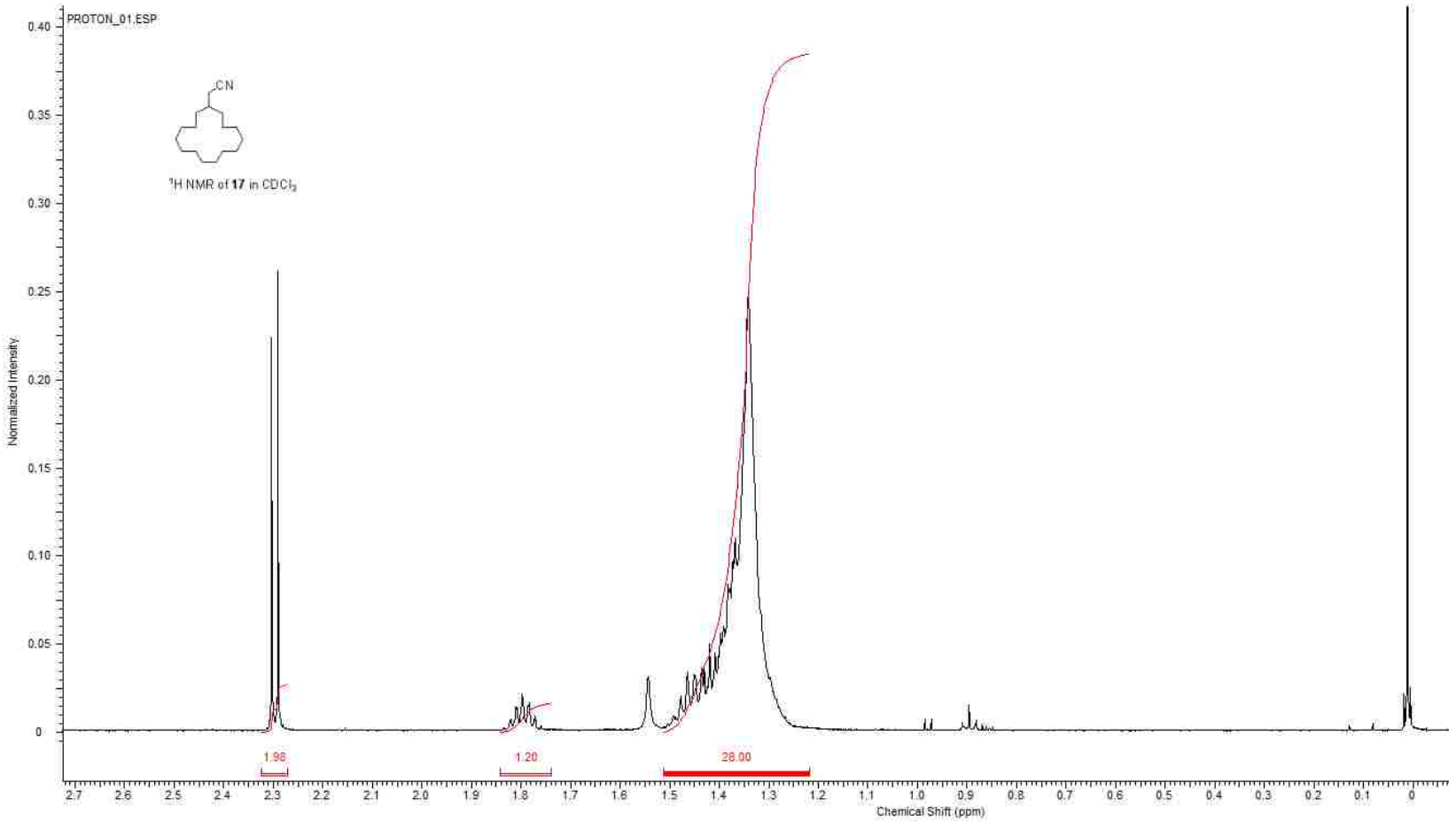
PROTON_01.ESP
CN
$^1$H NMR of **17** in $CDCl_3$
Normalized Intensity
0.40
0.35
0.30
0.25
0.20
0.15
0.10
0.05
0
1.96
1.20
28.00
2.7 2.6 2.5 2.4 2.3 2.2 2.1 2.0 1.9 1.8 1.7 1.6 1.5 1.4 1.3 1.2 1.1 1.0 0.9 0.8 0.7 0.6 0.5 0.4 0.3 0.2 0.1 0
Chemical Shift (ppm)

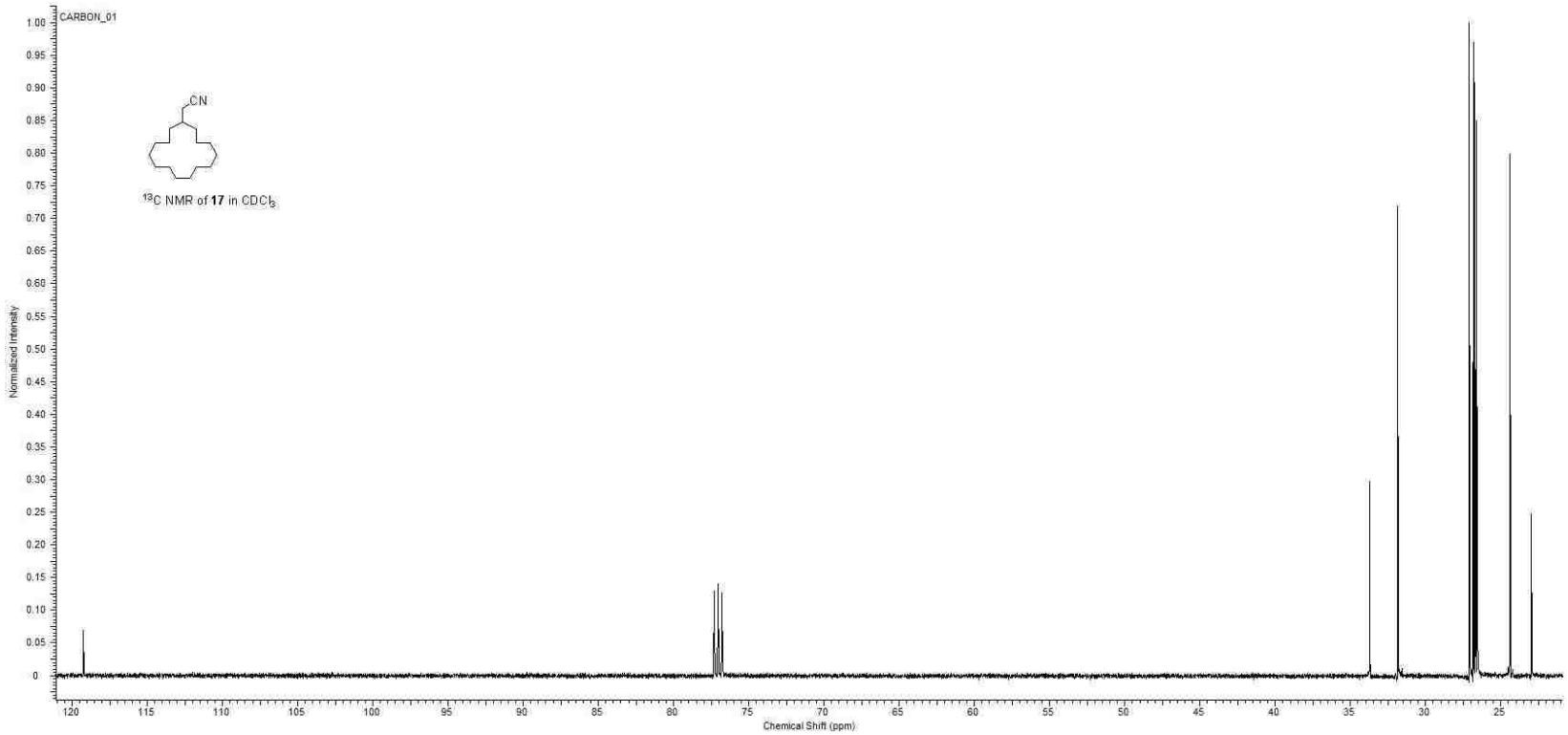
CARBON_01
CN
$^{13}$C NMR of **17** in $CDCl_3$
Normalized Intensity
Chemical Shift (ppm)

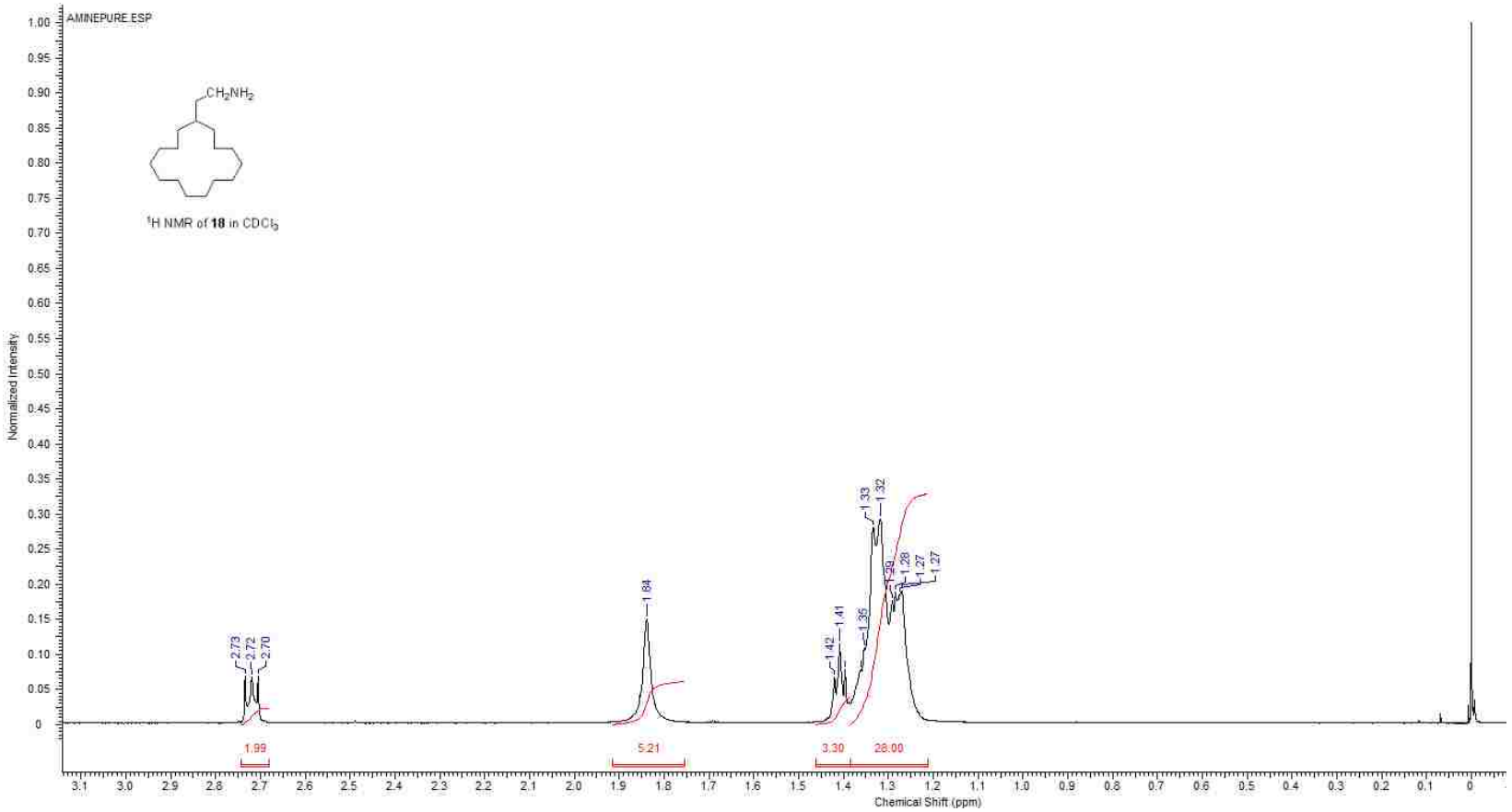
AMINEPURE ESP
$CH_2NH_2$
$^1$H NMR of **18** in $CDCl_3$
Normalized Intensity
Chemical Shift (ppm)
2.73
2.72
2.70
1.84
1.42
1.41
1.35
1.33
1.32
1.29
1.28
1.27
1.27
1.99
5.21
3.30
28.00

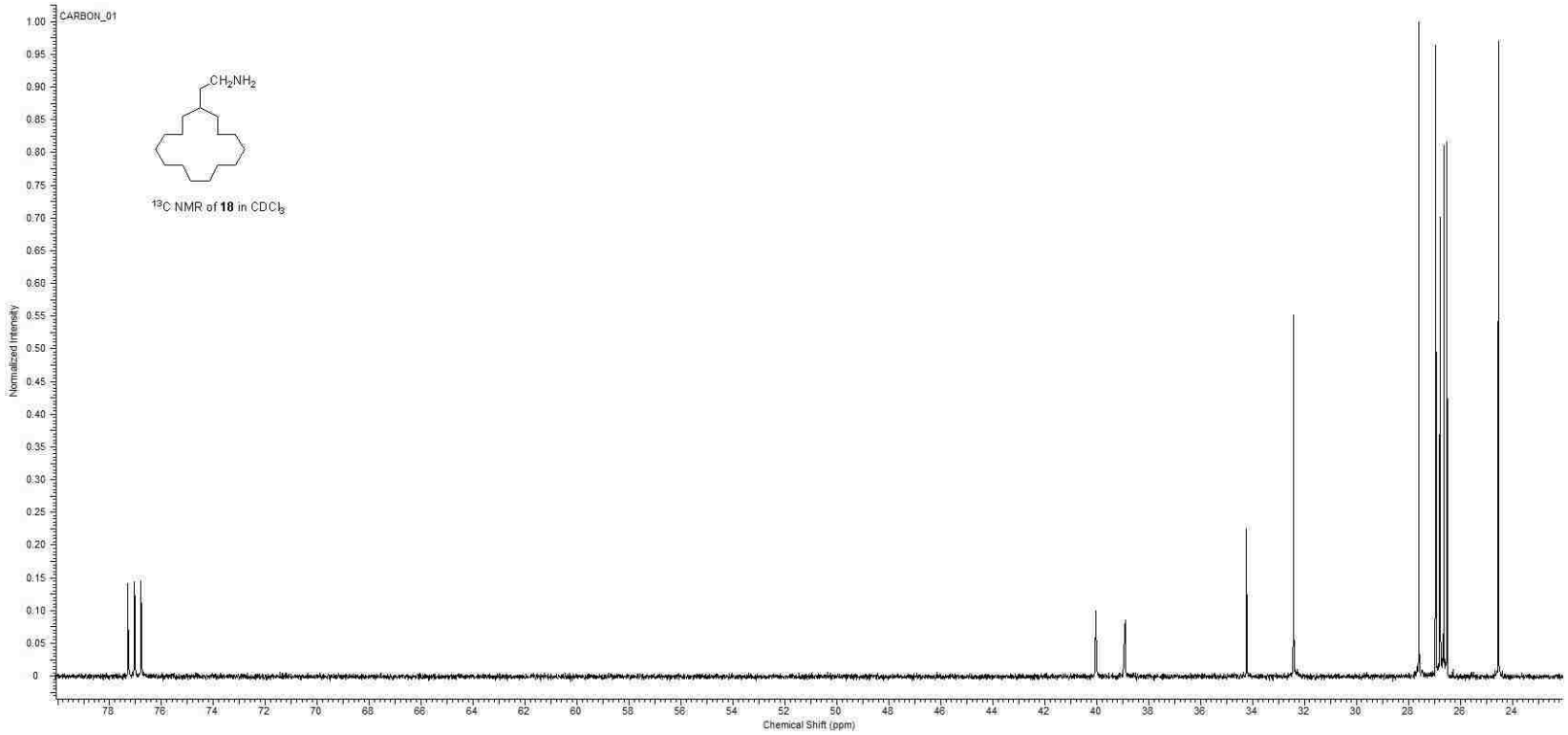
CARBON_01
CH2NH2
13C NMR of 18 in CDCl3
Normalized Intensity
Chemical Shift (ppm)

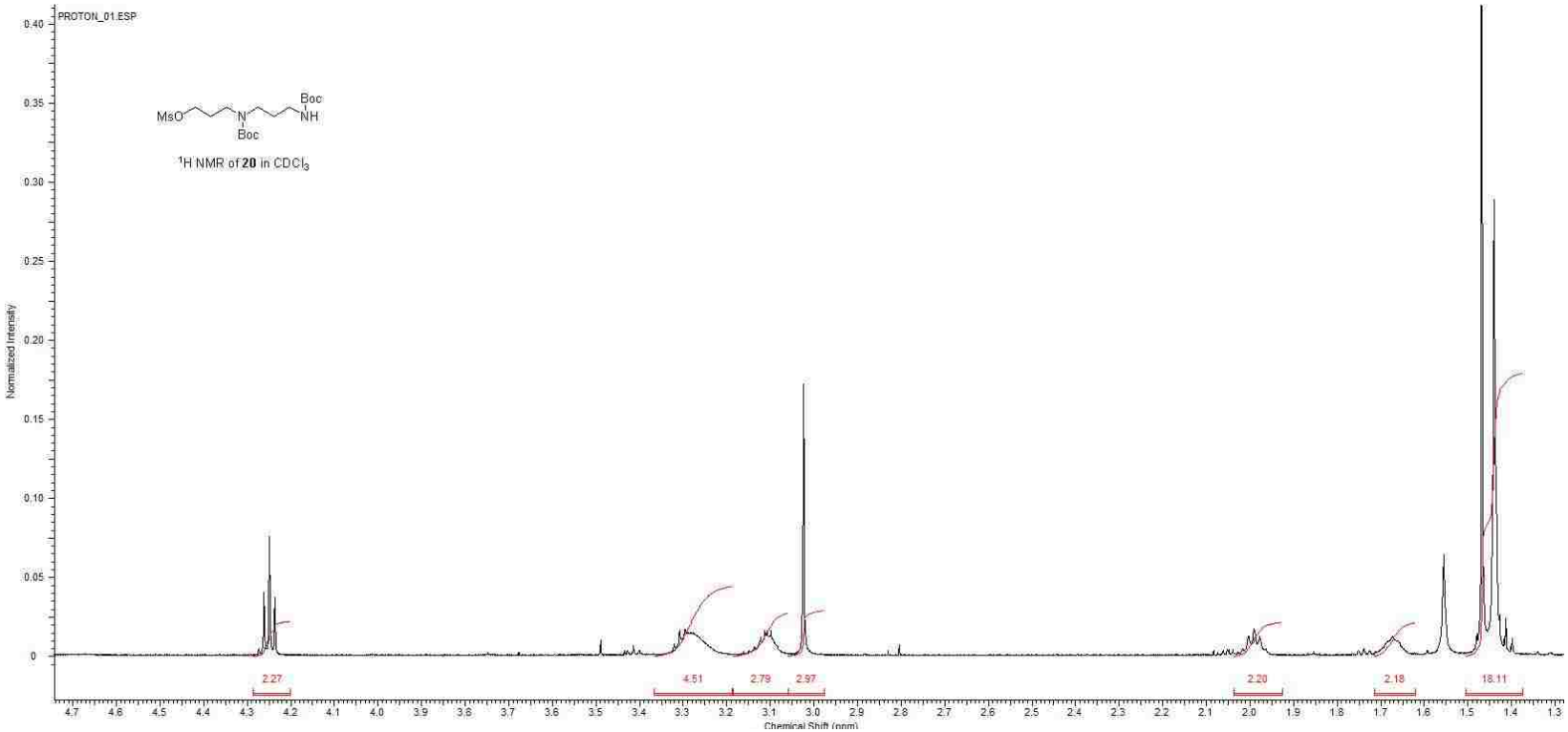
PROTON_01.ESP
MsO
N
Boc
Boc
NH
$^1$H NMR of **20** in $CDCl_3$
Normalized Intensity
2.27
4.51
2.79
2.97
2.20
2.18
18.11
Chemical Shift (ppm)

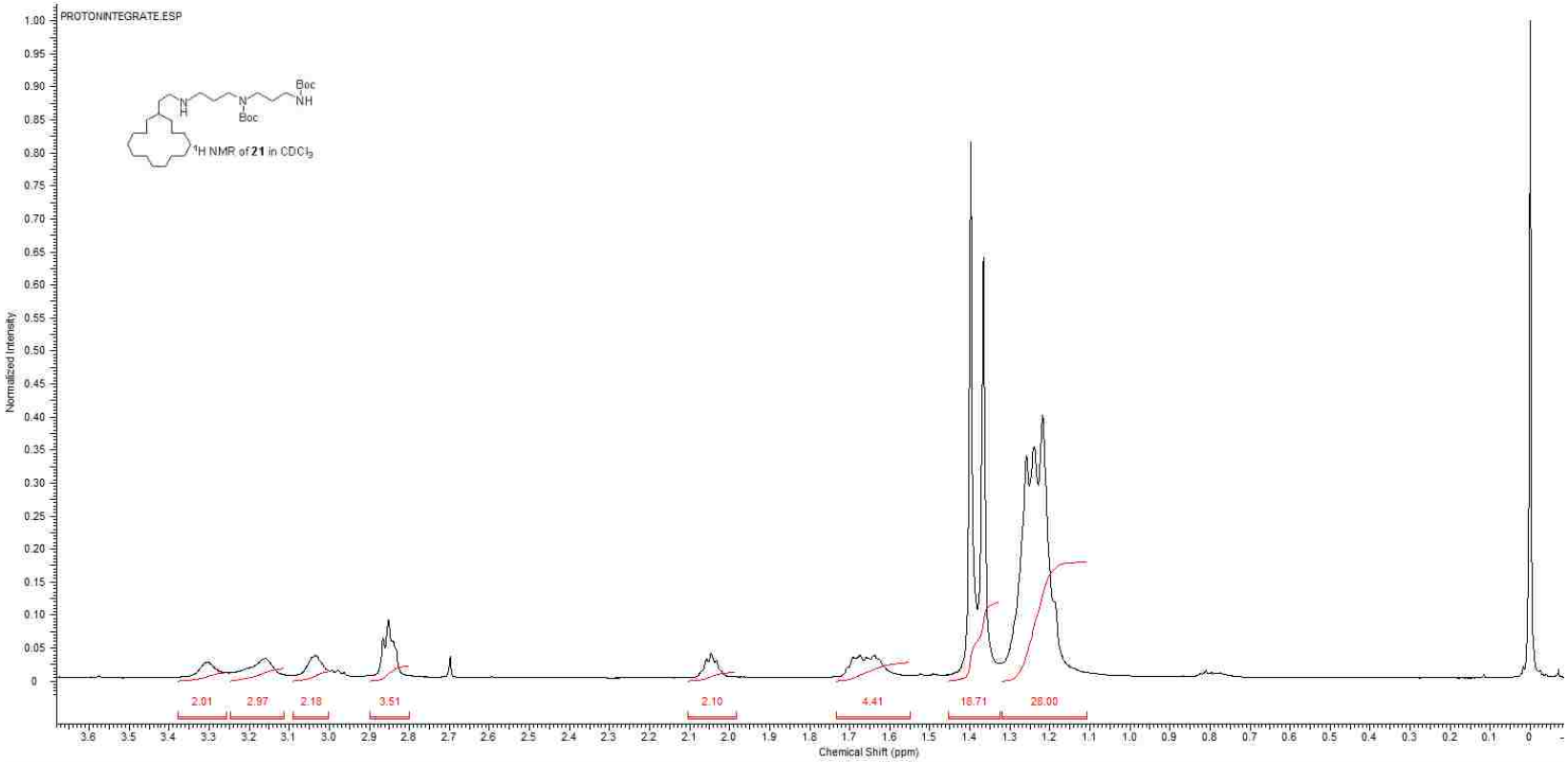
PROTONINTEGRATE.ESP
Boc
NH
N
H
N
Boc
$^1$H NMR of **21** in $CDCl_3$
Normalized Intensity
2.01
2.97
2.18
3.51
2.10
4.41
18.71
28.00
Chemical Shift (ppm)

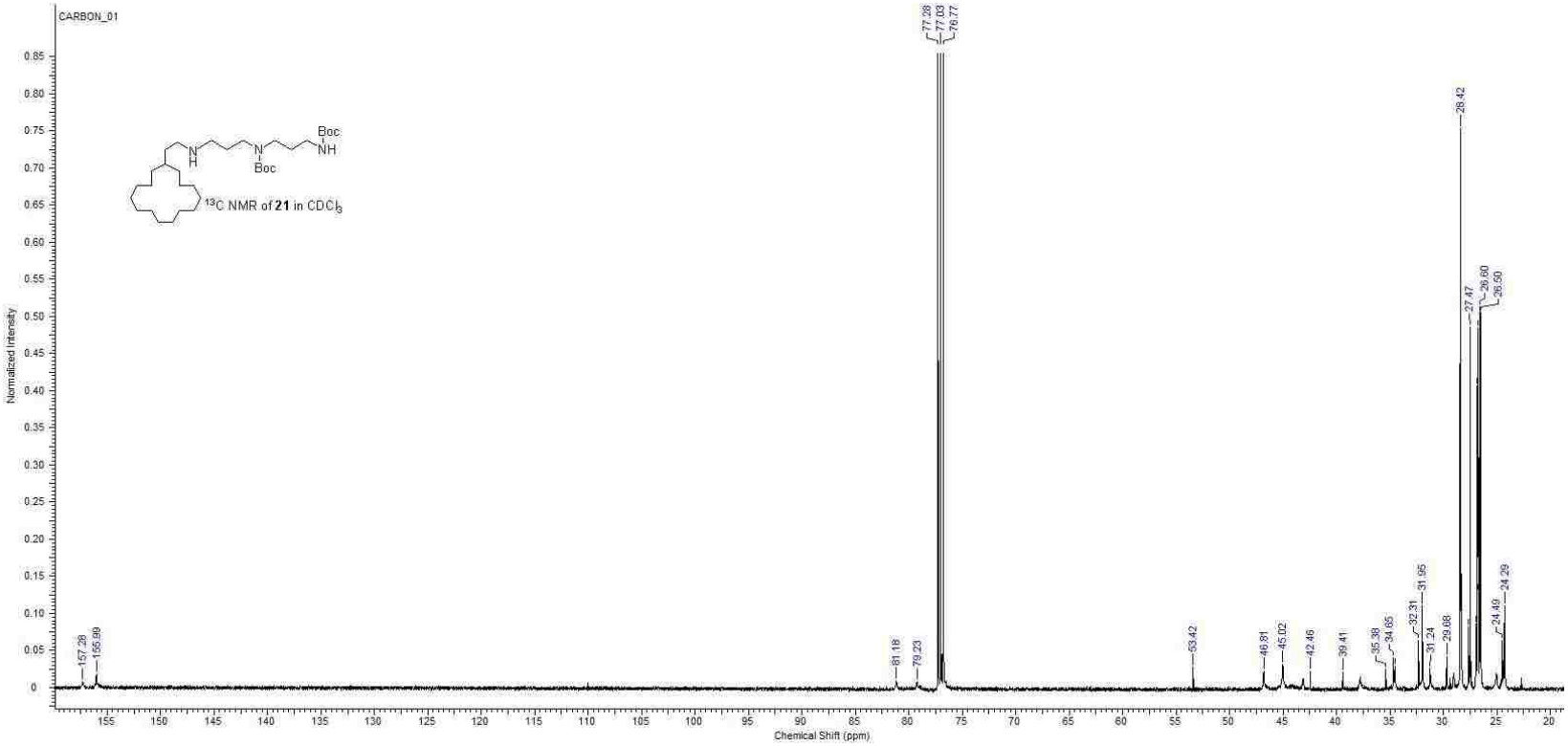
CARBON_01
Boc
NH
N
H
N
Boc
$^{13}$C NMR of **21** in $CDCl_3$
Normalized Intensity
Chemical Shift (ppm)
157.28
155.99
81.18
79.23
77.28
77.03
76.77
53.42
46.81
45.02
42.46
39.41
35.38
34.65
32.31
31.95
31.24
29.88
28.42
27.47
26.60
26.50
24.49
24.29

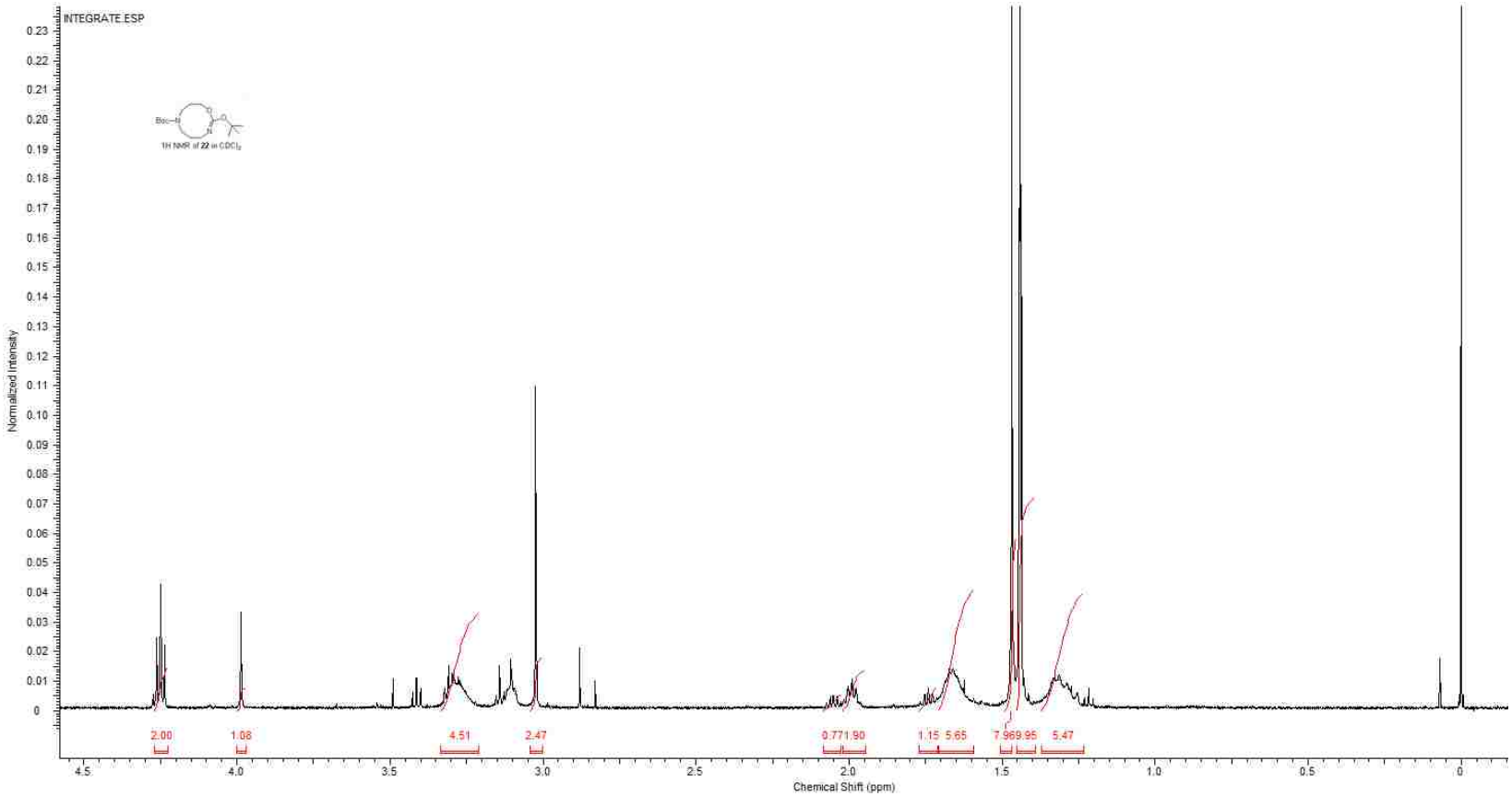
INTEGRATE.ESP
Normalized Intensity
Chemical Shift (ppm)
2.00
1.08
4.51
2.47
0.77
1.90
1.15
5.65
7.96
9.95
5.47

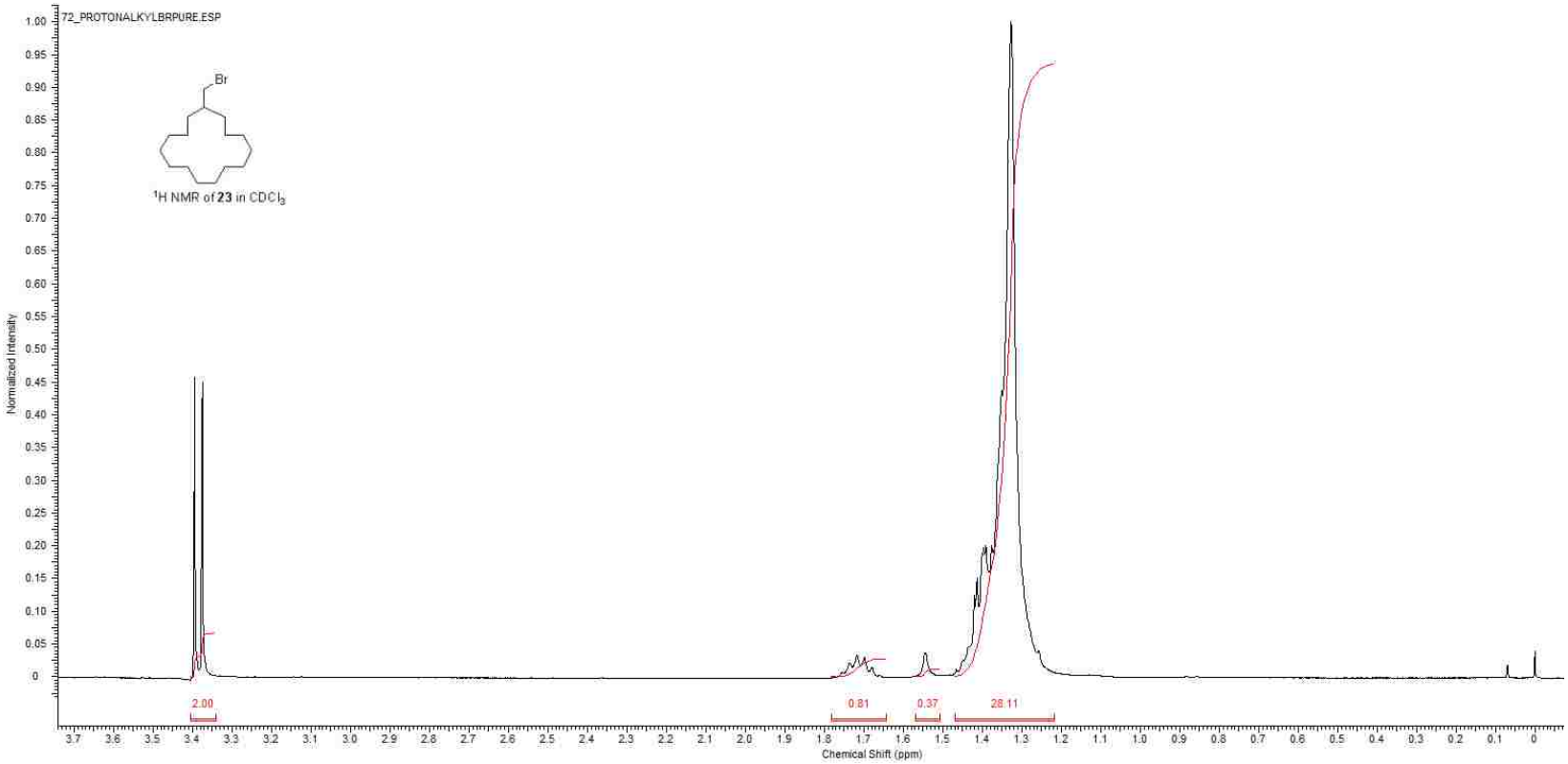
72_PROTONALKYLBRPURE.ESP
Br
$^1$H NMR of **23** in $CDCl_3$
Normalized Intensity
Chemical Shift (ppm)
2.00
0.81
0.37
28.11

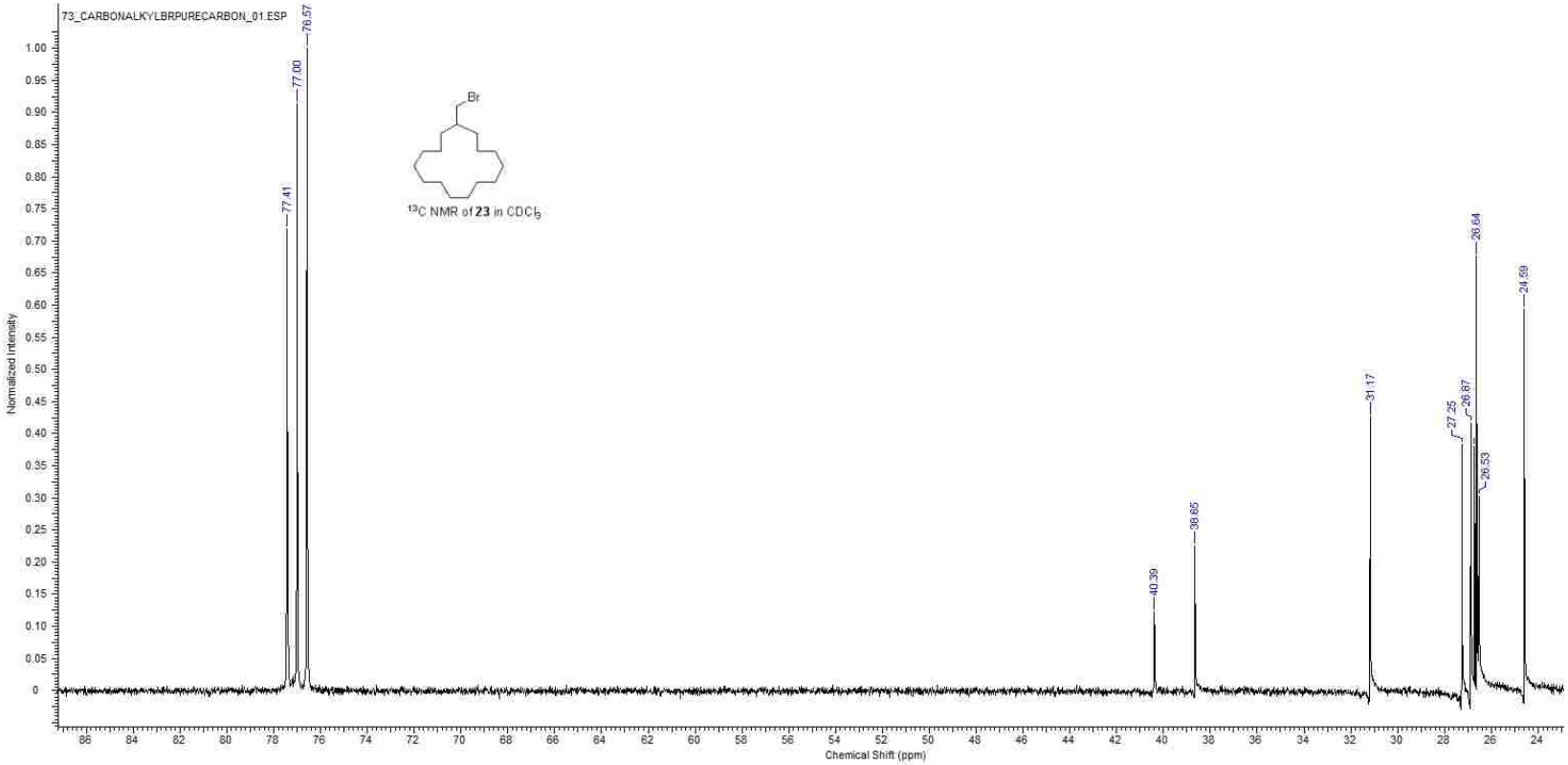
73_CARBONALKYLBRPURECARBON_01.ESP
Br
$^{13}$C NMR of **23** in $CDCl_3$
Normalized Intensity
Chemical Shift (ppm)
76.57
77.00
77.41
40.39
38.65
31.17
27.25
26.87
26.64
26.53
24.59

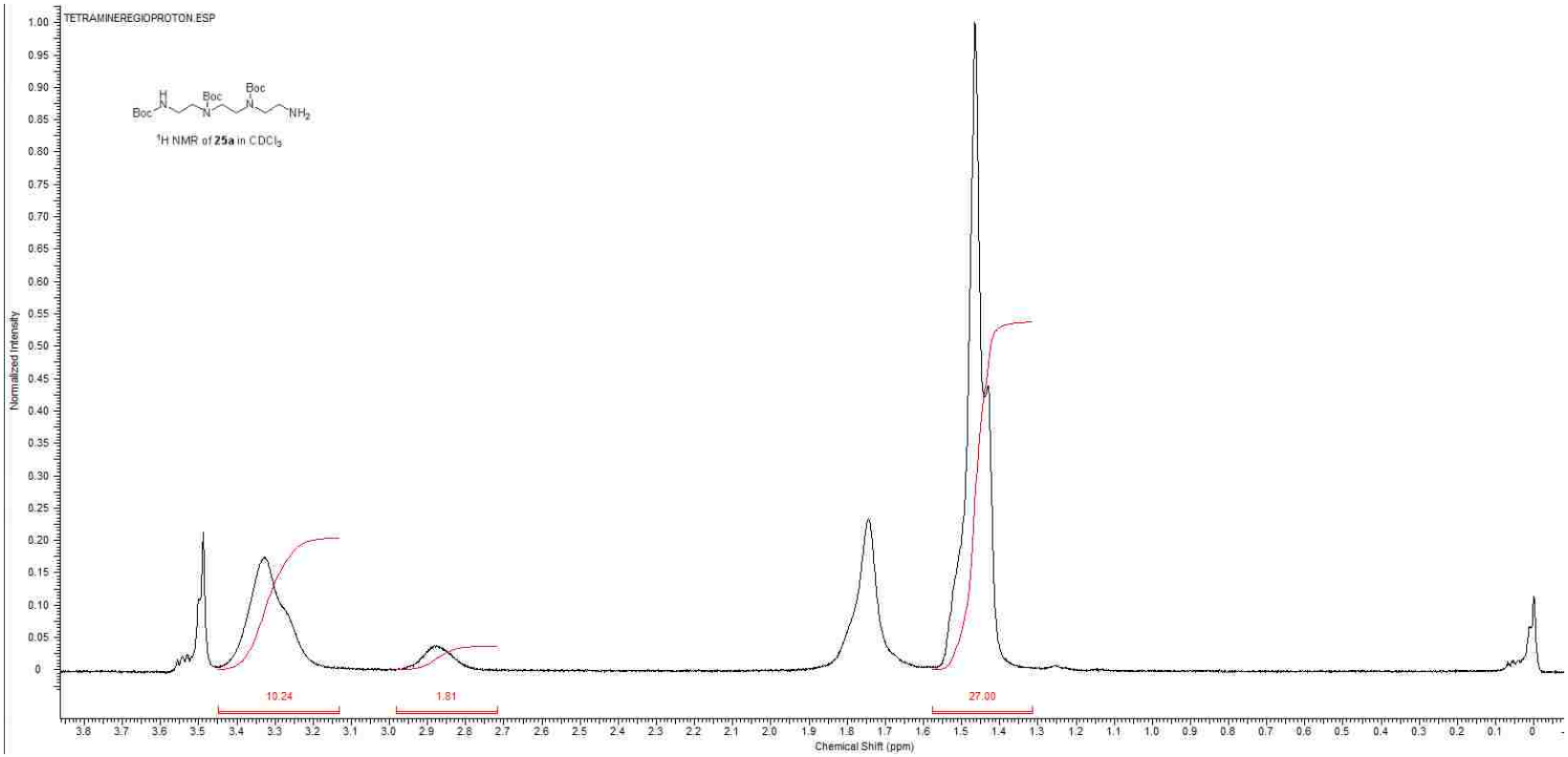
TETRAMINEREGIOPROTON.ESP
Boc
Boc
Boc
NH2
1H NMR of 25a in CDCl3
Normalized Intensity
10.24
1.81
27.00
Chemical Shift (ppm)

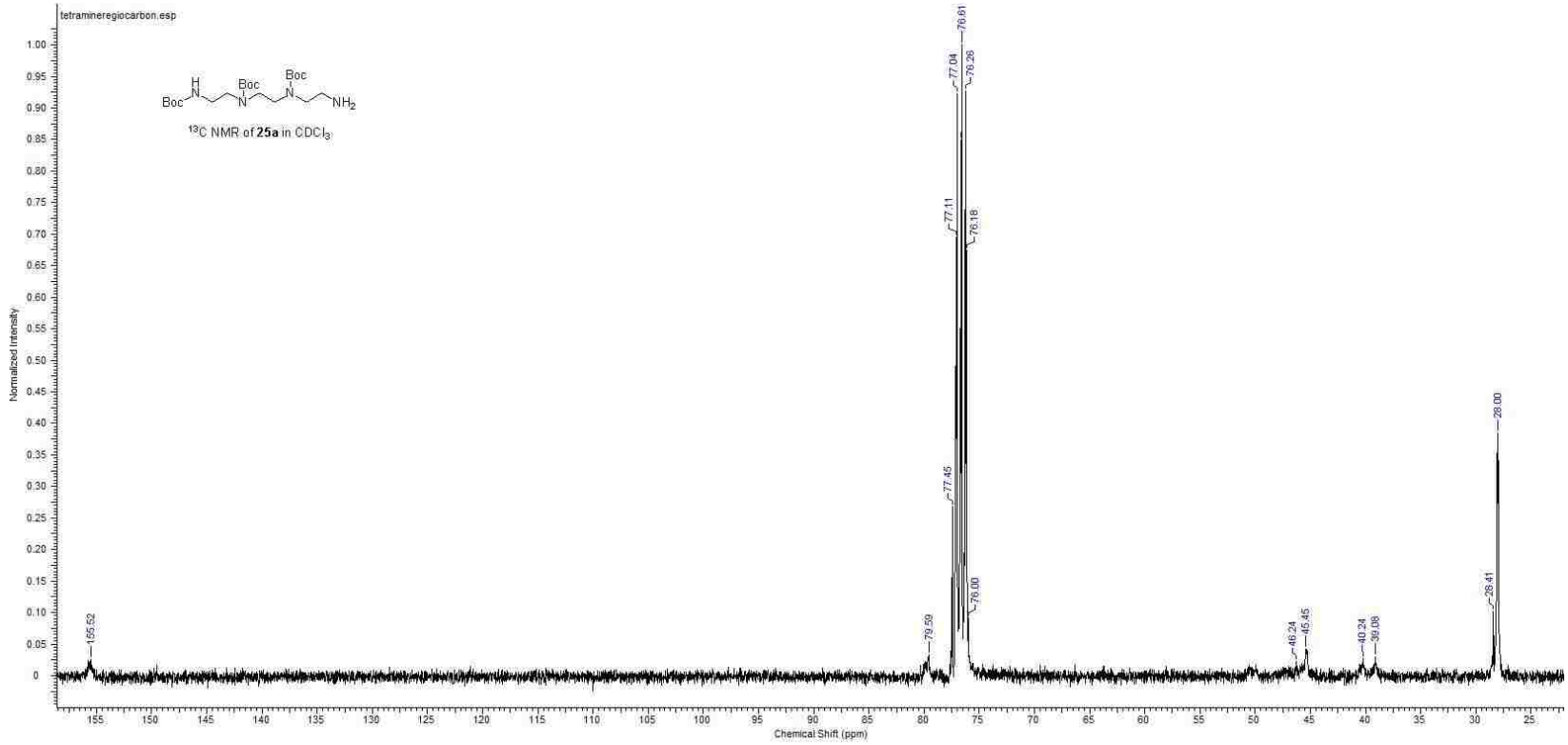
tetramineregiocarbon.esp
Boc
H
N
Boc
N
Boc
N
NH2
13C NMR of 25a in CDCl3
Normalized Intensity
Chemical Shift (ppm)
155.52
79.59
77.45
77.11
77.04
76.81
76.29
76.18
76.00
46.24
45.45
40.34
39.08
28.41
28.00

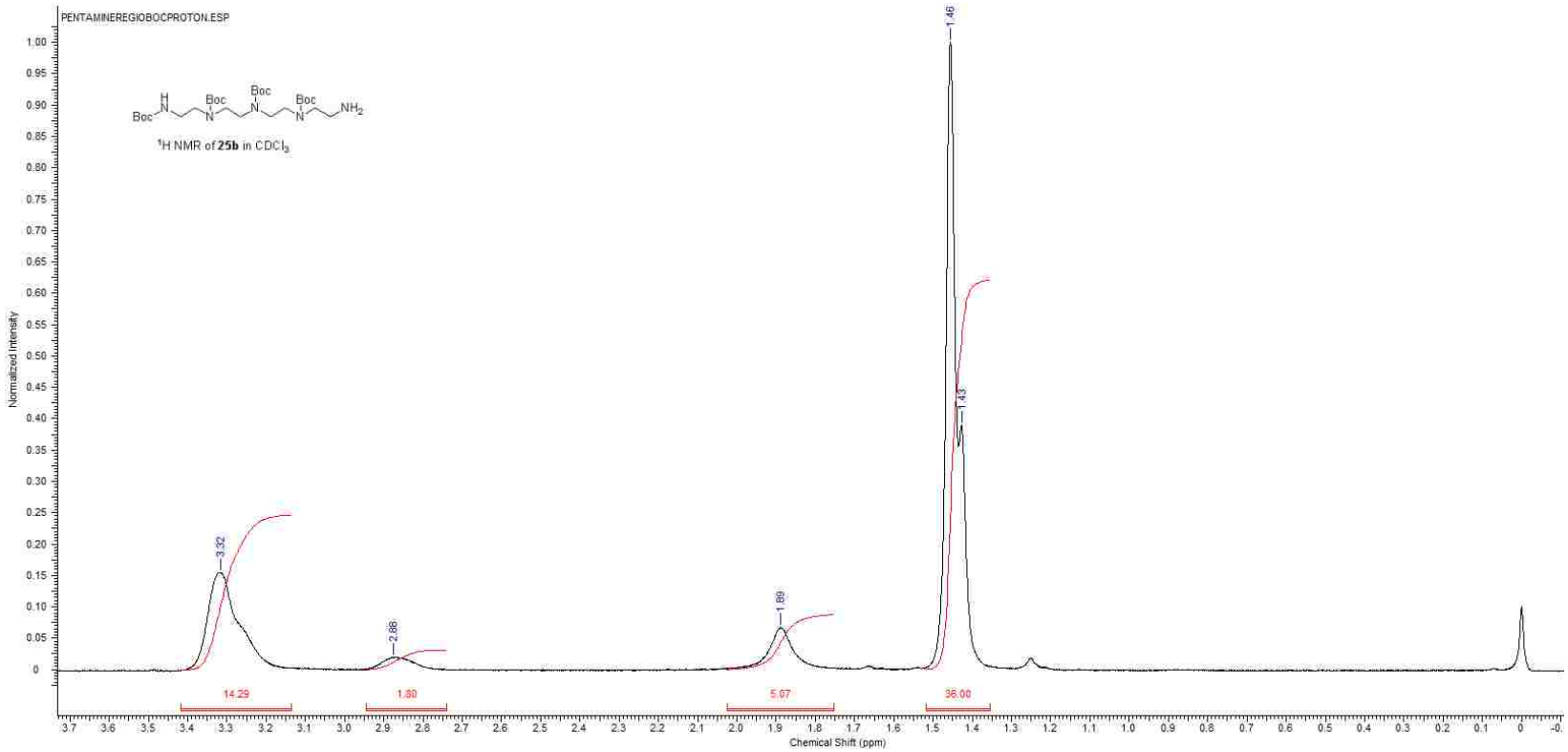
PENTAMINEREGIOBOCPROTON.ESP
Boc
Boc
Boc
Boc
NH2
1H NMR of 25b in CDCl3
Normalized Intensity
Chemical Shift (ppm)
3.32
2.86
1.89
1.46
1.43
14.29
1.80
5.07
36.00

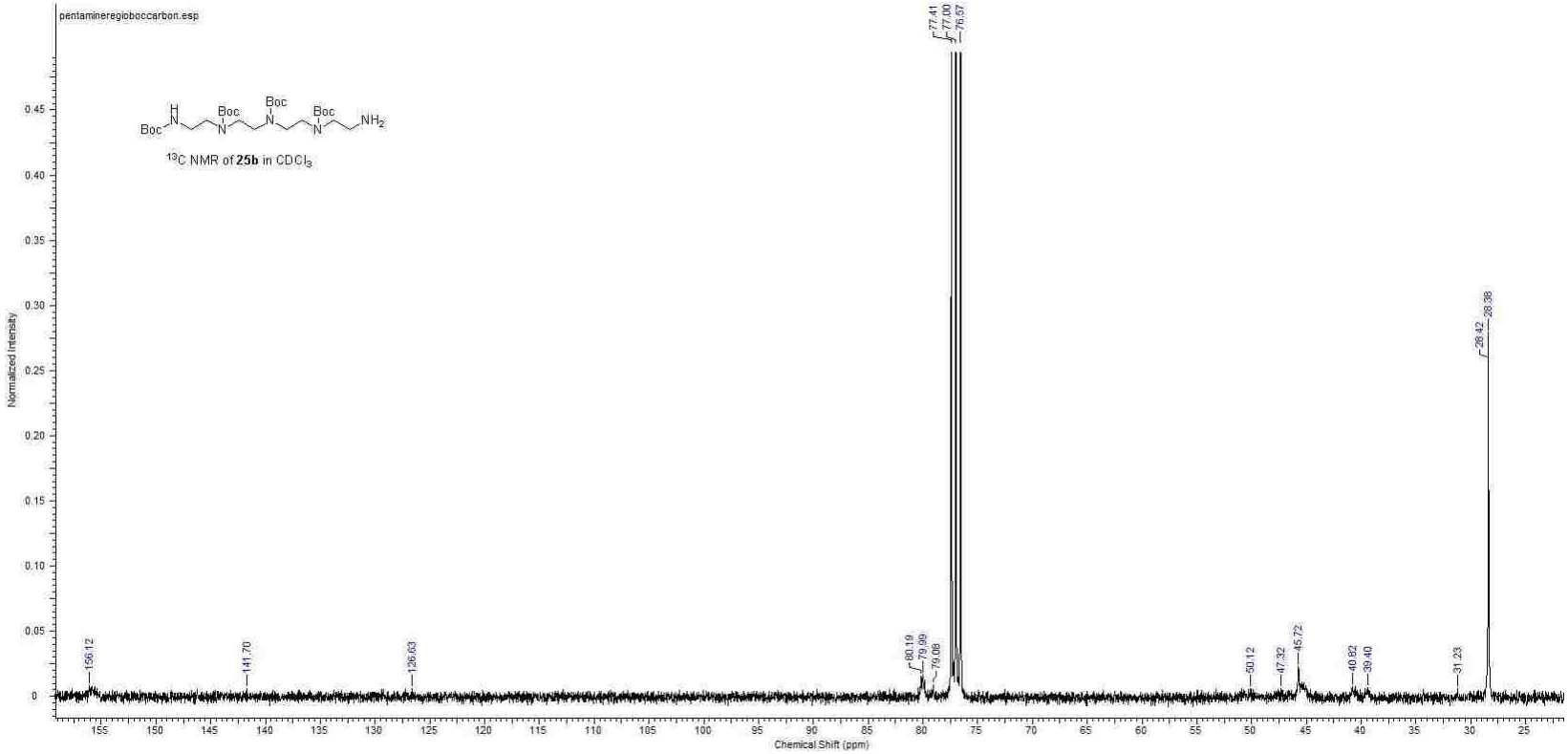
pentamineregioboccarbon.esp
Boc
Boc
Boc
Boc
NH2
13C NMR of 25b in CDCl3
Normalized Intensity
Chemical Shift (ppm)
156.12
141.70
126.63
80.19
79.99
79.08
77.41
77.00
76.57
50.12
47.32
45.72
40.82
39.40
31.23
28.42
28.36

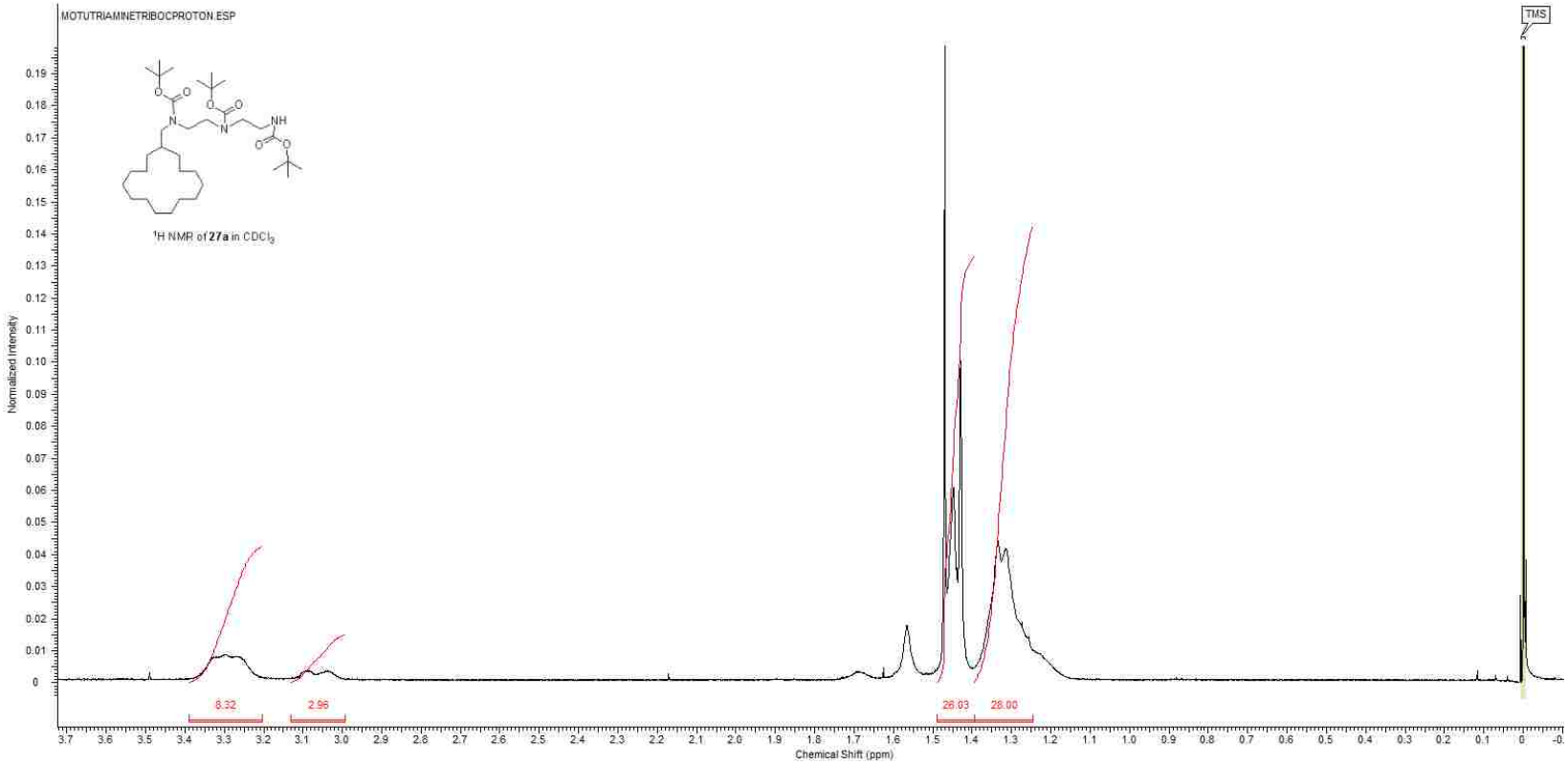
MOTUTRIAMINETRIBOCPROTON.ESP
TMS
$^1$H NMR of **27a** in $CDCl_3$
Normalized Intensity
Chemical Shift (ppm)
8.32
2.96
26.03
26.00

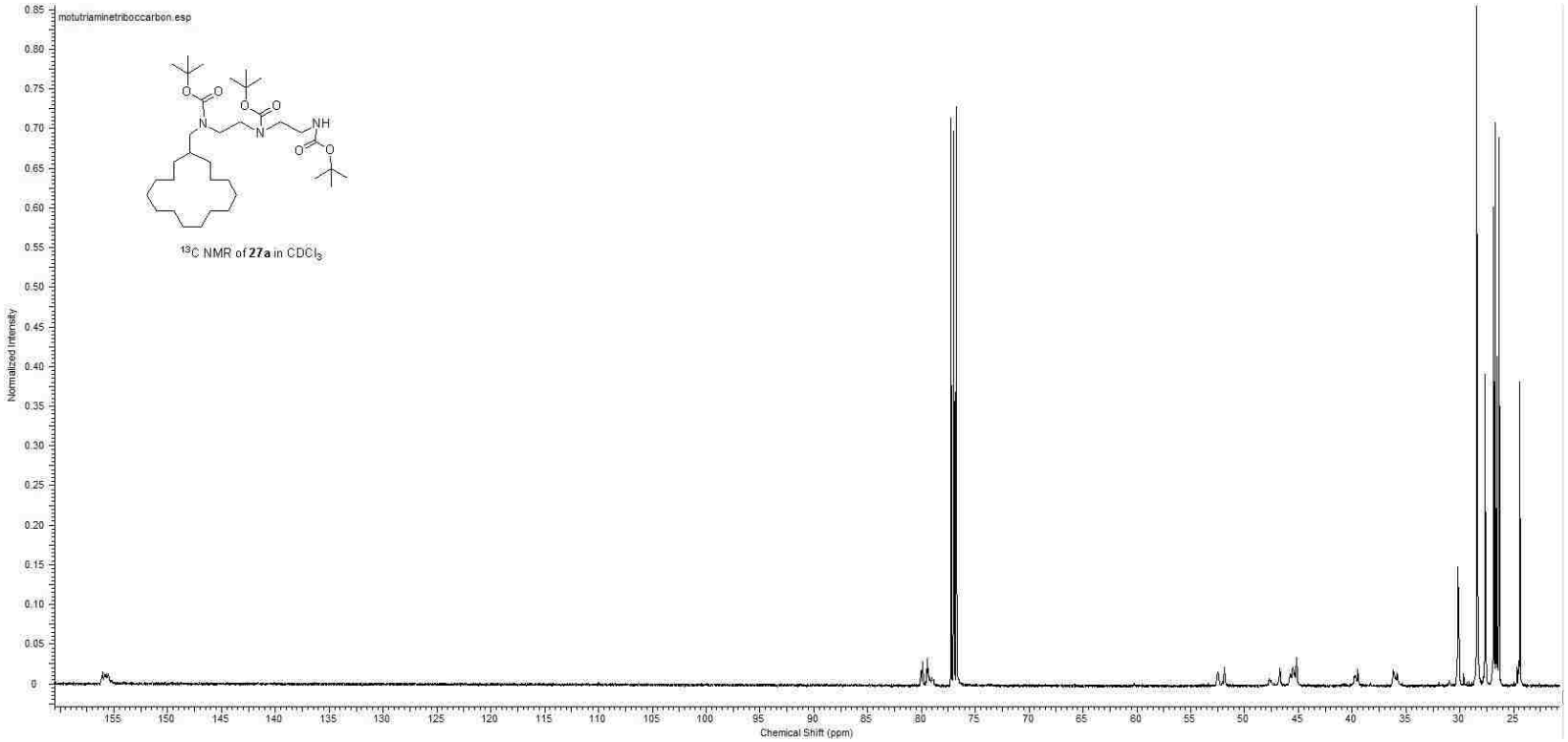
mototriaminetriboccarbon.esp
$^{13}$C NMR of **27a** in $CDCl_3$
Normalized Intensity
Chemical Shift (ppm)

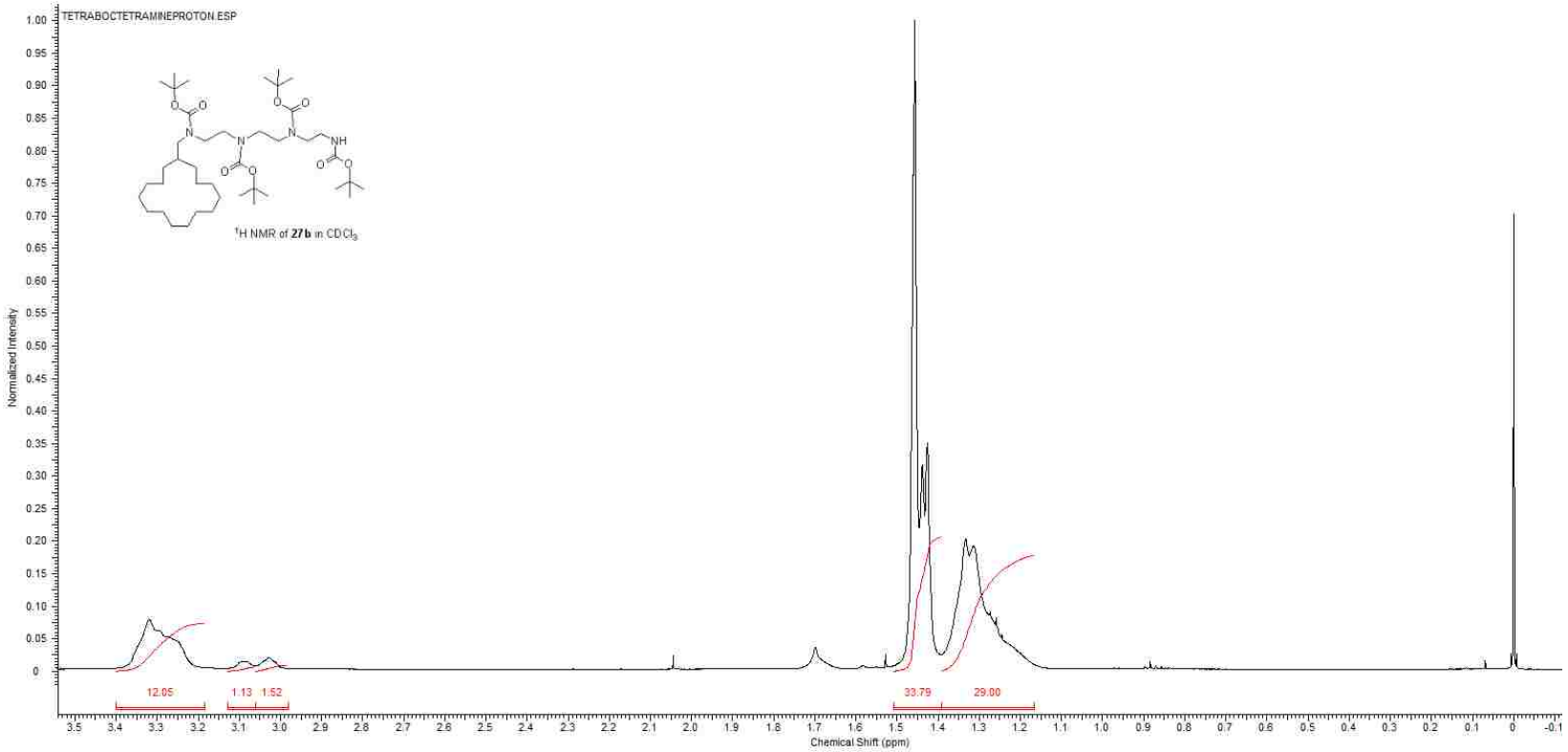
TETRABOCTETRAMINEPROTON.ESP
$^1$H NMR of **27b** in $CDCl_3$
Normalized Intensity
Chemical Shift (ppm)
12.05
1.13
1.52
33.79
29.00

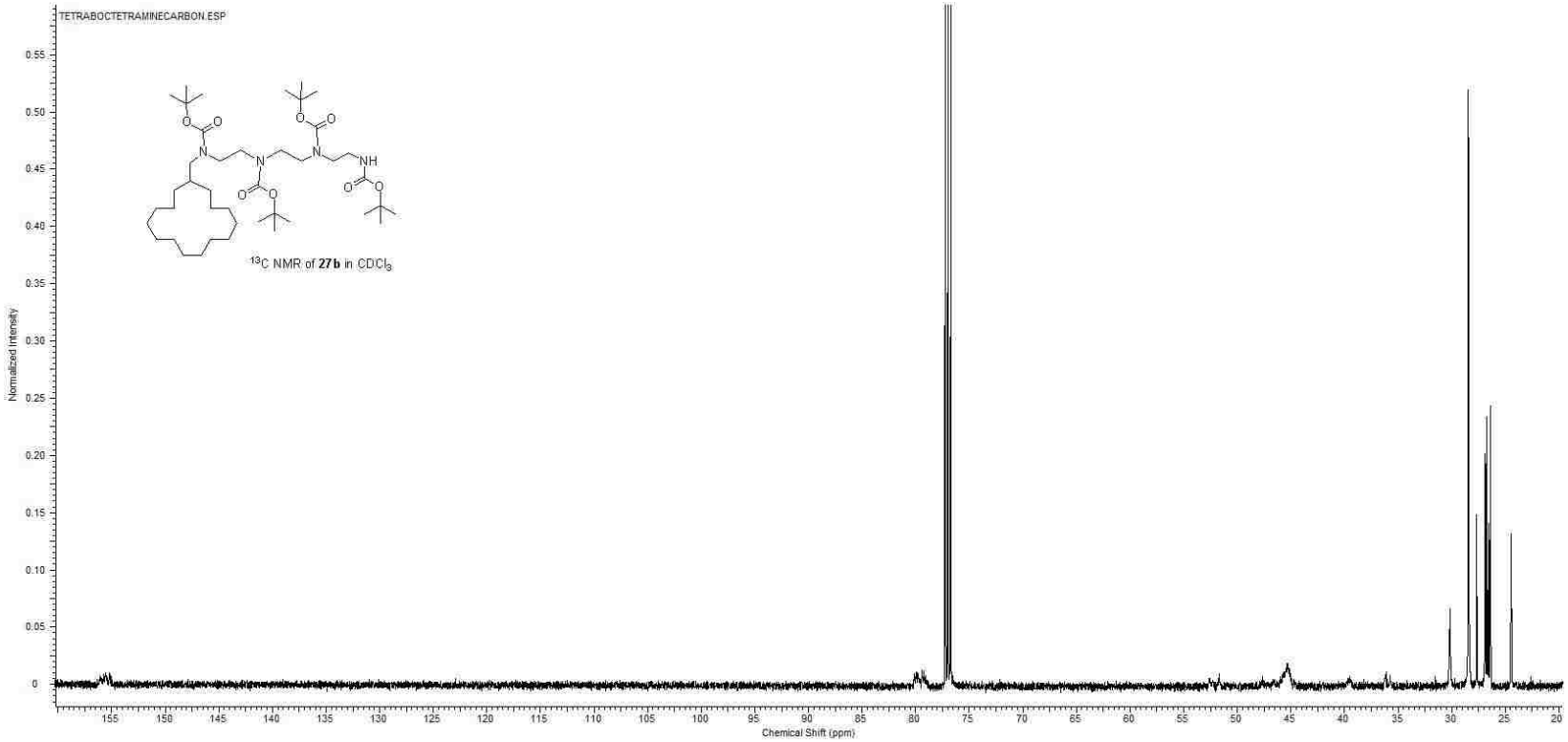
TETRABOCTETRAMINECARBON.ESP
$^{13}$C NMR of **27b** in $CDCl_3$
Normalized Intensity
Chemical Shift (ppm)

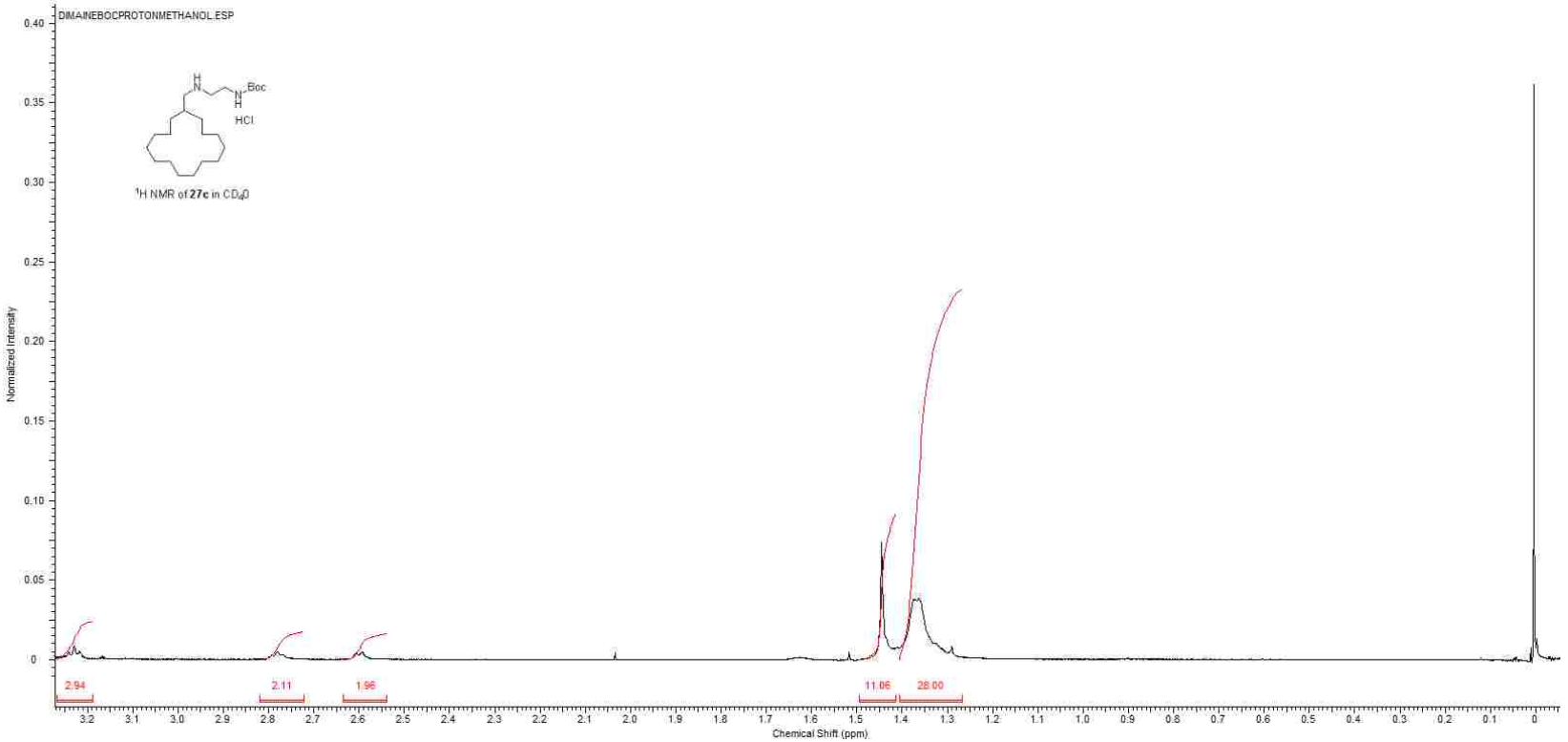
DIMAINEBOCPROTONMETHANOL.ESP
Boc
HCl
$^1$H NMR of **27c** in $CD_3O$
Normalized Intensity
Chemical Shift (ppm)
2.94
2.11
1.96
11.06
28.00

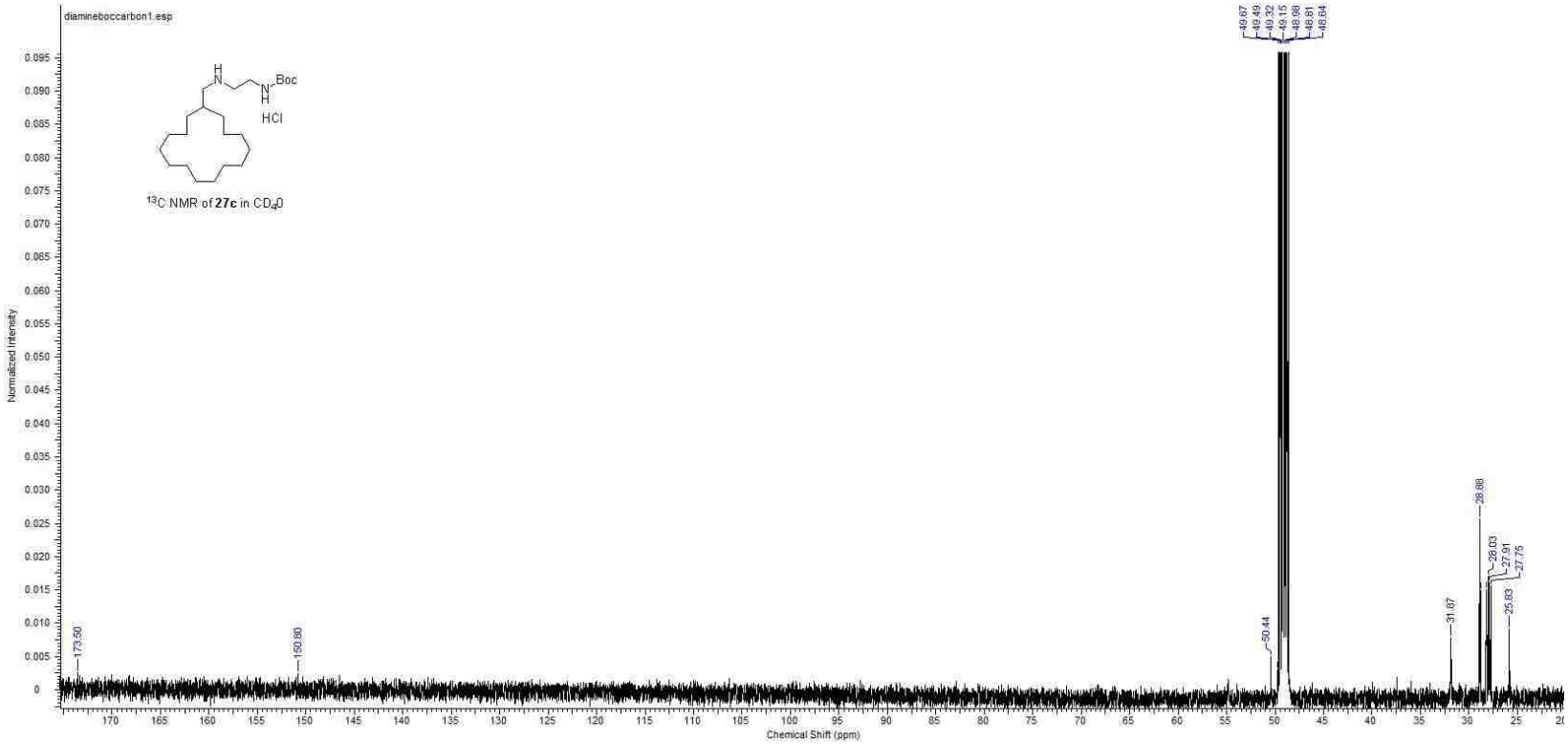
diamineboccarbon1.esp
Boc
HCl
$^{13}$C NMR of **27c** in $CD_3OD$
Normalized Intensity
Chemical Shift (ppm)
49.67
49.49
49.32
49.15
48.98
48.81
48.64
28.68
28.03
27.91
27.75
31.67
25.83
50.44
173.50
150.80

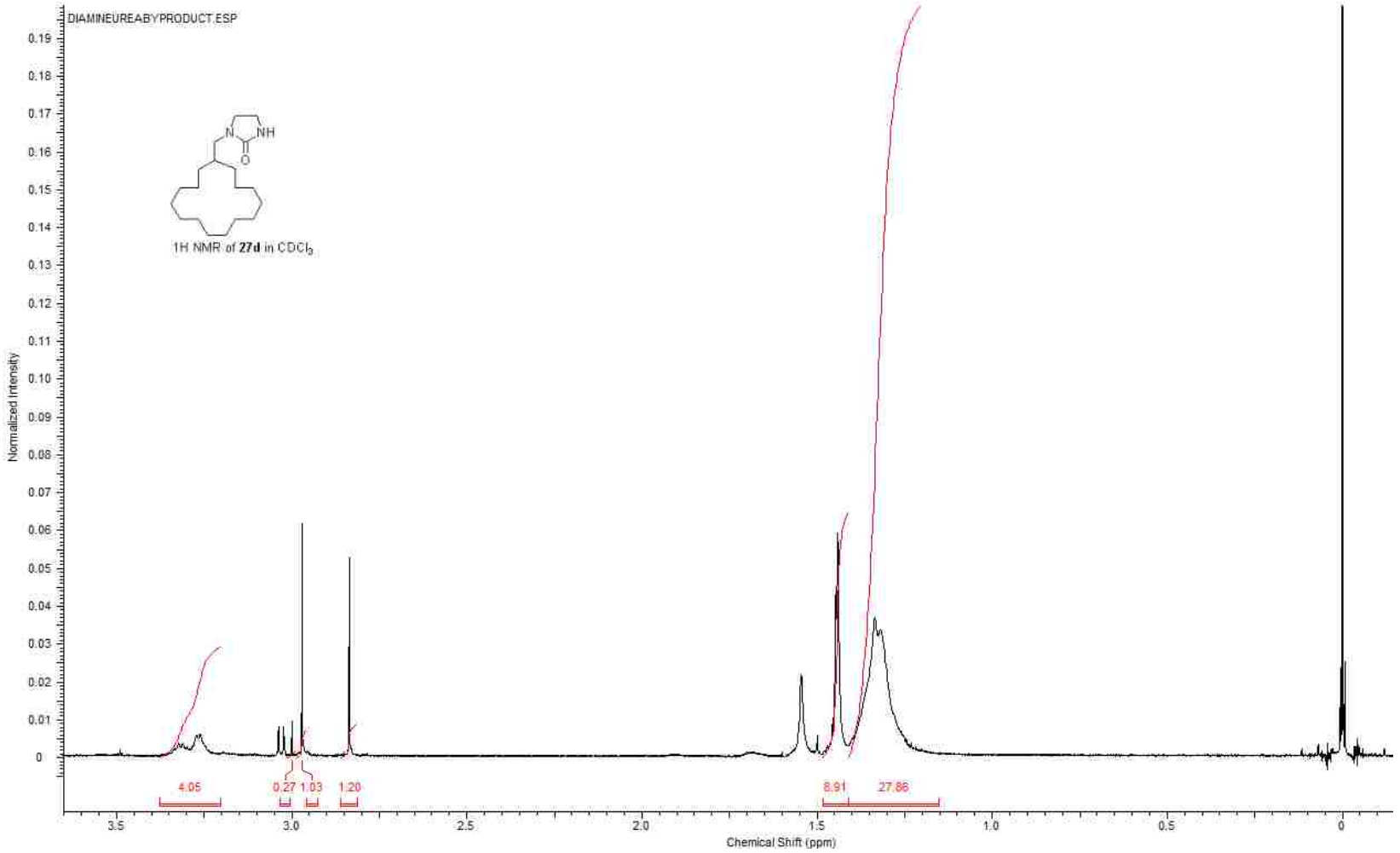
DIAMINEUREABYPRODUCT.ESP
1H NMR of 27d in CDCl3
Normalized Intensity
Chemical Shift (ppm)
4.05
0.27
1.03
1.20
8.91
27.86

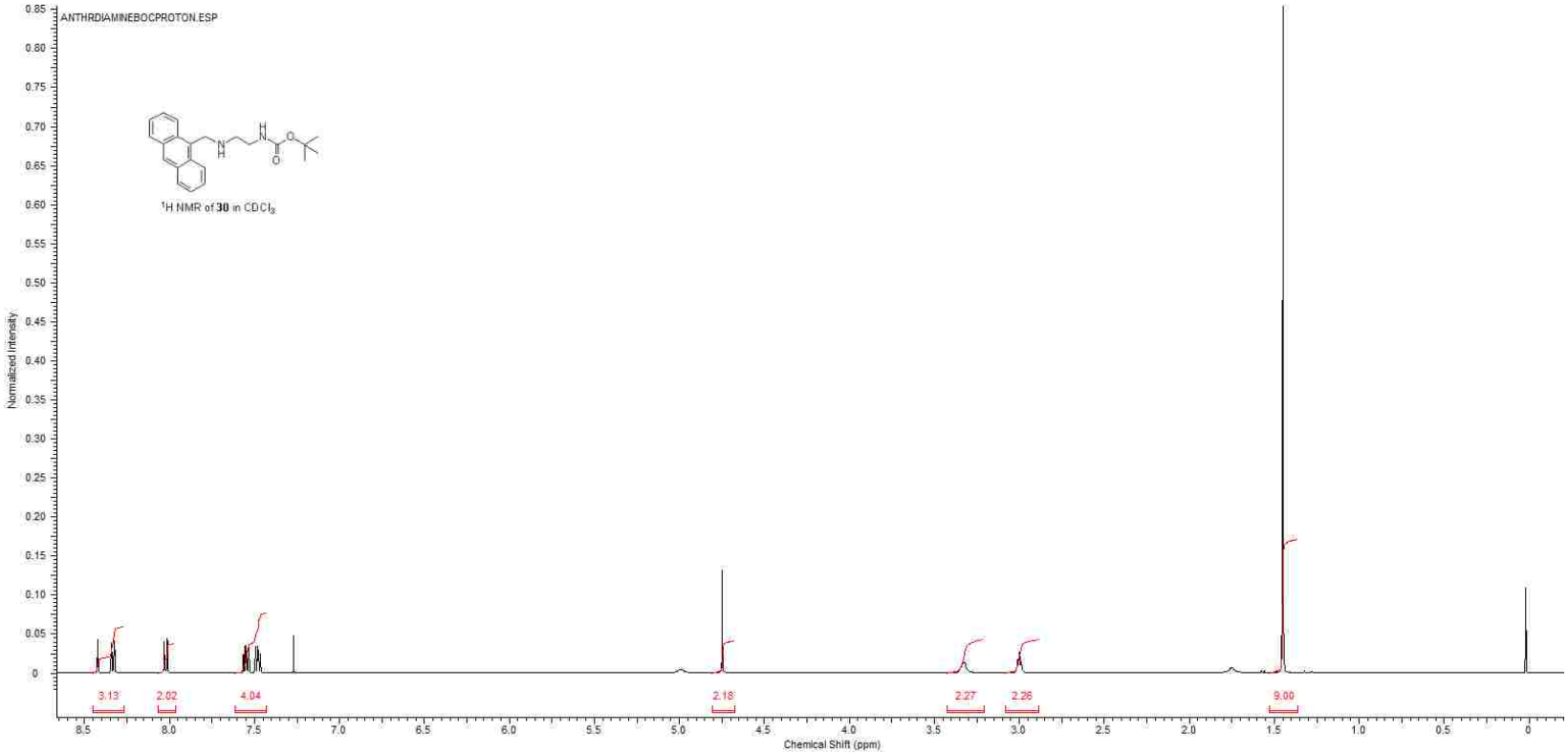
ANTHRDIAMINEBOCPROTON.ESP
$^1$H NMR of **30** in $CDCl_3$
Normalized Intensity
Chemical Shift (ppm)
3.13
2.02
4.04
2.18
2.27
2.26
9.00

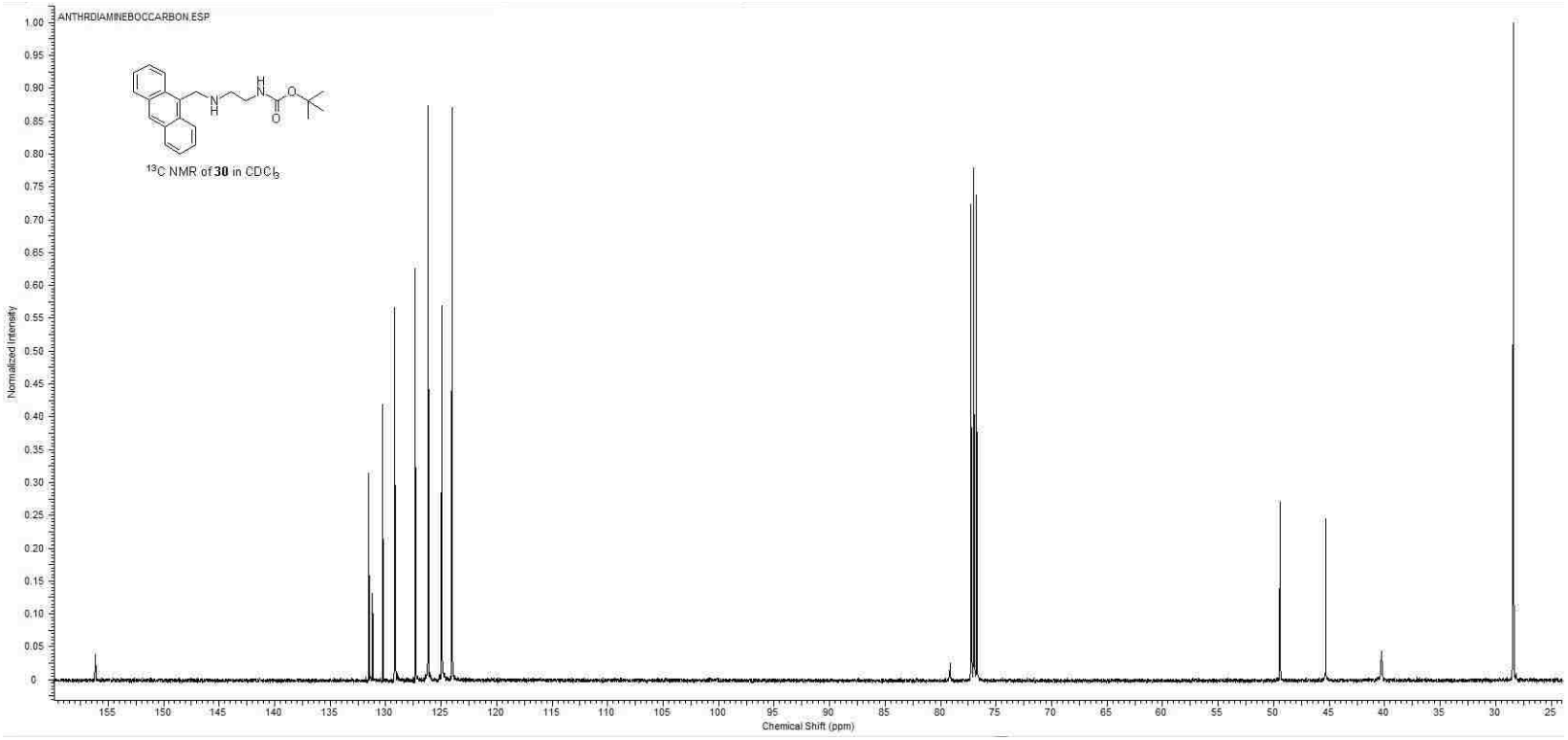
ANTHRDIAMINEBOCCARBON.ESP
$^{13}$C NMR of **30** in $CDCl_3$
Normalized Intensity
Chemical Shift (ppm)

## REFERENCES


1. Williams, D. E.; Lassota, P.; Andersen, R. J., Motuporamines A-C, cytotoxic alkaloids isolated from the marine sponge *Xestospongia exigua* (Kirkpatrick). *J. Org. Chem.* **1998,** *63*, 4838-4841.

2. Weeks, R. S.; Vanderwerf, S. M.; Carlson, C. L.; Burns, M. R.; O'Day, C. L.; Cai, F.; Devens, B. H.; Webb, H. K., Novel lysine-spermine conjugate inhibits polyamine transport and inhibits cell growth when given with DFMO. *Exp Cell Res* **2000,** *261* (1), 293-302.

3. Park, M. H., The post-translational synthesis of a polyamine-derived amino acid, hypusine, in the eukaryotic translation initiation factor 5A (eIF5A). *J Biochem* **2006,** *139* (2), 161-9.

4. Palmer, A. J.; Wallace, H. M., The polyamine transport system as a target for anticancer drug development. *Amino Acids* **2010,** *38* (2), 415-22.

5. Muth, A.; Pandey, V.; Kaur, N.; Wason, M.; Baker, C.; Han, X.; Johnson, T. R.; Altomare, D. A.; Phanstiel, O., IV, Synthesis and biological evaluation of antimetastatic agents predicated upon dihydromotuporamine C and its carbocyclic derivatives. *J Med Chem* **2014,** *57* (10), 4023-4034.

6. Muth, A.; Madan, M.; Archer, J. J.; Ocampo, N.; Rodriguez, L.; Phanstiel, O. t., Polyamine transport inhibitors: design, synthesis, and combination therapies with difluoromethylornithine. *J Med Chem* **2014,** *57* (2), 348-63.

7. Heaton, M. A.; Flintoff, W. F., Methylglyoxal-bis(guanylhydrazone)-Resistant Chinese Hamster Ovary Cells: Genetic Evidence That More Than A Single Locus Controls Uptake. *J. Cell. Physiol.* **1988,** *136*, 133-139.

8. Mandel, J. L.; Flintoff, W. F., Isolation of mutant mammalian cells altered in polyamine transport. *J. Cell. Physiol.* **1978,** *97*, 335-344.

9. Williams, D. E.; Craig, K. S.; Patrick, B.; McHardy, L. M.; van Soest, R.; Roberge, M.; Andersen, R. J., Motuporamines, anti-invasion and anti-angiogenic alkaloids from the marine sponge *Xestospongia exigua* (Kirtpatrick): Isolation, structure elucidation, analogue synthesis, and conformational analysis. *J. Org. Chem.* **2002,** *67*, 245-258.

10. (a) Kaur, N.; Delcros, J. G.; Archer, J.; Weagraff, N. Z.; Martin, B.; Phanstiel Iv, O., Designing the polyamine pharmacophore: influence of N-substituents on the transport behavior of polyamine conjugates. *Journal of medicinal chemistry* **2008,** *51* (8), 2551-60; (b) Kaur, N.; Delcros, J.-G.; Martin, B.; Phanstiel, O., Synthesis and biological evaluation of dihydromotuporamine derivatives in cells containing active polyamine transporters. *J. Med. Chem.* **2005,** *48*, 3832-3839.

11. Roskelley, C. D.; Williams, D. E.; McHardy, L. M.; Leong, K. G.; Armelle, T.; Karsan, A.; Andersen, R. J.; Dedhar, S.; Roberge, M., Inhibition of tumor cell invasion and angiogenesis by motuporamines. *Cancer Res.* **2001,** *61*, 6788-6794.

12. (a) Hyvonen, M. T.; Ucal, S.; Pasanen, M.; Peraniemi, S.; Weisell, J.; Khomutov, M.; Khomutov, A. R.; Vepsalainen, J.; Alhonen, L.; Keinanen, T. A., Triethylenetetramine modulates polyamine and energy metabolism and inhibits cancer cell proliferation. *Biochem J* **2016,** *473* (10), 1433-41; (b) Liu, J.; Guo, L.; Yin, F.; Zheng, X.; Chen, G.; Wang, Y.,

Characterization and antitumor activity of triethylene tetramine, a novel telomerase inhibitor. *Biomed Pharmacother* **2008,** *62* (7), 480-5.

13. McHardy, L. M.; Sinotte, R.; Troussard, A.; Sheldon, C.; Church, J.; Williams, D. E.; Andersen, R. J.; Dedhar, S.; Roberge, M.; Roskelley, C. D., The tumor invasion inhibitor dihydromotuporamine C activates RHO, remodels stress fibers and focal adhesions, and stimulates sodium-proton exchange. *Cancer Res* **2004,** *64* (4), 1468-1474.

14. Baetz, K.; McHardy, L.; Gable, K.; Tamsin, T.; Reberioux, D.; Bryan, J.; Andersen, R. J.; Dunn, T.; Hieter, P.; Roberge, M., Yeast genome-wide drug-induced haploinsufficiency screen to determine drug mode of action. *PNAS* **2004,** *101,* 4525-4530.

15. Asano, S.; Kitatani, K.; Taniguchi, M.; Hashimoto, M.; Zama, K.; Mitsutake, S.; Igarashi, Y.; Takeya, H.; Kigawa, J.; Hayashi, A.; Umehara, H.; Okazaki, T., Regulation of cell migration by sphingomyelin synthases: sphingomyelin in lipid rafts decreases responsiveness to signaling by the CXCL12/CXCR4 pathway. *Mol. Cell Biol.* **2012,** *32* (16), 3242-3252.

16. Furstner, A.; Rumbo, A., Ring-closing alkyne metathesis. Stereoselective synthesis of the cytotoxic marine alkaloid motuporamine C. *J. Org. Chem.* **2000,** *65,* 2608-2611.

17. Yang, C. T.; Zhang, Z. Q.; Liang, J.; Liu, J. H.; Lu, X. Y.; Chen, H. H.; Liu, L., Copper-catalyzed cross-coupling of nonactivated secondary alkyl halides and tosylates with secondary alkyl Grignard reagents. *Journal of the American Chemical Society* **2012,** *134* (27), 11124-7.

18. Prugh, J. D.; Birchenough, L. A.; Egbertson, M. S., A Simple Method of Protecting a Secondary Amine with Tert-Butyloxycarbonyl (Boc) in the Presence of a Primary Amine. *Synthetic Commun* **1992,** *22* (16), 2357-2360.

19. Khomutov, A. R.; Shvetsov, A. S.; Vepsalainen, J. J.; Kritzyn, A. M., Novel acid-free cleavage of N-(2-hydroxyarylidene) protected amines. *Tetrahedron Lett* **2001,** *42* (15), 2887-2889.

20. Abdel-Magid, A. F.; Carson, K. G.; Harris, B. D.; Maryanoff, C. A.; Shah, R. D., Reductive Amination of Aldehydes and Ketones with Sodium Triacetoxyborohydride. Studies on Direct and Indirect Reductive Amination Procedures(1). *The Journal of organic chemistry* **1996,** *61* (11), 3849-3862.

21. Gardner, R. A.; Delcros, J.-G.; Konate, F.; Breitbeil, F.; Martin, B.; Sigman, M.; Phanstiel, O., *N*1-Substituent effects in the selective delivery of polyamine-conjugates into cells containing active polyamine transporters. *J. Med. Chem.* **2004,** *47*, 6055-6069.

22. Bruns, C. J.; Harbison, M. T.; Kuniyasu, H.; Eue, I.; Fidler, I. J., In vivo selection and characterization of metastatic variants from human pancreatic adenocarcinoma by using orthotopic implantation in nude mice. *Neoplasia* **1999,** *1* (1), 50-62.

23. Seiler, N.; Delcros, J. G.; Moulinoux, J. P., Polyamine transport in mammalian cells. An update. *Int J Biochem Cell Biol* **1996,** *28* (8), 843-61.

24. Phanstiel, O., IV ; Kaur, N.; Delcros, J.-G., Structure-activity investigations of polyamine-anthracene conjugates and their uptake via the polyamine transporter. *Amino Acids* **2007,** *33*, 305-313.

25. Roy, U. K.; Rial, N. S.; Kachel, K. L.; Gerner, E. W., Activated K-RAS increases polyamine uptake in human colon cancer cells through modulation of caveolar endocytosis. *Mol Carcinog* **2008,** *47* (7), 538-53.